Scuola Internazionale Superiore di Studi Avanzati

From neuronal networks to behavior: dynamics of spontaneous activity and onset of movement in the leech

Thesis submitted for the degree of Doctor Philosophiae

Neurobiology sector

January 2007

Candidate

Alberto Mazzoni

Supervisor

Vincent Torre

A Sara

Index

Plan of the work

The first section of the Introduction will briefly describe the anatomy of the leech and the known mechanisms of neuronal control of the movements in this animal. The second section will review previous results on the importance and the dynamics of the spontaneous activity in the nervous system. The third section will present some mathematical tools we used in our analysis, with a particular emphasis on criticality theory that is, in our opinion, a key tool to describe the irregular self-regulated spontaneous activity of neuronal networks.
The first two sections of the Results have been published in two different papers. The following two sections present papers in preparation and must therefore be considered works in progress.

List of publications

The first two sections of the Results reproduce the following published papers

Mazzoni A, Garcia Perez E, Zoccolan D, Graziosi S, Torre V (2005) Quantitative characterization and classification of leech behavior. J.Neurophysiol 93:580-593.

Garcia-Perez E, Mazzoni A, Zoccolan D, Robinson HPC, Torre V (2005) Statistics of decision making in the leech. J Neurosci 25:2597-2608.

Abbreviations

FR: firing rate

ISI: inter-spike interval

IBI: inter-burst interval

NMDA: N-methyl-d-aspartate

GABA: γ-aminobutyric acid

APV: 2-Aminophosphonovaleric acid

PTX: Picrotoxin

SOC: self organized criticality

CPG: central pattern generator

HSB: highly synchronized burst

MEA: multielectrode array

LFP: local field potential

MN: motor neuron

DP: dorsal posterior root

PP: posterior posterior root

AA: anterior anterior root

MA: median anterior root

ABSTRACT

Animal behavior was once seen as a chain of reactions to stimuli from the environment. From chemotaxis in bacteria to mammals withdrawing from painful stimuli, most of the actions taken by animals are clearly driven by external inputs. Reflexes were among the first phenomena to be studied to have an insight on the dynamics of the nervous system. Later, a step forward was the discovery of central pattern generators: once a behavior is started by a stimulus, some neuronal networks are able to maintain it without further inputs from the environment. The nervous system of all animals, however, is so complex that is displaying a rich dynamics even in the absence of external inputs or, in a more realistic situation, when no single input is able to drive a clear-cut reaction. In the same way, at the motor output level, animals keep moving in the absence of evident stimuli. These spontaneous behaviors are still far from being understood.

Difficult problems are often easier to solve in simple systems. The leech has a relatively simple nervous system, composed of ~10^3 neurons disposed in a regular structure, but at the same time displays a variety of different behaviors. It seems then a good preparation to approach the spontaneous dynamics problem.

The aim of my PhD research is to describe the spontaneous behavior of the leech and the spontaneous activity of its nervous system.

A first, necessary step for this study was to develop a method of automatic classification and analysis of the leech movements. Thanks to this method we described accurately the properties of the different behaviors: we focused particularly on the largely unknown irregular exploratory behavior, which is found to display a broad range of oscillation frequencies and displacement speeds, but with some recurrent movement patterns. Finding the complete list of the leech spontaneous behaviors, and the probability of the transitions between them, it was possible to demonstrate that decision making in the leech is a Markovian process.

The spontaneous activity in the isolated leech ganglion was found to be characterized by long-term correlations and a large variability in bursts size and duration. The same dynamics was observed in dissociated culture of rat hippocampal neurons, despite the difference in the structure between the two networks. We studied the effects of pharmacological modulations of inhibitory and excitatory processes on the spontaneous activity, and the role of single identified motor neurons in

spontaneous bursts. Finally we proposed a simple statistical model accounting for experimental results.

We studied then the spontaneous activity of the leech ganglion when it was connected to the other ganglia and in the semi-intact moving animal. Inputs received from the head and tail brain caused a drastic change in the activity of the ganglion, increasing synchronization among neurons and leading to a regime dominated by very large bursts. By recording at the same the movements of the leech and its nervous activity it was possible to have a better understanding of the relationship between the motor neuron bursts and the onset of movements.

1-The leech

1.a Structure of the leech nervous system

The species of leech that was the subject of my researches is the *Hirudo medicinalis*, which has been intensively studied from the ancient times due to its use in medicine. Physicians collected many data about the anatomy of the leech, making it an ideal subject for early studies on development of the nervous system and neuron morphology in the late 19th and early 20th century. In the last 50 years, as we will partially see later, several fundamental issues of neuroscience, from action potential generation to sensory-motor integration to regeneration, have been addressed in the leech central nervous system. One of the reasons for this relies on its simple structure.

The leech is a segmented animal: 102 annuli are visible on the dark green surface of the skin, and the internal structure of the body is divided into 32 segments. The first 4 are the head segments, the following 21 the body segments and the last 7 segments are fused to form the tail sucker (Payton in Muller et al. 1981). The 32 metameric segments are innervated by one head ganglion, 21 body ganglia (usually numbered starting from the head), and 7 fused tail ganglia. We will call the head and tail ganglia "brains" for their regulatory role in respect to the body ganglia. The ganglia are joined by a connective, composed of three bundles of fibres and covered by a fibrous sheath. Pairs of nerve roots arise from each side of the body ganglion, and each one is bifurcating to originate 4 main roots on each side (see Fig. 1).

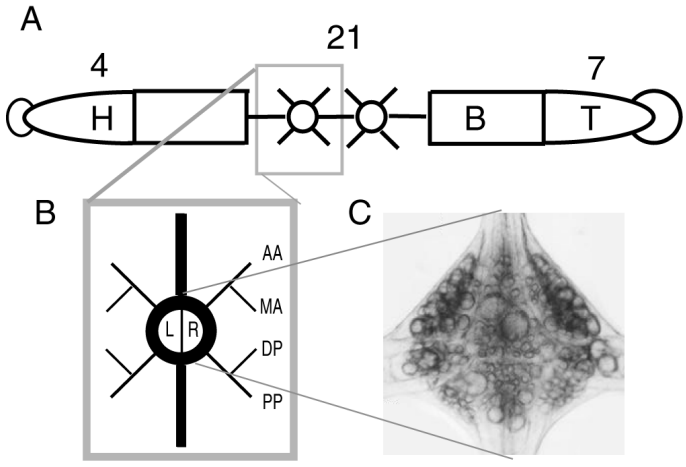

Figure 1 Structure of the nervous system of the leech. ***A*** *The whole body divided into three sectors: Head, Body and Tail.* ***B*** *The structure of a single ganglion divided into Left and Right semi-ganglia and projecting four main roots: Anterior Anterior, Median Anterior, Dorsal Posterior and Posterior Posterior.* ***C*** *Picture of an isolated ganglion with visible neurons (from S.Blackshaw)*

There are no peripheral reflexes that contribute to the body movements: all movements are originated in the ganglia. Each segmental ganglion is composed of 400 nerve cell bodies, except ganglia 5 and 6, which innervate the sex organs and contain over 700 nerve cell bodies. The neurons are divided into six packets with axonal processes passing trough a central neuropil. Their position and connection are very stable from ganglion to ganglion and from leech to leech, and their diameter varies from 10 to 60 μm.

Neurons in leech ganglia can be divided into three main categories: sensory neurons, motor neurons, interneurons. The leech has different kinds of sensory neurons, since it reacts to a variety of natural stimuli: it is sensitive to light (Peterson 1983) by means of 10 paired eyes on the dorsal surface of the head and 14 sensilla per segment on the body, to chemical and thermal stimuli affecting the feeding behavior (Zhang et al. 2000), and to water waves by means of sensilla distributed over the whole body (Philips and Friesen 1982). Since the very beginning (Nicholls and Baylor 1968), however, the most studied have been the mechanosensory neurons. At each side of each ganglion there are two neurons sensitive to light touch (T cells), three neurons sensitive to pressure (P cells) and two neurons sensitive to noxious stimuli (N cells), all innervating the skin of the segment corresponding to their ganglion and the neighboring ones (Nicholls et al. 1992). The well defined border of the innervated skin areas, the accurate sensitivity to the intensity of the pressure applied, and the ability to directly trigger a local bending (see section 1b) made these neurons an optimal subject to study the computational properties of sensory-motor integration. The population coding identifies the localization of the stimulus thanks to the tuning properties of the single neurons (Lewis and Kristan 1998a), and to the differences in spike count and timing between neurons with overlapping sensory fields (Thomson and Kristan 2006).

Motor neurons are innervating the five kinds of muscles originating the movements of the leech: annulus erector, longitudinal, circular, oblique, and dorsoventral (Payton in Muller et al. 1981, Kristan et al. 2005). The contraction of the annulus erector muscles, located just under the skin, causes each annulus to form a sharp ridge. The following three are disposed into concentric layers: from the outside inward, longitudinal muscles contraction produces shortening, circular muscles contraction produces a reduction in cross-section and elongation, and oblique muscles contraction causes stiffening at an intermediate body length. Dorsoventral muscle fibres traverse the body cavity, and their contraction elongates the body. There are 32 identified motor neurons (MN) in each semi-ganglion of the leech (see Appendix D of Muller et al. 1981 and the addition in Norris and Calabrese 1987). Each motor neuron connects to a single muscle type: AE excite the annulus erector muscles, HE the lateral heart tubes to keep the blood pumping, whereas the role of motor neuron 10 is unknown. The other known connections are summarized in Table 1

muscles / neuron role	Longitudinal	Circular	Oblique	Dorsoventral
excitors	3,4*,5,6,8,17,106,107, 108,L	11,12,112,CV	110,111	109,117*
inhibitors	1,2,7,9,101,102,119			

Table 1 Motor neurons and associated muscles *All MN are projecting controlaterally except those indicated with *.*

Each motor neuron innervates a field that extends longitudinally into adjacent body segments and there overlaps with the fields of homologous neurons (Payton in Muller et al. 1981). Excitatory MN increase the amplitude and the rate of the contractions of the corresponding muscles when their firing rate exceeds a characteristic threshold, whereas inhibitory MN oppose the activity of excitors both at a muscle level and by inhibiting them in the ganglion (Mason and Kristan 1982). Motor neurons response to stimuli is generally very variable, but their statistical independence allows a reliable population coding (Arisi et al. 2001, Zoccolan et al. 2002).

The majority of neuronal somata of the leech are interneurons without direct connection to the periphery. Most of the known interneurons have been identified for participating in the networks underlying some of the behaviors that we will present in the section 1b.

Neuron in the leech ganglia are known to form electrical synapses and chemical synapses with a variety of receptors such as acethilcoline (Muller in Muller et al. 1981). In the Results we will focus on the presence of glutamate NMDA excitatory receptors (Burrell and Sahley 2004) and GABA inhibitory receptors (Cline 1986).

1b Neuronal control of leech behavior

The whole range of possible behaviors of the leech can be decomposed into four basic movements occurring at the level of the single segment (Kristan et al. 2005):

a) bending, i.e. a contraction of longitudinal muscles on one side, often associated with relaxation on the other side
b) shortening, i.e. a synchronous contraction of all longitudinal muscles
c) elongation, i.e. a contraction of circular muscles
d) flattening, i.e. a contraction of the dorsoventral muscles

Two reactive behaviors, elicited by tactile stimulation, have been extensively studied: the local bending and the shortening.

The local bending has been studied delivering stimuli with touching devices, electrical stimulations of the skin, or directly with intracellular depolarization of mechanosensory neurons. In any of these cases the segment bends, and the bending extends to a number of neighboring segments depending on the intensity of the stimulation (Wittenberg and Kristan 1992a). The P cells detect and localize the position of the stimulus in the skin, since each one of them has a cosine shape receptive field (Lewis and Kristan 1998a). P cells activate interneurons, seventeen of which have been identified (Lockery and Kristan 1990), and these interneurons still have cosine shaped receptive field (Lewis and Kristan 1998a). The process leading from the coding of the stimuli position to the local bending has been recently well characterized (Lewis and Kristan 1998 b and c). Interneurons activate the excitatory motor neurons corresponding to the stimulated area to induce contraction, and the inhibitory motor neurons of the opposite areas to induce relaxation through direct inhibition of muscles and inhibition of the corresponding excitatory motor neurons (see Fig. 2).

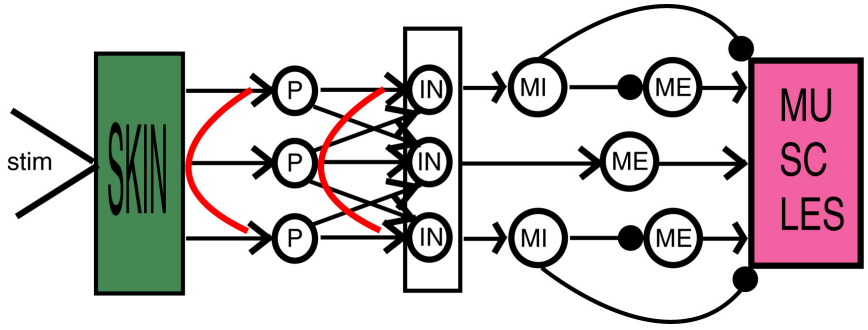

Figure 2 Local bending network. *From left to right: the applied stimulus, the skin, the Pressure (P) mechanosensory neurons, the Interneurons (IN), then the Inhibitory Motor neurons (MI) and the Excitatory Motor neurons (ME) triggering the contraction of the muscles. The red lines indicate that the excitation is greater for the mechanosensory neurons and interneurons corresponding to the stimulated area. This results in a contraction of the muscles of the stimulated area and a relaxation of the muscles away from the stimulus.*

Monitoring the leech skin with an optical flow technique, combined with intracellular recording (Zoccolan et al. 2001) it was demonstrated that local bending is a linear combination of the contributions of longitudinal and circular MN (Zoccolan and Torre 2002).

Stimulating the anterior end of the leech produces a whole body shortening involving the contraction of all longitudinal muscles. The stimulation activates an unpaired interneuron called S cell, and this neuron propagates the signal along the body of the leech (Bagnoli et al. 1975). The S cells projects through the Faivre's nerve, the smallest connective bundle, axons ending with electric junctions passing the action potential to the S cell of the following ganglion. S cells conduct signals with a speed of 5-6 ms per segment, high compared with 15-17 ms per segment of other pathways (Shaw and Kristan 1995). S cells connect with L cells, motor neurons activating the longitudinal muscles (see Tab 1), but these connections do not seem to be effective in inducing a motor response (Shaw and Kristan 1999). This means that more interneurons could be involved. The network is probably composed of a fast sub-threshold pathway activated by the S cells chain, followed by a slower but stronger signal. Stimulation of the midbody segments can induce local shortening (Wittenberg and Kristan 1992b).

The two behaviors presented are local reactions of the leech to the stimuli. The locomotion of the leech relies instead on two periodic behaviors: swimming and crawling, the choice among which depends on the level of water with respect to the body volume (Esch et al. 2002). The leech swims by flattening and extending the body, and producing undulatory waves by alternating contractions of dorsal and ventral longitudinal muscles. The rearward progression is caused by the inter-segmental delay of the contractions, and exerts on the water the pressure necessary to move the body. At all the swimming speeds the body wall maintains a waveform equal to approximately one wavelength. The complete cycle varies from 0.4 to 2 s. (Brodfuerher and Thorogood 2001). We will present our estimate of the cycle period in the first section of the Results.

The swimming network over the whole body is composed of four functional classes of neurons: trigger neurons in the brain ganglia, gating interneurons in the body ganglia, a Central Pattern Generator (CPG) composed of body ganglia interneuron, and finally inhibitory and excitatory motor neurons activating longitudinal muscles (see Fig. 3).

Trigger neurons have been identified in the head brain (Brodfuehrer and Friesen 1986): their axons project on the entire length of the connective, with input and output sites in the body ganglia. Brief stimulation of trigger neurons can elicit swimming activity; a stimulation of Tr2 during swimming can stop it (O'Gara and Friesen 1995).

Stimulations delivered to the head induce swimming through activation of the P and N sensory neurons, that are eliciting activity in the trigger neurons. Swimming can be induced also through stimulations delivered to the segments in the back half of the leech. The presence of the head brain is not even necessary for swimming: on the contrary, headless preparations have stronger evoked

swimming activity, whereas a depressing effect on swimming is seen after removal of the tail brain (Brodfuherer et al. 1993).

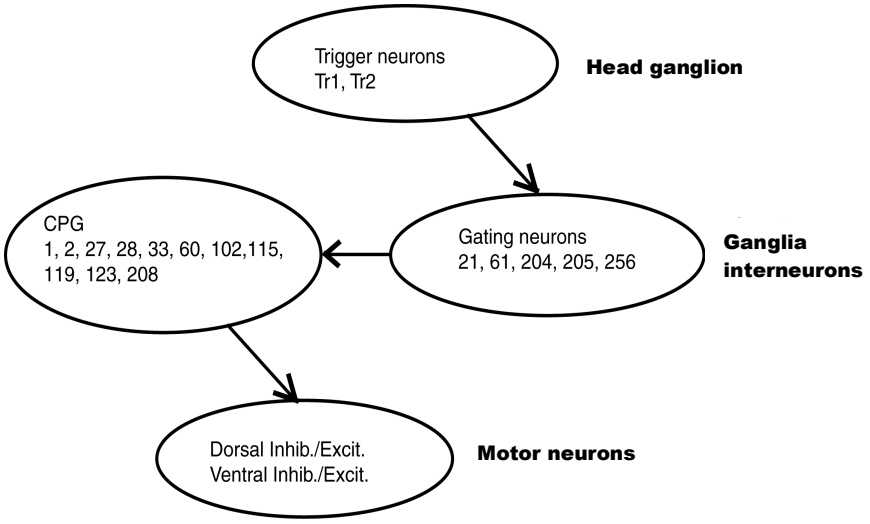

Figure 3 Swimming network *Four functional sets of neurons compose the swimming signal pathway: trigger neurons, gating interneurons and CPG interneurons in the ganglia, and motor neurons activating the muscles*

Gating neurons, especially 204 and 205, have a great importance in determining and modulating the swimming activity (Weeks 1981). 204 and 205 are unpaired excitatory neurons located in body ganglia 9-16 and sending axons in most ganglia of the nerve cord. Depolarization of these cells triggers swimming activity in the nerve cord, through an excitatory drive to some interneurons composing the CPG. Cell 204, in all ganglia, is activated by a triggering input of Tr1, while the only identified target for Tr2 is interneuron 256, that is terminating swimming (Taylor et al. 2003). Serotonin-containing cells 21/61 can initiate swimming, although less robustly than 204 and 205 (Nusbaum et al. 1987). Serotonin and other amines are known to have multiple effects on initiating, modulating and stopping swimming (see Kristan et al. 2005 for a review).

Isolated ganglia from the anterior end to the midpoint of the ventral nerve cord are capable of generating swim-like oscillations, but not individual posterior ganglia. In addition, there is a U-shaped gradient of cycle period. Isolated mid-cord ganglia produce oscillations with a shorter cycle period than individual anterior ganglia or than short chains of posterior ganglia. For all these reasons, the rhythmical activity relies more on the inter-segmental interactions than on the dynamics of the single segmental oscillator.

Inter-segmental connections span for six segments and are asymmetric: neurons project their axons toward the tail or toward the head according to the phase of their firing relatively to the swim period (Hill et al. 2003). Both experiments with isolated nerve cord preparation and models reproduce the

swim oscillation, but with a phase delay between consecutive segments of approximately 8° while in the intact animal this delay is of 17° (a complete cycle with 21 active segments). This is due to the fact that sensory feedbacks from ventral stretch receptor are able to modulate the phase delay (Cang and Friesen 2000).

When the level of the water is not sufficient to allow swimming, the leech crawls. Crawling consists in the following actions: releasing the front sucker, elongating the body, attaching the front sucker, starting body contraction, releasing the rear sucker, completing body contraction, attaching the rear sucker. These actions form a step and the overall duration is of 2-10 seconds. The elongation and contraction phases propagate from the anterior to the posterior end of the animal. In the first section of the Results we will present our estimates on both the duration of the single step and of the crawling episode. The crawling period is usually more irregular than swimming period (Cacciatore et al. 2000).

Elongation is produced by the contraction of the circular muscles, and contraction by the co-contraction of all longitudinal muscles, resulting in a shortening of the segment. The corresponding MNs activity is composed of alternating bursting in the MNs projecting into the two different kinds of muscles (Eisenhart et al. 2000). The burst duration and the overall period are much longer in isolated nerve cord recordings than in the semi-intact preparations, and than what would be expected from behavioral data. This means that sensory feedbacks are modulating the activity of the CPG that is underlying the movement.

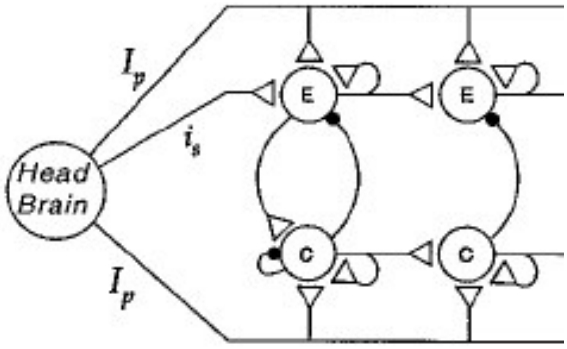

Figure 5 General model of neuronal network underlying crawling. *Reproduced from Cacciatore et al. (2000). E = Elongation and C = contraction units, i_s = serial and I_P = parallel inputs. Serial inputs from the brain trigger the elongation/contraction oscillation in the segments that propagate downward to the tail. Parallel inputs set the inter-segmental delay.*

The basic model developed for the mechanisms originating crawling consists in a chain of elongation units (one for each segment) and a chain of contracting units (one for each segment).
A trigger signal from the brain activates the first elongation unit. This activates the contraction unit of the same segment and the elongation unit of the following segment. The contraction unit stops the activity of the elongation unit, and triggers the contraction unit of the following segment, which activates and does the same. Self excitatory feedbacks stabilize the firing. The modulation of the firing rate of the trigger influences the duration of the steps, but not enough to reproduce behavioral data, so probably the duration is determined by a parallel input acting on each element of the chain. The identification of the elements of the units has still to come.
Once that single behaviors have been identified, it is interesting to address the problem of the transitions between behaviors. We will consider these transitions as decision making processes, where the possible choices are the behaviors. In the second section of the Results we will present a model describing the structure of decision making in the intact leech, based on the complete classification of the possible spontaneous behaviors that will be described in the first section.
The presence of stimuli bias the decision making process. Feeding, that we are not going to describe here, is dominant in the behavioral hierarchy (Misell et al. 1998), and stimuli to the anterior end of the leech cause whole body shortening to substitute ongoing behavior (Shawn and Kristan 1995). Depolarization of the neuron R3b1 in the head brain can induce either swimming or crawling (Esch et al. 2002), according to the sensory feedback informing the leech about the level of the surrounding water. R3b1 is also able to induce rarely a hybrid swimming/crawling behavior, during which the leech elongates and oscillates at the same time. This finding, together with the presence of interactions between the shortening circuit and both gating and trigger neurons of the swimming circuit, suggest that the process of decision is distributed instead of related to the switching of single neurons at a higher hierarchical level.
The recent introduction of voltage sensitive dyes to monitor the activity of the ganglion of the leech, combined with Principal Component Analysis (PCA) to deal with the large amount of data collected, was a big step forward in the analysis of the overlapping of the CPGs related to different behaviors, and of the process of decision making (Briggman et al. 2006).
In Briggman and Kristan (2005) the activity of 80% of the neurons in the ganglion was monitored during both swimming and crawling. It was found that the overlap in the set of the neurons oscillating during the two behaviors is very large: 93% of the neurons oscillating during swimming do the same during crawling.
In a previous paper, the ganglion was monitored while performing the decision between swimming and crawling, after the delivery of a stimulus able to lead to both behaviors (Brigmann et al. 2005).

The activity of the system was represented as a point in a phase space having a number of dimensions equal to the number of the identified neurons, i.e. approximately 140. Thanks to PCA, three linear combinations of neurons activity were found to account for 70% of the variance of the data set, allowing a 3D insightful representation of the dynamics of the neuronal network. Monitoring in time the activity of the ganglion results in a trajectory in the three-dimensional phase space, with different paths associated to swimming and crawling. In this way it was possible to determine the time necessary for the leech to choose between the two behaviors as the time of significant discrepancy between the two trajectories associated to the behaviors, and to determine the set of neuron able to predict the outcome of the decision measuring the direction of this discrepancy. Inside this set, neuron 208 was able to bias significantly but not exclusively the decision, if hyperpolarized or depolarized during a stimulus, respectively toward swimming or crawling. This suggests also that the border between CPG and decision network could be more blurred than previously believed. The authors argue that the variability in the efficacy of trigger neurons could depend on the internal state of the ganglion previous to the delivery of the stimuli is discussed, as previously done by Brodfuehrer et al. (1993). In the last two sections of the Results we will try to give a description of the spontaneous activity of the ganglion, which might represent this internal state.

2 Spontaneous activity

Neuronal networks are not passive mechanisms waiting for something to happen and then reacting to it. Neuronal networks display intense, and usually irregular, activity even in the absence of stimuli, or in the more realistic case of the absence of any significant single stimulus determining their dynamics. In the history of neuroscience, researchers have first unveiled the ways the nervous system reacts to external stimuli through simple reflex mechanisms, then how central pattern generators, once triggered, are able to self-sustain a periodic activity (Marder 2001). Now the problem of dynamics and functional role of irregular spontaneous activity must be addressed.

In this section I will review some papers demonstrating that the spontaneous activity in neuronal networks is often as strong as the evoked activity, and moreover that it is not homogenous noise but is structured. Then I will present studies regarding the main functional role actually attributed to the spontaneous activity, which is to contribute to determine the development of the nervous system. Finally I will describe the known effects of spontaneous activity on the computational properties of the adult nervous system, and some theoretical models proposed to understand the spontaneous activity dynamics.

To explain the large variability of the response of many neuronal networks *in vivo* to the delivery of a repeated stimulus (Stein et al. 2005), the standard approach has been to assume that the response is the sum of a reliable response signal and uncorrelated background noise. The signal is then recovered by averaging over many repeated trials. This reflects the idea that the signal of the single neuron is intrinsically noisy, but since this noise is random, the brain is able to obtain reliable responses using population codes. The validity of this approach was questioned in a seminal paper (Arieli et al. 1996) describing the spontaneous and evoked activity in the cat visual cortex, recorded simultaneously with dyes and electrodes. They found that often the spontaneous activity of the different neurons was synchronized, even in the absence of common inputs. As a consequence, the spontaneous activity displayed coherent structures, larger than the stimulus driven activity: “the effect of the stimulus might be likened to the additional ripples caused by tossing a stone into a wavy sea”. Since the noise was not random, the averaging procedure described above was not correct. The correct procedure to estimate in a first approximation the stimulus driven activity was to subtract from the total response the initial pre-stimulus activity. The resulting patterns were very similar across trials, meaning that the variability of the response was indeed due to the ongoing processes.

A similar analysis was performed at the level of intracellular recordings in Azouz and Gray (1999). The membrane potential of neurons in the visual cortex was recorded before and after the presentation of a visual stimulus. The response magnitude was found to be linearly correlated with the starting potential due to the spontaneous activity. The spike count was correlated with the intensity of the high frequency fluctuations in the potential before the application of the stimuli. The spontaneous activity was found to have a structure both in time -as shown by means of autocorrelation function- and in space, since non neighboring neurons were synchronized.

Many interesting studies on these topics have been carried out in the ferret visual cortex. In many experiments performed in this preparation, the spontaneous activity was displaying long range correlation both in time and space, reflecting the presence of memory and organization. Interestingly, the correlation was irregular: neurons were not firing exactly synchronously and network bursts were not having a periodic behavior (Chiu and Weliki 2001). The connectivity organization of neurons was found not to account completely for the observed correlation: the activity is somehow self-organizing (Chiu and Weliki 2002). The effect of this correlation on the response to visual stimuli was studied recording the activity of the same set of neurons when the animals were or in the dark, or exposed to random images, or to movies with natural scenes. The result was that correlation in space and time of the spontaneous activity was very similar in the three conditions even if the correlations in the images were completely different. This means that the correlation in the activity induced by the inputs was small compared to the one present in the ongoing activity (Fiser et al. 2004). Both absolute values in the correlations and sensitivity to visual inputs increased significantly during the development of the animal.

The important functional role of spontaneous activity in development has been proven in a variety of preparations (see O'Donovan 1999 for a review, although a bit outdated). During development, the spontaneous activity is intense and in the form of long-lasting bursts alternated to periods of quiescent activity, due to the hyper excitable nature of the networks in this early stage in which chloride mediated neurotransmission is excitatory (Ben Ari et al. 1989).

In Jones and Jones (2000), the spontaneous activity in the chicken embryo was found to be highly irregular and at the same time displaying different characteristics in different neurons, according to their future functional role (in this case, belonging to the auditory system or not). The hypothesis is that early connections and morphological properties cause synchronized bursts in neurons belonging to the same system, and that then these bursts work as a signal leading to the correct development. In the ferret retina, before the onset of vision, the information about the connections to be made has been found to be retained in the spontaneous activity (Butts and Rokhsar 2001). The developmental mechanism is sensitive to activity in the timescales of several hundreds of ms, and

the unit of information seems consequently to be the burst (with an amount of information proportional to the size) rather than the single spike. Focusing on the neurotransmitters involved, rather than on information, the role of spontaneous activity and particularly of long-lasting irregular bursts has been proven also in the neonatal rat hippocampus *in vivo* (Leinekugel et al. 2002). In dissociated cultures from rat hippocampus, the effect of spontaneous activity in morphogenesis was mediated by long bursts modulating the intracellular calcium level, known to have a role in neurite outgrowth (van Pelt et al. 2004). The activity was composed also in this case of long-lasting irregular bursts, even if regularities were found on very long time scales (hours and days). In the developing spinal cord of the chicken embryo, the spontaneous activity modulates the efficacy of AMPA and GABA synapses (Gonzales-Islas and Wenner 2006). Spontaneous activity in development has then a key role in setting the balance between inhibition and excitation that is present in the adult neuronal networks (Haider et al. 2006). The common conclusion of all these studies is that during development there are feedback mechanisms between growth and efficacy of neuronal connections and spontaneous activity. These feedbacks lead the neuronal networks to have their final structure; spontaneous activity and functional architecture are therefore strictly connected.

More unclear is the functional role of the ongoing activity in the adult animal. The different studies on how neuronal networks compute in the presence of significant background activity have been recently reviewed in Destexhe and Contreras (2006). The importance of background activity can be understood by looking at the transition between sleep and awake state. In both situations there is spontaneous bursting, but in the first bursting is characterized by all-or-none behavior: long intense bursts periodically alternate with long, hyperpolarized quiet intervals. In the awake brain bursting activity is far more irregular, and in-between bursts the membrane potential of the neurons always remains close to the firing threshold. The responsiveness of neurons is affected by this difference: computation is improved in the awake state (and this is far from being surprising) and this improvement is obtained thanks to the strong and irregular background activity (and this is a bit surprising, in my opinion). This reminds the phenomenon of stochastic resonance (Wiesenfeld and Moss 1995): in nonlinear networks the signal-to-noise ratio can reach the maximum level for nonzero values of the noise.

In a variety of studies (reviewed in Destexhe et al. 2003), Destexhe and collaborators injected neurons *in vitro* with currents simulating the synaptic bombardment of the background activity present in *in vivo* neuronal networks. Three are the main effects of ongoing activity on the computational properties of single neurons. The first is a shift in neuron responsiveness. For isolated neurons the responsiveness is a step function: the neuron is never responding if the stimulus

is under a given threshold and always if this threshold is passed. In the presence of ongoing network dynamics the responsiveness becomes a probabilistic function: very low stimuli have a small but nonzero probability to trigger a response (Ho and Destexhe 2000). This allows the network to propagate faithfully the received signals, while avoiding the onset of disrupting oscillatory activity. Second, the efficacy of synaptic inputs in initiating a spike does not depend strictly on the location of the input in the dendrite (Rudolph and Destexhe 2003a). Third, the presence of strong and irregular background activity neurons increases the sensitivity to high frequency inputs (Rudolph and Destexhe 2003b). All this advantages have a drawback: that they originate probabilistic and not deterministic response. This should be compensated for by populations of neurons processing information in parallel (Shadlen and Newsome 1998).

Studies on the computation dynamics at the network level, describing the way the irregular activity is originated and not only its consequences, still have not reached such clear cut results. Recording the activity is difficult at a network level because multi-electrode results are under sampling the population of neurons, while with optical recordings and local field potentials the risk is to average out neuronal specificity. Some preliminary results have been obtained in network models. In van Vreeswijk and Sompolinski (1996), a model including strong excitatory and inhibitory synapses sparsely connected displays spontaneous chaotic dynamics. Nonetheless the network response to stimuli is linear, and more accurate in time than that of the single unit. In Vogels and Abbott (2005) a sparse, connected network of spiking model neurons generates chaotic patterns of activity. These patterns were found to account for the noise necessary to propagate fluctuations in firing rates across feedforward layers of the network. However, the synaptic strengths required for these models to work are not matching experimental results.

A model closer to known functional connections is the one proposed in Cai et al. (2005) to describe spontaneous activity in the visual cortex. The authors implemented in the model architectural and synaptic data regarding the organization of neurons in V1 cortex, such as the presence of orientation columns and slow decaying NMDA receptors. By varying the parameters, the model displays rhythmic and homogeneous dynamics, but is also able to recreate the highly fluctuating bursting activity seen in *in vivo* networks.

Another set of interesting works is the one by Segev, Ben-Jacobi and collaborators, springing from the multi-unit recordings of spontaneous activity in dissociated cultures described in Segev et al. (2001). The networks exhibited “synchronized bursting events” characterized by long-term correlation, manifested by power law decay of the power spectrum density. Time sequences of spikes and bursts were both well fitted by Levy distributions with power law tails. The authors state that these phenomena could originate by self regulation in the activity, executed via neuronal

internal autonomous means (Hulata et al. 2004). In following papers they propose a model of self-organization accounting for these data based on three characteristics: a) the network is not homogeneous, i.e. some neurons display fatigue during the bursts while others display facilitation (Persi et al. 2004) b) the balance of inhibition and excitation is self regulated c) there is an internal source of noisy activity that they suppose could be originated by the glia cells (Volman et al. 2003).

It is possible to find some common points in the different model proposed, but a general solution of the problem is still far. In the end it could also be that many networks display irregular bursting activity because it has some computational advantages, but that different networks reach this state trough different mechanisms.

Regarding the next steps to be taken to understand spontaneous activity, we agree with Destexhe and Contreras (2006) when they say "explicitly considering the state of the network and its effect on computations or responsiveness to external inputs (...) one may find inspiration from physics, in particular from studies of how different dynamic states of matter provide different properties with respect to interactions with the environment." In the next section we will review some tools of statistical mechanics used in neuroscience, some of which might lead to a better understanding of the spontaneous activity of neuronal networks.

3 Statistical mechanics tools for neuroscience

"Many systems in nature are far too complex to analyse directly. (...) Despite this, such systems often show simple, striking behavior. Statistical mechanics explains the simple behavior of complex systems." (Sethna 2006)

A key feature of biological systems is their complexity. Biological systems are composed of a high number of elements at any level of analysis (many molecular structures in the membrane of a neuron, many neurons in any functional subset of the nervous system), and these elements are usually strongly connected. Nevertheless, biological systems show striking simple behaviors such as robustness (Barkai and Leibler 1997; Levin 2006).

Whether the field is called *systems biology* (Kitano 2002a) or *computational biology* (Kitano 2002b), there is a widespread agreement over the need of a closer interaction between the subfields of mathematics dealing with the analysis of systems and biology, interaction that can result into a mutual enrichment (Cohen 2004). During both information processing (Averbek et al. 2006) and sensory-motor integration (Grillner 2003), the nervous system works as a large and complex network reliably performing accurate behavior, so it is an ideal subject for this interaction.

Even the use of simple mathematical tools from statistics can lead to interesting insights.

In the first section of the Results we will find the complete set of the leech movement patterns in the absence of stimuli. Once that the set of behavioral states BS={α, β, ... } is defined, it is possible to describe the leech behavior as a chain [B(1)➔ B(2) ➔ .... ➔ B(n)] where each B(i) corresponds to an element of BS and each step B(i)➔ B(j) to the decision of the leech to switch from behavior B(i) to behavior B(j). Since it is impossible to determine what the leech will do next, this is a random (i.e. non-deterministic) process. A random process in which the probability distribution of the future state is determined only by the present one is called Markov process (Papoulis 1984). In the second section of the Results section we will show that decision making in the leech is a Markov process. This kind of processes can have many interesting properties: a Markov process is ergodic if any state can be reached from any other state in a finite number of steps, and balanced if there is no preferred direction in the transitions. If both properties stand the process is guaranteed to converge to a an equilibrium probability distribution (Sethna 2006), in such a way that the fraction of time spent in every behavior is stable, which is the case of the leech. Furthermore, Markov Decision Process are widely used in the study of optimal decisions, mostly in machine programming: if a reward function is implemented for every decision it is then possible to determine optimal behaviors and even to have an active process of reinforcement learning (Sutton and Barto 1998). Markov

processes have already been used in neurobiology to model the dynamics of synaptic gating (Legendre 1998; Diba 2004).

In the third section of the Results we will analyse the spontaneous activity of leech ganglia and hippocampal rat dissociated cultures, and we will see how, when considering large networks, the spontaneous firing statistics follows a Poisson model for small bin sizes but not when the size exceeds 500 ms. A similar result was described in Rieke et al. (1997) for single neurons. We will go further, finding a model that is correctly describing the activity at long time scales: the firing statistics in this case follows a lognormal distribution (Crow and Shimitzu 1987; Limpert et al. 2001). Probability distributions fitting the data are useful mainly because we know what kind of processes originates them, and we can hypothesize that the same dynamics originates the data. The Poisson model working for small bins tells us that on these time scale spikes from different neurons can be considered independent, while the presence of a lognormal distribution for larger bins means that at these time scales a) the correlations cannot be neglected and b) the global activity can be seen as multiplicative noise (Mikhailov and Calenbhur 2002), resulting from the amplification of the fluctuations of the single neurons. There is also another reason why the transition from the Poisson model to the lognormal model is so important. There are just three classes of stable probability distribution functions (PDF): Gaussian, Cauchy and Levy distributions, the last one having an asymptotic power law behavior (Sornette 2004). Every PDF that for large values is decaying faster than $1/|x|^3$, under a sufficiently high number of convolutions converges to a Gaussian distribution. If the distribution is decaying slower than that, it converges to a Levy distribution. This allows us to distinguish two broad classes of distributions: short tailed, converging to Gaussian ("mild distributions") and long tailed, converging to Levy ("wild distributions"). Classical examples are the height and the wealth: the probability of finding someone two times taller than you is zero, whereas the probability of finding someone two (or even four) times wealthier than you is definitely non-zero. Considering the system as one object, mild distributions are generated by negative feedback dynamics (there is an optimal size for human beings and large deviations from this size reduce chances of survival), whereas wild distributions are generated by positive feedback dynamics (the more money you have, the more money you are going to make; the less you have, the less chances to make it). Looking at the interaction of the system elements, mild distributions are generated by weakly correlated or uncorrelated systems and wild ones by strongly correlated systems – your height does not affect other people's height, your money interacts with other people's money. Long tailed distributions such as power laws have several interesting properties: for instance, the largest events of the distribution accounts for a significant fraction of the total, so tails are not as negligible as for Gaussian distributions.

It has been found that in neurobiology power laws correctly describe phenomena in which long range and/or strong correlations are involved. The time course of firing adaptation processes is better described by power laws rather than by an exponential decay (Drew and Abbott 2006), because of the multiple timescales involved in the process (Fairhall et al. 2001). Fluctuations in working memory circuits display power laws similar to a random walk, reflecting the presence of long-term correlations among the fluctuations of the different neurons (Miller and Wang 2006). Coming back to the spontaneous activity, finding that the distribution of the firing rate is long tailed suggests that the neurons are strongly interacting, i.e. that the correlation among the elements of the network is high.

Determining the level of the interaction among neurons in a neuronal network is a key step to understand its behavior and this can be easily done by means of the correlation function. Correlations among pre-synaptic neurons can be detected at a single neuron level, since they cause an increase in the conductance and in the amplitude of membrane potential fluctuations (Rudolph and Destexhe 2004). Spike-count correlations among different neurons in a network can explain the onset of periodic collective oscillations (Brecht et al. 1999, Galan et al. 2006) and how the architecture of neuronal networks is determined in such a way to optimize information processing (Krahe et al. 2002, Schneidman et al. 2006, Sclens et al. 2006).

Once that the correlation structure of a system is known, it is possible to use more advanced tools from statistical mechanics to study it, such as phase models. As a system undergoes a phase transition not only its properties are changing abruptly, but the symmetry of the system changes, and it is possible to describe this change by means of an order parameter. The value of the correlation among the elements can often be such a parameter, for instance when the system goes from an uncorrelated to a correlated state like in the transition from gas to liquid. We will see in the third section of the Results how the decrease of inhibition or excitation using receptors blockers can be described as the onset of two different phases of the neuronal network activity. Previous works (Shadlen and Newsome 1998, Haider et al. 2006) demonstrated that a fine balance between excitation and inhibition is necessary to optimize the computational properties of the neurons.

Critical states theory could explain the large variability of the spontaneous activity and many others of its properties, like the stability of the fine tuning between inhibition and excitation.

Similar dynamics near phase transitions are found among very different systems: this characteristic is referred to as universality of phase transitions. Moreover, the similarity consists usually in the presence of local scale invariance in space and time. Figure 6 represents the phase transition dynamics occurring in a system when the correlation among its elements is varied.

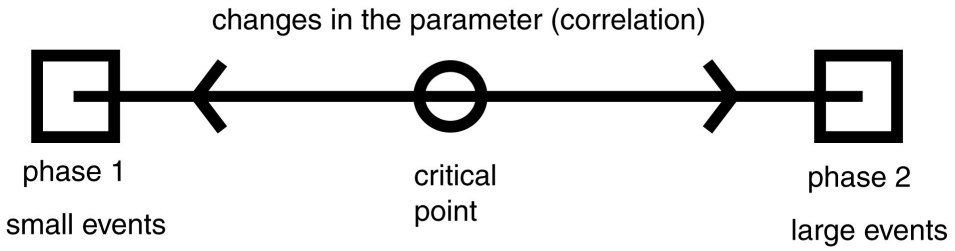

Figure 6 Critical point *Criticality is present just for a given value of correlation. Any decrease leads to a stable phase characterized by short range correlations and small events, and any increase to a highly synchronized stable phase displaying large events.*

The circle in the center is an unstable equilibrium point: if correlation is slightly decreased or increased the system will flow to a stable state (a phase) characterized by small or large events respectively. If correlation has exactly the critical value, events of all size will be present.

In Figure 7 we add to the horizontal axes representing changes in correlation a vertical axes representing changes in the analysis scale. The process of increasing the scale of analysis of a system is called coarse graining. This process will lead to diverging behaviors if we start from one of the two phases, but to a fixed point (the red circle in the figure) if we start from the critical point (the black circle) (Sethna 2006). The red circle is scale invariant because, being a fixed point for the coarse-graining process, if we change the scale of analysis again, we will find always the same dynamics. This means that for scales larger than a given threshold, the system displays scale invariance. Many properties of a scale invariant system will have a power law distribution since power laws are inherently scale invariant: if $f(x) = x^a$, and we rescale the variable x for a B factor, we will have $f(Bx) = B^a x^a \propto f(x)$: the function will not change its shape. Furthermore, different systems having different laws at a microscopic scale (that are ignored because of the coarse graining process) will reach the same critical point, thus displaying the same scale-invariant behavior.

Figures 6 and 7 explain the three main characteristics of critical states a) presence of events of all sizes b) scale invariance c) similarity between different systems. All of these are key properties of spontaneous activity of neuronal networks as we will show in the third section of the Results.

Critical points are typically unstable, but in some systems negative feedbacks make the critical state stable, while preserving large fluctuations and all the characteristics we described. We will refer to this phenomenon as Self Organized Criticality (SOC).

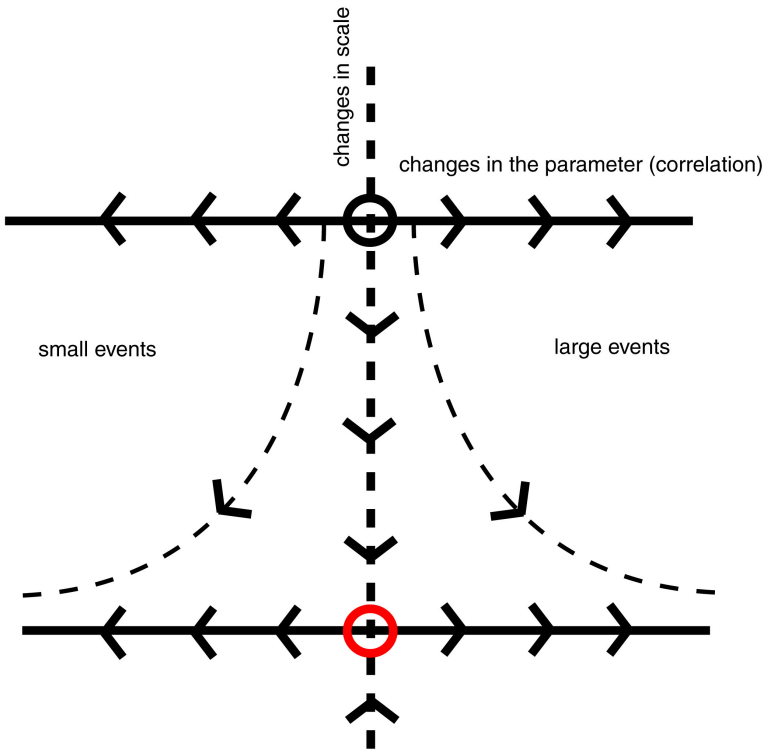

Figure 7 Criticality and scale invariance. *Same as Fig. 6 but with a vertical degree of freedom representing the scale of analysis. Increasing the scale of analysis lead to divergent behaviors for systems outside the critical point. Systems at criticality instead eventually reach a stable point (the red circle) so that the dynamics is not affected by other changes in the scale (scale invariance).*

3.a Self Organized Criticality and neuronal activity

SOC describes the activity of systems composed by interacting on/off elements, that can be activated by an external drive or by mutual excitation, and having the following properties

1. Elements have highly non linear behavior: an element is activated if the interaction with the neighbours exceeds a given threshold.
2. The external driving rate is slow compared to the interaction timescale (interaction-dominated activity).
3. Energy is conserved: the energy put in the system by the external drive leaves eventually the system through its boundaries.

SOC theory states that, under a broad range of conditions, these systems have the following interconnected properties

a) The system dynamics has a critical state as stable attractor
b) In the critical state every active element activates on average one neighbour

c) The activity has a 1/f power spectrum
d) Activation in the system spreads in "avalanches" having size and duration distribution described by power laws

For reviews see Jensen (1998) and Sornette (2004).
We have seen that usually critical states are the unstable equilibrium point in between two stable phases, but unstable systems are rare to be seen in natural conditions. The point a) states that the critical dynamics described by SOC theory can actually represent robust natural phenomena such as biological systems. In fact, many properties of SOC systems are common in nature: property b) ensure that information transmission is optimized (Kinouchi and Copelli 2006), property c) indicates that there is correlation on multiple timescales (Jensen 1998), and we have seen in the previous section that many systems display power law behavior.
A drastic simplification could summarize SOC theory in the statement

Network with dynamics (1,2,3) ➔ Network activity with properties (a,b,c,d)

It must be noticed that the opposite implication is not true. For instance, many other mechanisms can generate an activity having the properties c) and/or d) (Sornette 2004), so before concluding that a system displays SOC the inter-element dynamics has to analysed.
At the moment there is no complete formalism for SOC theory. We will present here the "branching parameter / mean field" approach of Zapperi (Zapperi et al. 1995, Vespignani and Zapperi 1998) since it is the one that we used in the third section of the Results.
Condition 2) is equivalent to say that if t* is the typical timescale of an avalanche of activations and T is the average interval between external activations, then $t^*/T \to 0$ (no external activation during avalanches).
Condition 3) immediately translates into property b): the average number σ of elements that are activated by an active cell must be one.
If the two conditions stands, the probability distribution of the avalanches size P(s) will be

$$P(s) = As^{-3/2} \exp(s/S)$$

that is, a power law distribution with slope –3/2 followed by an exponential decay for sizes bigger than a threshold S, which depends on the number of elements in the network (Eurich et al. 2002).

Similarly the probability distribution of the avalanches duration P(d) will be

$$P(d) = Ad^{-2} \exp(d / D)$$

that is, a power law distribution with slope –2 followed by an exponential decay for durations larger than a threshold D that again depends on the number of elements in the network.

By changing the two parameters t*/T and σ, it is possible to drive the system outside criticality to phases characterized instead than by scale invariance, just by large avalanches (super-critical dynamics) or by small avalanches (sub-critical dynamics). It is possible to drive the system to the sub-critical state by decreasing σ: if we reduce the interactions, the number of elements activated by an active element will become smaller than 1. Long correlations in space and time will be lost and just small and local events will be displayed: P(s) and P(d) will decay faster than in the critical states (Eurich et al. 2002). Increasing on the contrary the efficiency of the interactions drives the system to the super-critical state. Super-critical states, differently than sub-critical ones, can be reached also by changing the other parameter: if the driving rate is increased there is the possibility of external inputs arriving during the avalanches. Both changes keep the system away from the stable resting state. Most of the events will then involve a large fraction of the system: P(s) and P(d) will have a peak corresponding to large avalanches (Vespignani and Zapperi 1998, Eurich et al. 2002).

Two papers described neurons activity as SOC: Linkenkaer-Hansen et al. (2001) and Beggs and Plenz (2003).

In the first paper (Linkenkaer-Hansen et al. 2001) the activities recorded were the spontaneous EEG and MEG of the human brain. On long timescales, between 5 and 1000 seconds, the activity showed 1/f power spectrum. As we said in the previous pages, long-range temporal correlation, 1/f power spectrum is a necessary but not sufficient conditions for the presence of SOC. The authors introduce SOC only in the discussion saying that it is "a general framework of how local interactions create large-scale dynamics, which could account for the long-range temporal correlations and the power-law scaling behavior observed for spontaneous oscillations."

A recent paper by Bedard et al. (2006), however, shows that the 1/f power spectrum of the EEG in the cat is due to the frequency-dependent filter of the brain tissue, since the underlying Local Field Potential (LFP) has a different kind of temporal correlations, demonstrating that the dynamics is not SOC.

In the second paper (Beggs and Plenz 2003), LFPs of the spontaneous activity of cultured slices of rat cortex were recorded on multielectrode arrays. The first finding is that the apparently synchronous activation of the electrodes was in fact a fast propagating activity, as shown by the variability of electrodes crosscorrelation functions. They proceeded then to define "neuronal avalanches" in four steps: a) an "event" (i.e. a population spike) occurs every time the LFP crosses a given threshold; b) the recording time is divided into small frames of a duration varying from 1 to 16 ms, and the number of events occurring in each frame is counted; c) frames during which at least one event occurs are called "active"; the other frames are called "silent"; d) a "neuronal avalanche" is defined as a strip of consecutive active frames preceded and ended by a silent frame. The correspondence with SOC models is straightforward: every frame corresponds to an interaction step, so the duration of an avalanche is defined as the number of frames composing it, and the size as total number of electrodes involved. In this way is possible to test directly SOC theory predictions. Avalanches size followed a power law over between one and two orders of magnitude. with a slope varying with the chosen frame size. When the frame size was chosen in order to correspond to the average interval between two events the slope became exactly –3/2, in agreement with expectations. When different subsets of the electrodes were considered, the avalanche size distribution remained a power law with –3/2 slope, proving that the activity exhibits an appreciable range of scale invariance. The threshold size for exponential cut-off was proportional to the number of electrodes analysed. When inhibition was decreased by application of the GABA-receptor antagonist picrotoxin, the size distribution was bimodal with a peak for large sizes. The branching parameter σ was measured directly as the ratio of descendant electrodes to ancestor electrodes for two consecutive time bins at the beginning of an avalanche. Values found were close to theoretical prediction for SOC states: $\sigma=1.04\pm0.2$ for avalanches starting with one electrode, and $\sigma=0.9\pm0.2$ for avalanches starting with more than one electrode. Finally a numerical simulation of avalanche dynamics in a feedforward network demonstrates that information is optimal if the activity propagates with σ close to the critical value 1. This work suggests that the dynamics underlying spontaneous activity can be described by SOC. The method used to identify avalanches in the electrical activity of the nervous system can be used to check theoretical predictions in other preparations and conditions without relying only on power spectrum analysis. The same procedure was used from the authors in following papers, to study the presence of recurrent patterns in the avalanches and their role in memory (Beggs and Plenz 2004), and to investigate the effects of dopamine in the long range interactions in the rat cortex (Stewart and Plenz 2006).

In the third section of the Results we will use similar models to describe the spontaneous activity in the isolated leech ganglion and in dissociated cultures of rat hippocampal neurons.

It must be stressed that, originating from statistical mechanics, SOC theory deals with global properties of the system, without giving insights on the dynamics of the single elements. If the spontaneous activity of neuronal networks can be described as SOC, however, many phenomena can be explained and interesting predictions can be made.

We have seen in the previous section that the spontaneous activity is characterized by a) large variability of events size, b) long range temporal correlations, and these are distinctive features of critical systems. SOC theory, moreover, predicts a) the precise probability distribution of size and duration of spontaneous activity burst, given by the equations on the top of page 23, b) the power spectral density of the spontaneous activity, that should have a 1/f behavior for sufficiently low frequencies.

During the spontaneous activity inhibitory and excitatory interactions are in a balance: SOC theory proposes that this phenomenon could simply stem from the energy balance of the network, and predicts that the average number of neurons triggered by a firing neuron should be one. The fact that inhibitory and excitatory receptor blockers respectively increase or decrease the bursting activity is well known: SOC theory predicts more accurately the corresponding burst size and duration distributions.

SOC theory predicts also how the neuronal network size should affect the bursting activity, and that an increase in external inputs should have an effect similar to the increase of the interaction among the elements of the network. SOC models could be useful to understand how all of these properties are originated during development and how do they affect computational and functional processes in the intact animals.

We are not claiming that SOC unveils completely spontaneous activity in neuronal networks. A complete description of the spontaneous activity must of course account also for neuronal mechanisms that are not included in SOC models. SOC can be however an interesting piece of such a description, explaining the statistical properties of spontaneous activity at a network level.

Bibliography

Arieli A, Sterkin A, Grinvald A, Aertsen A (1996) Dynamics of ongoing activity: explanation of the large variability in evoked cortical responses Science 273: 1868-1871

Arisi I, Zoccolan D, Torre V (2001) Distributed motor pattern underlying whole-body shortening in the medicinal leech. J Neurophysiol 86:2475-2488

Averbeck BB,. Latham PE, Pouget A (2006) Neural correlations, population coding and computation. Nature Rev. Neurosci. 7:358-366

Azouz R, Gray CM (1999) Cellular mechanism contributing to response variability of cortical neurons *in vivo* J. Neurosci 19:2209-2223

Bagnoli P, Brunelli M,Magni F, Pellegrino M (1975) The neuron of the fast conducting system in hirudo medicinalis: identification and synaptic connections with primary afferent neurons. Arch. Ital. Biol 113:21-43

Bak P, Tang C, Wiesenfeld K (1987) Self-Organized Criticality: an explanation of 1/f noise. Physical Review Letters 59:381-385

Bak P, Tang C, Wiesenfeld K (1988) Self-Organized Criticality. Physical Review A 38:364-374

Barkai N, Leibler S (1997) Robustness in simple biochemical networks. Nature 387: 913-17

Bedard C, Kroger H, Destexhe A (2006) Does the 1/f frequency scaling of brain signals reflect self-organized critical states? 11:118102 1-4

Beggs JM, Plenz D (2003) Neuronal avalanches in neocortical circuits. J Neurosci 23: 11167-11177

Beggs JM, Plenz D (2004) Neuronal avalanches are diverse and precise activity patterns that are stable for many hours in cortical slice cultures. J Neurosci 24: 5216-5229

Ben Ari Y, Cherubini E, Corradetti R, Gaiarsa JL (1989) Giant synaptic potentials in immature rat CA3 hippocampal neurones J Physiol 416:303-325.

Brecht M, Wolf S, Andreas KE (1999) Patterns of synchronization in the superior colliculus of anesthetized cats. J Neurosci. 19: 3567 - 3579

Briggman KL, Abarbanel HDL, Kristan WB (2005) Optical imaging of neuronal populations during decision making Science 307:896-901

Briggman KL, Abarbanel HDL, Kristan WB (2006) Imaging dedicated and multifunctional neural circuits generating distinct behaviors J. Neurosci. 26:10925-10933

Briggman KL, Kristan WB (2006) From crawling to cognition: analysing the dynamical interaction among populations of neurons Curr. Op. Neurob. 16:135-144

Brodfuehrer PD, Friesen WO (1986) Control of leech swimming activity by the cephalic ganglia. J Neurobiol. 17: 697-705

Brodfuehrer PD, Kogelnik AM, Friesen WO, Cohen AH (1993) Effect of the tail ganglion on swimming activity in the leech. Behav Neural Biol. 59: 162-166

Brodfuehrer PD, Thorogood MSE (2001) Identified neurons and leech swimming behavior. Prog. in Neurobiol. 63: 371-381

Burrell BD, Sahley CL (2004) Multiple forms of Long-Term Potentiation and Long-Term-Depression converge on a single interneuron in the leech CNS J Neurosci 24:4011-4019

Butts DA, Rokhsar DS (2001) The information content of spontaneous retinal waves J Neurosci 27:961-973

Cacciatore TW, Rozenshteyn R, Kristan WB (2000) Kinematics and modelling of leech crawling: evidence for an oscillatory behavior produced by propagating waves of excitation J Neurosci 20: 1643-1655

Cai D, Rangan AV, McLaughin DW (2005) Architectural and synaptic mechanisms underlying coherent spontaneous activity in V1 PNAS 102:5868-5873

Cang J, Friesen WO (2000) Sensory modification of leech swimming rhythmic activity of ventral stretch receptors can change inter-segmental phase relationships J Neurosci 20: 7822-7829

Chiu C, Weliki M (2001) Spontaneous activity in developing ferret visual cortex *in vivo* J Neurosci 21:8906-8914

Chiu C, Weliki M (2002) Relationship of correlated spontaneous activity to functional ocular dominance in the developing visual cortex Neuron 35:1123-1134

Cline HT (1986) Evidence for GABA as a neurotransmitter in the leech J Neurosci 6:2848-2856

Cohen JE (2004) Mathematics is biology's next microscope, only better; biology is mathematics' next physics, only better. PLoS Biol 2(12): e439.

Crow EL, Shimitzu K (1987) Lognormal distributions. New York: Marcel Dekker.

Destexhe A, Rudolph M, Parè D (2003) The high-conductance state of neocortical neurons *in vivo* Nat. Rev. Neurosci 4:739-751

Destexhe A, Contreras D (2006) Neuronal computations with stochastic network states. Science 314: 85-90

Diba K, Lester AH, Koch C (2004) Intrinsic noise in cultured hippocampal neurons: experiment and modeling.. J Neurosci. (43):9723–9733

Drew PJ, Abbott LF (2006) Models and properties of power law adaptation in neural systems. J Neurophysiol 96:826-833

Drossel B, Schwabl F (1992) Self organized critical forest-fire model Physical Review E 69:1629-1632

Eisenhart FJ, Cacciatore TW, Kristan WB (2000) A central pattern generator underlies crawling in the medicinal leech J Comp Physiol A 186: 631-643

Esch T, Mesce KA, Kristan WB (2002) Evidence for sequential decision making in the medicinal leech. J Neurosci 22:11045:11054

Eurich CW, Herrman JM, Ernst UA (2002) Finite-size effects of avalanche dynamics Physical Review E 66: 66137-1:15

Fairhall AL, Lewen GD, Bialek W, de Ruyter van Steveninck RR. (2001) Efficiency and ambiguity in an adaptive neural code. Nature 412: 787–792

Fiser J, Chiu C, Weliki M (2004) Small modulation of ongoing cortical dynamics by sensory input during natural vision. Nature 431:573-578

Freeman WJ, Holmes MD, West GA, Vanhatalo S (2006) Fine spatiotemporal structure of phase in human intracranial EEG Clin. Neurophysiol. 117:1228-12243

Friesen WO, Hocker CG (2001) Functional analyses of the leech swim oscillator J Neurophysiol. 86:824-835

Galán RF, Fourcaud-Trocmé N, Ermentrout GB, Urban NN (2006) Correlation-induced synchronization of oscillations in olfactory bulb neurons. J Neurosci. 26: 3646 - 3655

Garcia-Perez E, Zoccolan D, Pinato G, Torre V (2004) Dynamics and reproducibility of a moderately complex sensory-motor response in the medicinal leech J Neurophysiol 92:1783-1795

Gonzales-Islas C, Wenner P (2006) Spontaneous network activity in the embryonic spinal cord regulates AMPAergic and GABAergic synaptic strength Neuron 49:563-575

Grillner S (2003) The motor infrastructure: from ion channels to neuronal networks. Nature Rev. Neurosci. 4: 573-586

Haider B, Duque A, Hasenstaub AR, McCormick DA (2006) Neocortical activity *in vivo* is generated trough a dynamic balance of excitation and inhibition J Neurosci 26:4535-4545

Hill AAV, Masino MA, Calabrese RL (2003) Inter-segmental coordination of rhythmic motor patterns J Neurophysiol 90:531-538.

Ho N, Destexhe A (2000) Synaptic background activity enhances the responsiveness of neocortical pyramidal neurons J Neurophysiol 84: 1488-1496

Hulata E, Baruchi I, Segev R, Shapira Y, Ben-Jacob E (2004) Self-regulated complexity in cultured neuronal networks. Phys. Rev. Lett. 92: 198105

Jensen HJ (1998) Self organized criticality: emergent complex behavior in physical and biological systems Cambridge UK: Cambridge University Press.

Jones TA, Jones SM (2000) Spontaneous activity in the statoacoustic ganglion of the chicken embryo J Neurophysiol 83:1452-1468

Kinouchi O, Copelli M (2006) Physics of psychophysics: dynamic range of excitable networks is optimized at criticality Nature Physics 2:348-351

Kitano H (2002a) Systems biology: a brief overview. Science 295: 1662-1664

Kitano H (2002b) Computational systems biology. Nature 420: 206-210

Krahe R, Kreiman G, Gabbiani F, Koch C, Metzner W (2002) Stimulus encoding and feature extraction by multiple sensory neurons**.** J Neurosci. 22: 2374 - 2382

Kristan WB, Calabrese RL, Friesen OW (2005) Neuronal control of leech behavior Prog. In Neurobiol. 76:279-327

Legendre P (1998) Voltage dependence of the Glycine receptor–channel kinetics in the zebrafish hindbrain. J Neurophys. 82: 2120 - 2129

Leinekugel X, Khazipov R, Cannon R, Hirase H, Ben-Ari Y, Buszaki G (2002) Correlated bursts of activity in the neonatal hippocampus *in vivo*. Science 296: 2049-2052

Levin SA (2006) Fundamental questions in biology. PLoS Biol 4(9): e300

Lewis JE, Kristan WB (1998a) Representation of touch location by a population of leech sensory neurons. J. Neurophysiol. 80: 2584–2592

Lewis JE, Kristan WB (1998b) A neuronal network for computing population vectors in the leech Nature 391: 76-79

Lewis JE, Kristan WB (1998c) Quantitative analysis of a directed behavior in the medicinal leech: implications for organizing motor output. J. Neurosci. 18: 1571–1582

Limpert E, Stahel AW, Abbt M (2001) Log-normal distributions across the sciences: keys and clues. Bioscience 51: 341-352

Linkenkaer-Hansen K, Nikouline VV, Palvas JM, Ilmoniemi RJ (2001) Long range temporal correlations and scaling behavior in human brain oscillations 21:1370-1377

Lockery SR, Kristan WB (1990) Distributed processing of sensory information in the leech. II. Identification of interneurons contributing to the local bending reflex. 10:1816-1829

Segev R, Benveniste M, Shapira Y, Hulata E, Cohen N, Palevski A, Kapon E, Ben-Jacobi E (2001) Long-term behavior of lithographically prepared *in vitro* neuronal networks Phis. Rev. Lett 88:118102

Marder E (2001) Moving rhythms Nature 410:755

Mason B, Kristan WB (1982) Neuronal excitation, inhibition and modulation of leech longitudinal muscles J Comp Physiol 146: 527-536

Mikhailov AS, Calenbuhr V (2002) From cells to societies: models of complex coherent action. Berlin: Springer Verlag.

Miller P, Wang XJ (2006) Power-law neuronal fluctuations in a recurrent network model of parametric working memory**.** J Neurophysiol, 95: 1099 - 1114

Misell LM, Shaw BK, Kristan WB (1998) Behavioral hierarchy in the medicinal leech, *Hirudo medicinalis;* feeding as a dominant behavior. Behav. Brain Res. 90:13-21

Muller KJ, Nicholls JG, Stent GS (1981) Neurobiology of the leech Cold Spring Harbor Laboratory: New York.

Nicholls JG, Baylor DA (1968) Specific modalities and receptive fields of sensory neurons in CNS of the leech. J. Neurophysiol. 31: 740–756.

Nicholls JG, Martin RA, Wallace BG (1992) From Neuron to Brain 3rd edition Sinauer Associates: Sunderland MA

Norris BJ, Calabrese RL (1987) Identification of motor neurons that contain a FMRFamidelike peptide and the effects of FMRFamide on longitudinal muscle in the medicinal leech Hirudo Medicinalis J Comp Neurol 266:95-111

Nusbaum MP, Friesen WO, Kristan WB, Pearce RA (1987) Neural mechanisms generating the leech swimming rhythm: swim-initiator neurons excite the network of swim oscillator neurons. J Comp Physiol A 161: 355-366

O'Donovan (1999) The origin of spontaneous activity in developing networks of the vertebrate nervous system Curr.Opin. Neurobiol. 9: 94-104

O'Gara BA, Friesen WO (1995) Termination of leech swimming activity by a previously identified swim trigger neuron. J Comp Physiol A 177:627-636

Papoulis, A (1984) Brownian movement and markoff processes pp. 515-553 in Probability, random variables and stochastic processes New York: McGraw-Hill.

Persi E, Horn D, Volman V, Segev R, Ben-Jacob E (2004) Modelling of synchronized bursting events: the importance of inhomogeneity. Neural computation 16:2577-2595

Peterson EL (1983) Visual processing in the leech central nervous system Nature 303: 240-242

Rieke F, Warland D, van Steveninck RdR, Bialek W (1997) Spikes. Exploring the neural code. Cambdrige MA: MIT Press.

Rudolph M, Destexhe A (2003a) A fast conducting, stochastic integrative model for neocortical neurons *in vivo* J Neurosci 23:2466-2476

Rudolph M, Destexhe A (2003b) Gain modulation and frequency locking under conductance noise Neurocomputing 52:907-912

Rudolph M, Destexhe A (2004) Inferring network activity from synaptic noise. J Physiol – Paris 98: 452-466

Schneidman E, Berry JM, Segev R, BialekW (2006) Weak pairwise correlations imply strongly correlated network states in a neural population. Nature 440:1007-1012

Sethna JP (2006) Statistical mechanics: Entropy, order parameters, and complexity. Oxford: Oxford University Press.

Shadlen MN, Newsome TW (1998) The variable discharge of cortical neurons: implications for connectivity, computation, and information coding. J Neurosci 10: 3870-3896

Shaw BK, Kristan WB (1995) The whole-body shortening reflex of the medicinal leech: motor pattern, sensory basis, and interneuronal pathways. J Comp Physiol A 177:667-6681

Shaw BK, Kristan WB (1999) Relative roles of the S cell network and parallel interneuronal pathways in the whole-body shortening reflex of the medicinal leech. 82:1114-1123

Shlens J, Field GD, Gauthier JL,Grivich MI, Petrusca D, Sher A, Litke MA, Chichilnisky EJ (2006) The structure of multi-neuron firing patterns in primate retina. J Neurosci 32:8254–8266

Sornette D (2004) Critical phenomena in natural sciences. Berlin: Springer Verlag.

Stein RB, Gossen ER, Jones KE (2005) Neuronal variability: noise or part of the signal? Nat. Rev. Neur. 6:389-397

Stewart CV, Plenz D (2006) Inverted-U profile of dopamine-NMDA-mediated spontaneous avalanche recurrence in superficial layers of rat prefrontal cortex. J Neurosci 31:8148-8159

Sutton RS, Barto GA (1998) Reinforcement learning: an introduction. Cambdrige MA: MIT Press.

Szczupak L, Kristan WB (1995) Widespread mechanosensory activation of the serotonergic system of the medicinal leech J Neurophyisiol 74:2614-2624

Taylor AL, Cottrell GW, Kleinfeld D, Kristan WB (2003) Imaging reveals synaptic targets of a swim-terminating neuron in the leech CNS. J Neurosci 23:11402-11410

Thomson EE, Kristan WB (2006) Encoding and decoding touch location in the leech CNS J Neurosci 8009-8016

van Pelt J, Wolters PS, Corner AM, Rutten WLC, Ramakers GJA (2004) Long-term characterization of firing dynamics of spontaneous bursts in cultured neural networks. IEEE Trans. Biom. Eng. 51:2051-2062

Vespignani A, Zapperi S (1998) How self-organized criticality works: a unified mean field picture Physical Review E 57: 6345-6362

Vogels TP, Abbott LF (2005) Signal propagation and logic gating in networks of integrate-and-fire neurons. J Neurosci 25:10786-10795

Volman V, Baruchi I, Persi E, Ben-Jacob E (2003) Generative modelling of regulated dynamical behavior in cultured neuronal networks Physica A 335:249-278

Weeks JC (1981) Neuronal basis of leech swimming: separation of swim initiation, pattern generation, and inter-segmental coordination by selective lesions. J Neurophysiol 45:698-723

Wiesenfeld K, Moss F (1995) Stochastic resonance and the benefits of noise: from ice ages to SQUIDs. Nature 373:33-36.

Wittemberg G, Kristan WB (1992a) Analysis and modelling of the multisegmental coordination of shortening behavior in the medicinal leech. II. Role of identified interneurons J Neurophysiol 68:1693-1707

Wittemberg G, Kristan WB (1992b) Analysis and modelling of the multisegmental coordination of shortening behavior in the medicinal leech. I: Motor output pattern J Neurophysiol 68:1683-1692

Worrell GA, Cranstoun SD, Echauz J, Litt B (2002) Evidence for self-organized criticality in human epileptic hippocampus Neuroreport 13:2017-2021

Zapperi S, Lauritsen KB, Stanley HE (1995) Self organized branching processes: mean field theory for avalanches Phys. Rev. Lett.

Zhang X, Wilson RJ, Li Y, Kleinhaus AL (2000) Chemical and thermal stimuli have short-lived effects on the retzius cell in the medicinal leech. J Neurobiol 43: 304-311

Zoccolan D, Giachetti A, Torre V (2001) The use of optical flow to characterize muscle contraction. J Neurosci Methods 110:65-80

Zoccolan D, Pinato G, Torre V (2002) Highly variable spike trains underlie reproducible sensorimotor responses in the medicinal leech. J Neurosci 22:10790-10800

Zoccolan D, Torre V (2002) Using optical flow to characterize sensory-motor interactions in a segment of the medicinal leech. J Neurosci. 22:2283-2298

Results

1

Quantitative characterization and classification of leech behavior.

Alberto Mazzoni, Elizabeth Garcia-Perez, Davide Zoccolan, Sergio Graziosi and Vincent Torre

J Neurophysiol 93:580-593

2

Statistics of decision making in the leech

Elizabeth Garcia-Perez, Alberto Mazzoni, Davide Zoccolan,
Hugh Robinson and Vincent Torre

J Neurosci 25:2597-2608.

Conclusions and perspectives

The two interrelated subjects of my PhD thesis were the spontaneous behavior of the leech and the spontaneous activity of its nervous system.

The first achievement was to develop a passive markers experimental procedure to track the displacements of the leech, and a classification algorithm based on time series analysis to identify and study movement patterns. By using these techniques we gave, to our knowledge, the first complete description of the kinematics of exploratory movements in the leech.

The complete list of the possible leech behaviors, in the absence of direct stimuli, was found. Behavior durations followed an exponential distribution function and transition rates between two behaviors were independent from previous actions. From these findings we obtained a Markovian model for decision making in the leech.

My research moved then to study the spontaneous activity in the leech nervous system.

We compared the spontaneous activity in the isolated leech ganglion and in dissociated cultures of rat hippocampal neurons, in order to analyse the differences between a structured and an unstructured neuronal network. These differences were smaller than expected. Single neurons had tonic firing dynamics, but they could switch to burst firing according to the activity of the network. Both neuronal networks displayed long-range temporal correlations: bursts size and duration were distributed according to power laws. Effects of NMDA and GABA receptors blockage on the bursting dynamics were similar in the two networks. We proposed a statistical description of spontaneous activity based on the theory of self-organized criticality, demonstrating that it can account for many of our results.

The spontaneous bursting activity was then studied in a greater detail in the leech. When the ganglion was not isolated, but connected to the rest of the nervous system, correlation among neurons increased, and the spontaneous activity was not characterized anymore by bursts of all sizes, but was instead dominated by highly synchronized events. By recording simultaneously the electrical activity in the ganglia and the leech behavior, we found that this highly synchronized bursts, triggered probably by inputs from both head and tail brain, caused the onset of movement in the leech.

The results presented in this thesis open the possibility for many future lines of research.

By using the same analysis procedure we applied to spontaneous movements, it would be possible to study the way stimuli affect the behavior. We are performing preliminary experiments on the effects of serotonin, which is known to interact with neuronal networks responsible for swimming,

on the moving intact leech. A first question to be answered is whether the properties of the swimming behavior, such as speed of movement, oscillation frequency and inter-segmental delay, are different in the presence of serotonin. Previous studies demonstrated that serotonin induces the leech to spend more time swimming, but it could be interesting to see if this is happening because the average duration of swimming episodes is increased, and/or because the transition rates from other behaviors toward swimming are higher.

More electrophysiological studies are going to be necessary to find the neuronal networks underlying the process of decision making in the leech. Transitions between behaviors are likely to be due to the activity of trigger neurons in the leech brain. Semi-intact experiments, with the head brain exposed and the body moving, could help to build a bridge between our behavioral results and the neurons activity. Statistical properties of the spontaneous firing of trigger neurons should affect the probability of transitions between behaviors.

In the second part of the thesis we have described many properties of the spontaneous activity in the leech ganglion. From a theoretical point of view, having found dynamics reminding of SOC in a hierarchical network was quite surprising and raised many questions. We are currently working on a simulated network, implementing suggestions from SOC theory and from experimental results on the functional architecture of the leech ganglion, trying to reproduce the results we have found on spontaneous activity. Further studies on the interaction among neurons in the absence of stimuli are required. An important improvement could be the use of voltage sensitive dyes, since this would increase the number of monitored neurons, and particularly would allow to record from the interneurons. Interneurons were not directly visible in our extracellular recordings, but they certainly play a key role in the spontaneous activity. A combination of electrophysiological recordings and voltage sensitive dyes, such as the one performed by Briggman and Kristan, could be used to shed light on the interplay, in activating CPG and starting movements, between trigger stimuli from the head, and the ongoing dynamics in the ganglia.

A limitation in our studies was the distance between the mid-body ganglion from which we recorded the electrical activity and the tail from which we recorded the movements. We are currently doing experiments with a semi-intact preparation similar to the one presented in the last two sections of the results, but with a piece of skin left attached to the inspected mid-body ganglion. In this way it will be possible to monitor the correlation between spontaneous bursts and movements more directly.

"*Non si tratta di affrancare la verita' da ogni sistema di potere – sarebbe una chimera dal momento che la verita' e' essa stessa potere – ma di staccare il potere della verita' dalle forme di egemonia (sociali, economiche, culturali) all'interno delle quali per il momento funziona*'

M Foucault – Microfisica del potere

"Bah... la realtà!' – Zanardi

Acknowledgements

I would like to thank...

Everyone because the world is a strongly connected network. And chances that we are connected are higher if you are reading this. So, whoever you are, consider yourself included.

The lab: Vincent, my guide in the science path, Liz without whom the preceding pages would have been white, my favourite Paolino, Frederic "el loco", Manu Schip, Leon Jacobo, Jelena "fan number one", Anil & Rajesh & Jummi for all the wonderful indian legends they told me, and all the rest of the crew with whom I shared the crowded room in these years...

My parents because still everything I know is what they taught me; my brothers following different, but similar paths for sharing sometimes part of their paths with me

Casa Pascoli: Fred, Toni, Pietro & Luca "l'inquilino virtuale" for the endless evenings with oranges and grappa and for sharing with me many successful experiments

Global people: Tania & Elena, Andrea & Andrea, Bove & Charles e tutti quelli che con determinazione e coraggio provano a spingere il mondo nella direzione giusta, e a volte ci riescono anche

The guitar girls and boys: Carlo, Michele, Viviana for making me love the song "Time after time" without ever listen to the recording

The Phasetransitioners: Manu & Bruno, Chiara & Fabio and the others with whom I shared another kind of interesting experiment and many days and feelings

And Sara - for bringing magic into my life from that very first night in the most beautiful corner of the world

Quantitative Characterization and Classification of Leech Behavior

Alberto Mazzoni, Elizabeth Garcia-Perez, Davide Zoccolan, Sergio Graziosi and Vincent Torre

J Neurophysiol 93:580-593, 2005. First published Aug 18, 2004; doi:10.1152/jn.00608.2004

J Neurophysiol 93: 580–593, 2005.
First published August 18, 2004; doi:10.1152/jn.00608.2004.

Quantitative Characterization and Classification of Leech Behavior

Alberto Mazzoni,[1] Elizabeth Garcia-Perez,[1] Davide Zoccolan,[1,2] Sergio Graziosi,[1] and Vincent Torre[1]
[1]*Scuola Internazionale Superiore di Studi Avanzati and Instituto Nazionale Fisica della Materia Section Trieste, Italy; and*
[2]*McGovern Institute for Brain Research, Massachusetts Institute of Technology, Cambridge, Massachusetts*

Submitted 15 June 2004; accepted in final form 6 August 2004

Mazzoni, Alberto, Elizabeth Garcia-Perez, Davide Zoccolan, Sergio Graziosi, and Vincent Torre. Quantitative characterization and classification of leech behavior. *J Neurophysiol* 93: 580–593, 2005. First published August 18, 2004; doi:10.1152/jn.00608.2004. This paper describes an automatic system for the analysis and classification of leech behavior. Three colored beads were attached to the dorsal side of a free moving or pinned leech, and color CCD camera images were taken of the animal. The leech was restrained to moving in a small tank or petri dish, where the water level can be varied. An automatic system based on color processing tracked the colored beads over time, allowing real-time monitoring of the leech motion for several hours. At the end of each experimental session, six time series (2 for each bead) describing the leech body motion were obtained. A statistical analysis based on the speed and frequency content of bead motion indicated the existence of several stereotypical patterns of motion, corresponding to different leech behaviors. The identified patterns corresponded to swimming, pseudo-swimming, crawling, exploratory behavior, stationary states, abrupt movements, and combinations of these behaviors. The automatic characterization of leech behavior demonstrated here represents an important step toward understanding leech behavior and its properties. This method can be used to characterize the behavior of other invertebrates and also for some small vertebrates.

INTRODUCTION

Behavior is the link between organisms and environment and between the nervous system and the ecosystem. Relating behavior to neuronal activity is a central aim of system neuroscience and a necessary step toward a full understanding of how the nervous system works (Averbeck and Lee 2003; Bucher et al. 2003; Prut and Perlmutter 2003a,b). The integration of animal behavior and the neurosciences provides important frameworks for hypothesizing neural mechanisms. Consequently, data acquisition is a crucial step to obtain an accurate quantitative characterization of behavior of the animal under investigation and of its reaction to the surrounding world (Reichardt 1961, 1965; Sommer and Wehner 2004; Wehner 2003). For this purpose, automatic data acquisition, particularly marker-based approaches, have been widely used in different ways. Some systems follow the position of the animal using ultrasound (Akaka and Houck 1980) and microwave Doppler radar (Martin and Unwin 1980), but these are high-cost techniques and can only examine gross motor behaviors. Some other attempts have been done with digitizing video images and then using this digital video as the input for object detection. This technique has the disadvantage that the size of the digital file increases quickly and, as a consequence, the duration of the experiment is limited to minutes (Baek et al. 2002; Hoy et al. 1996, 1997; McIver and Nelson 2000; Zakotnik et al. 2004). In addition, the processing of stored images should be done off-line. To avoid these problems, the tracking of a simple marker, natural or attached to the body of the animal, has been implemented. Natural markers are used only when a small tissue is under observation. Recent works explored this possibility to obtain a precise characterization of muscle contraction of the leech skin (Zoccolan et al. 2001; Zoccolan and Torre 2002). But this approach requires an off-line processing of the whole image and therefore is computationally rather expensive. When the organism of interest is small, natural color-based tracking combined with movement-based tracking, as in the case of ants (Balch et al. 2001), could be used, but in this case, if the animal remains motionless for long time, it cannot be tracked. On the other hand, markers attached to the analyzed body have been tracked. In the case of the fly, a marker placed on the fly's forehead is video-recorded (Stange and Hengstenberg 1996), and the position and orientation of the marker is extracted from the video image. This and some other similar approaches (Chrásková et al. 1999; Kruk 1997) used only one marker and therefore were restricted to the analysis of a single stereotyped behavior or to the study of a particular part of the body.

As an attempt to avoid all these problems, a multiple marker approach to quantify the locomotion patterns of a *Hirudo medicinalis* leech is proposed in this paper. We designed and automated tracking system capable of following the motion of a leech in real-time and for long periods (several hours) at a sampling rate $\leq$10 Hz. At the end of the experimental session, the system provided the position of each bead during each moment of the whole experiment. We also implemented an off-line analysis method, based on the speed and frequency content of each bead, to analyze the obtained time series. This statistical analysis allowed the identification of a variety of different leech behaviors and the determination of accurate quantitative features, such as elongation, trajectories, and speed, that cannot easily be measured. The generality of our method was tested by using free and restrained leeches, obtaining similar results. We concluded that this automatic quantitative parametrization of tracking movements could be useful not only for the leech behavior but also for some small animals, providing an important step toward the understanding of the neural mechanisms underlying animal behavior.

Following the introduction, this paper is organized into the following sections. In EXPERIMENTAL SET-UP, accuracy, sensitivity, and noise of the system are presented. CLASSIFICATION OF DIFFERENT BEHAVIORS shows the statistical analysis of the position and speed of the beads attached to the leech during

Address for reprint requests and other correspondence: V. Torre, c/o SISSA, Via Beirut 2, 34014 Trieste, Italy (E-mail: torre@sissa.it).

The costs of publication of this article were defrayed in part by the payment of page charges. The article must therefore be hereby marked "*advertisement*" in accordance with 18 U.S.C. Section 1734 solely to indicate this fact.

different behaviors. IDENTIFICATION OF DIFFERENT BEHAVIORS describes the procedure for classifying and determining the ending points (onset and termination) of a given motion to obtain the final identification of leech behaviors. EVALUATION OF THE AUTOMATIC SYSTEM attempts an evaluation of the proposed automatic behavior classification. Finally, in DISCUSSION, advantages, limitations, and possible extensions of the system are evaluated.

EXPERIMENTAL SET-UP

Animals and preparation

All the experiments were performed on intact leeches *Hirudo medicinalis*, obtained from Ricarimpex (Eysines, France) and kept at 5°C in water dechlorinated by aeration for 24 h. The animals were anesthetized in this water by adding 8% ethanol. Three plastic square beads (~2 mm diam) were attached to the dorsal side of the body with Vetbond super glue (WPI, Sarasota, FL), one of them near to the head (red), one in the midbody (green), and the third (blue) near the tail (see Fig. 1*B*). We started to monitor the behavior of the leech only when the animal was swimming and crawling normally, indicating full recovering from anesthesia (usually after 45 min).

Two different preparations were used: one in which the leech was completely free to move and another in which the leech was restrained by carefully inserting a pin through its rear sucker into the middle of a silicone elastomer (Sylgard)-coated dish. This restraining procedure did not produce any damage to the leech neuromuscular system and allowed the full rotation of the animal around the pin. Moreover, the pinned leeches were still able to use their rear sucker properly to stick on the bottom of the petri dish. Therefore in this restrained configuration, the leech body was very close to its natural posture during exploratory behavior, when the animal moves its anterior part back and forth while maintaining the rear sucker stuck on some support (Gray et al. 1938). When the behavior of a free-moving leech had to be characterized, the animal was moved to a tank (Fig. 1*B*). The level of water in the tank was changed to evoke preferentially swimming or crawling (Esch et al. 2002).

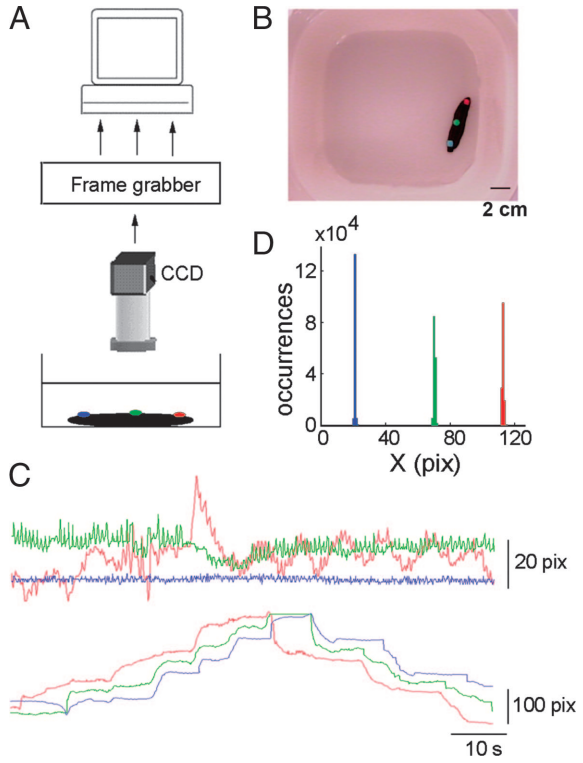

FIG. 1. *A*: scheme of the set-up: a color CCD camera mounted over a dissecting microscope viewed the leech from above with 3 colored beads attached to its dorsal side. Acquired time series were transferred to the computer hard disk. *B*: free moving leech in a rectangular plastic tank. Red, green, and blue beads were attached respectively to the head, midbody and tail of the animal. *C*: *x* displacement of the 3 beads during an exploratory (*top*) and a crawling episode (*bottom*). *D*: distribution of the recorded *x* coordinates of 3 immobile beads in an experiment aiming to establish the stability of the detecting system. The beads were recorded for 6 h.

Tracking colored beads

One color CCD camera with 640 × 480-pixel image size (Watec 231S) viewed the moving leech (Fig. 1*A*) from above in a petri dish or small tank (Fig. 1*B*). The camera was mounted on a dissecting microscope and connected via the S-Video-output (PAL) to a frame grabber (PCI-1411, National Instruments), which was installed on a personal computer. The colored beads placed on the back of the leech were tracked at 10 Hz by using software developed in our laboratory with LabVIEW 6.1 (National Instruments). This software took advantage of the ability of the frame grabber to acquire images directly in the HSL (hue, saturation, lightness) color space. The tracking algorithm was designed to work in real time with no frequency constraints (i.e., each frame was completely processed before the next was fed from the frame grabber). A standard PC (AMD Athlon1800+, 384 MB RAM DDR 266 kHz) was used in the experiments and was able to sample images and processed colored beads up to a frequency of 10 Hz. Preliminary results indicate that with a faster PC (P4 2.8 GHz FSB-800 kHz with Hyper Threading disabled, 2×512 MB RAM DDR 400 kHz double channel) tracking could be obtained at around 20 Hz. A user-customized color matching was performed to convert each acquired frame into three binary images, one for each bead, in which an ON bit represents a pixel in the corresponding color subspace. Sometimes, the leech twisted its body in such a way that one or more beads disappeared from the view of the camera. To detect these events, each binary map was then validated: if the number of matching pixels was less than eight, then the bead was reported as lost and the program recorded (0, 0) coordinates.

If a binary map was found to be valid, then different strategies were applied to calculate the center position of the bead, depending on the topological distribution of the positive pixels. If all the pixels were restricted inside a square of approximately the size of the bead (30 × 30 pixel), then the simple center of gravity was computed. On the other hand, if the positive pixels were spread around a wider area, the program searched for the 6 × 6-pixel region with the highest density of recognized pixels and returned the coordinates of its center. Finally, if in this last case more subzones all shared the same density of recognized pixels, the mean coordinates of the equivalent areas were recorded. Note that this software did not require saving all the processed images but just the coordinates of the selected beads. In this way, it was possible to monitor the leech behavior for several hours without filling hard disk space.

The position of the beads on the image plane was acquired as Cartesian coordinates and the following six time series were obtained

$$(x(n), y(n))_{\text{head/red}}$$

$$(x(n), y(n))_{\text{midbody/green}}$$

$$(x(n), y(n))_{\text{tail/blue}} \quad \text{for } n = 1 \ldots N \text{ steps} \tag{1}$$

where every step corresponds to 100 ms. Figure 1*C* shows the *x* displacement of the three beads while the leech was exploring the environment (*top*) with the tail (blue trace) attached to the bottom of the petri dish and the head moving around (red trace). When the leech was crawling (Fig. 1*C, bottom*), a succession of elongations and contractions were observed. When the leech was restrained to move around the pin inserted in its tail, the natural coordinate system to study its motion was a polar system centered on the position of the pin. Therefore each pair of Cartesian coordinates $(x, y)_{\text{color}}$ was transformed into a pair of planar polar coordinates $(\rho, \theta)_{\text{color}}$. Usually the pin was inserted approximately in the center of the dish, and its location used as the origin of the coordinate system

$$\rho_{\text{color}} = \sqrt{x^2_{\text{color}} + y^2_{\text{color}}} \tag{2}$$

$$\cos\theta_{\text{color}} = (x_{\text{color}}/\rho_{\text{color}}) \tag{3}$$

$$\sin\theta_{\text{color}} = (y_{\text{color}}/\rho_{\text{color}}) \tag{4}$$

The polar system has a clear geometrical and physiological meaning: ρ_{color} was the elongation of the leech body at the position marked by the bead (color), whereas θ_{color} was the angle between this position and a reference axis.

A sampling frequency of 10 Hz was sufficient to track the motion of a leech during swimming, as its frequency of oscillation—during this behavior—was between 1 and 2 Hz. In some cases, the behavior of the leech was video-recorded for further analysis.

The overall noise of recording system was measured by observing, for several hours, the apparent motion of the three beads attached to a black paper with a size similar to that of the leech. Figure 1*D* illustrates the distribution histograms of the position of the three colored beads in the absence of any active motion. The SD of the position of the *x* and *y* coordinates, i.e., the width of the histograms of Fig. 1*D,* was <1 pixel, indicating a precise and stable bead localization. Simultaneous precise localization of the three beads required appropriate setting of the illuminating light level and of the parameters used for color detection.

CLASSIFICATION OF DIFFERENT BEHAVIORS

Qualitative observation of leech behavior suggested the existence of a restricted number of stereotyped behaviors, such as swimming (Brodfuehrer and Thorogood 2001; Cang and Friesen 2002; Friesen et al. 1976; Stent et al. 1978) and crawling (Baader 1997; Eisenhart et al. 2000; Stern-Tomlinson et al. 1986). Our goal was to provide a quantitative classification of leech behavior based on the statistics of the leech body dynamics that could be compared with the classification usually obtained by visual inspection of the animal. Once the existence of a consistent matching between such a statistical classification of leech behavior and ethological observation was proved, an automatic classification of leech behavior over several hours could be obtained. In this section, it will be shown that by analyzing in time the trajectories of the colored beads attached to the leech, stationary, periodic, and exploratory behaviors could be identified. In addition to these prototypical behaviors, a number of other states were identified, such as peristaltic motion, abrupt movements, and some unclassified states. In *Exploratory states,* it will be shown how all these behaviors could be precisely identified and their endpoints determined.

Stationary states

This section shows how the statistics of the speed of the head (V_{head}) and of the midbody (V_{midbody}) were analyzed to identify stationary states. The speed $V_{\text{head/midbody}}$ was obtained in the following way: *1*) The time series $[x(n),y(n)]_{\text{head}}$ and $[x(n),y(n)]_{\text{midbody}}$ were numerically convolved with the time derivative $te^{(-t^2/2\sigma^2)}$ of a Gaussian function (Oppenheim and Schafer 1989), with σ equal to $z\Delta t$, where Δt is the sampling window of 100 ms and z is a positive integer. *2*) From these numerical time derivatives, dx_{head}/dt, dy_{head}/dt, dx_{midbody}/dt, and dy_{midbody}/dt of the original time series, the instantaneous values of V_{head} and V_{midbody} were computed as

$$V_{\text{head}}(n) = \sqrt{(dx_{\text{head}}/dt)^2(n) + (dy_{\text{head}}/dt)^2(n)} \tag{5}$$

$$V_{\text{midbody}}(n) = \sqrt{(dx_{\text{midbody}}/dt)^2(n) + (dy_{\text{midbody}}/dt)^2(n)} \tag{6}$$

Convolving a discrete function with a Gaussian function gives a smoothed approximation of the original data, where the measure of "smoothing" is regulated by the size of the SD. Convolving a function with the derivative of the Gaussian function is equivalent to evaluate the derivative of the smoothed function. The choice of the size (i.e., of the SD) of the convolution function is critical: a small size will result in small signal-to-noise ratio, whereas a large size will give an averaged value of the speed, losing local information. Figure 2, *A–C,* illustrates the distribution plots of (V_{head}, V_{midbody}) obtained from an experimental recording lasting 6 h obtained by convolution of the time series with the time derivative of a Gaussian filter with a value of σ equal to 0.5, 1, and 1.5 s, respectively. In this figure and in all similar plots obtained from recordings >2 h, a large isolated peak centered on the origin was observed.

This peak corresponded to a behavioral state in which both the head and the midbody of the leech were motionless and was present with all tested values of *z* varying from 5 to 25 (i.e., σ ranging from 0.5 to 2.5 s). This means that the identification of stationary states based on finding points in the time series with V_{head} and V_{midbody} near zero was robust against large variation of the width of the Gaussian used to compute the numerical time derivative of the head and midbody displacement. When a small value of *z* was used a smaller peak centered at a head speed of 25 pixel/s was observed (Fig. 2*A,* circled dark-gray peak). As will be shown, this peak corresponded to the characteristic speed of the swimming, but the final process used to identify swimming is explained in the next section. Figure 2*A* also shows a relevant fraction of events with a value of V_{head} equal to 0 but with a nonzero value of V_{midbody}. As discussed in a later section, this reflected a common pattern in which the leech moved its midbody, whereas its head and tail suckers were attached to the bottom of the recording chamber.

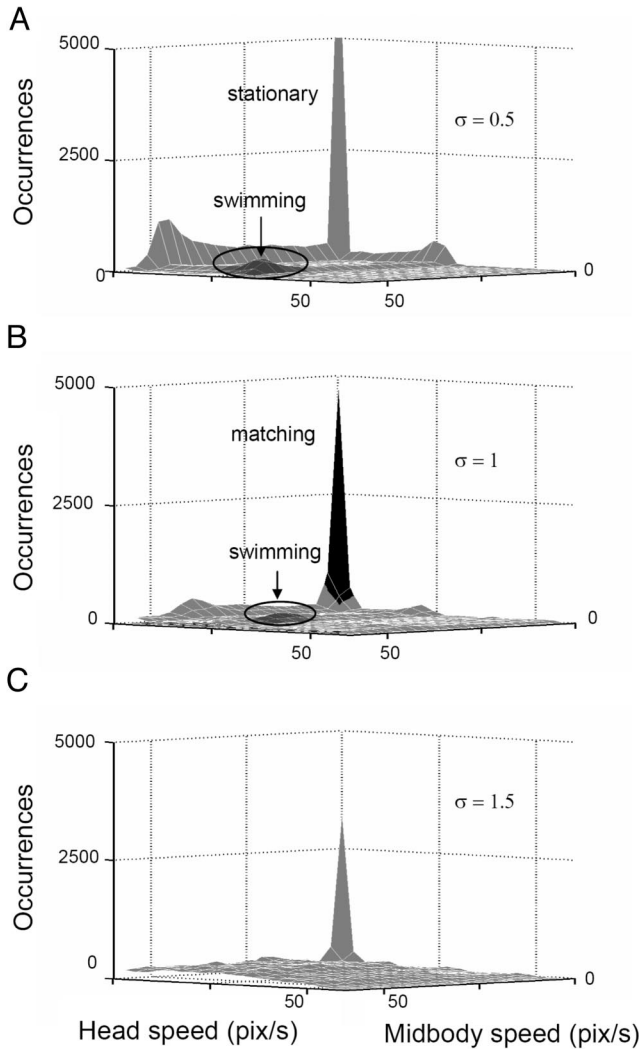

FIG. 2. *A–C*: distribution of (V_{head}, $V_{midbody}$) with a bin width of 3 pixel/s. In *A–C*, σ of the Gaussian function was equal to 0.5, 1, and 1.5 s, respectively. In *A*, a small circled dark-gray peak centered at speed of ~25 pixel/s for both V_{head} and $V_{midbody}$ indicated swimming episodes. In *B*, the peaks indicated in black were matched in Figs. 5–7 to identify still states in the time series.

As the SD of noise (see *Tracking colored beads*) of an immobile bead was ~1 pixel, a point in the time series was analyzed as stationary when V_{head} was <1 pixel/s. When V_{head} and V_{tail} were both <1 pixel/s, the leech was completely at rest. These points, indicated in black in Fig. 2*B*, were identified (i.e., matched) in the original time series and labeled as still points (see Figs. 4–6). The identification of these points represented the first step of the automatic classification.

Periodic states (swimming and crawling)

As a second step, periodic states were identified through the analysis of the spectral content of the time series. The analysis started by computing the total elongation $e(n)$ of the leech (see the horizontal line joining points H and T in Fig. 3*A*) defined as

$$e(n) = \sqrt{(x(n)_{head} - x(n)_{tail})^2 + (y(n)_{head} - y(n)_{tail})^2} \quad (7)$$

Elongation oscillated during swimming and crawling (at different frequencies) and varied noticeably in an irregular way during exploratory behavior. Then, for each point n of the resulting time series $e(n)$, the instantaneous speed defined in the previous section was tested. If $V_{head}(n) < 1$ pixel/s, the point was already classified as stationary and no further analysis was needed. If the speed was above this critical value, a time window centered on the point n, having a size T ranging from 20 s (for the high-frequency detection) to 50 s (for the low-frequency detection) was considered. In this time window, three quantities were computed. *1*) The maximal speed of the head defined as

$$V_T^{max}(n) = \max_{n-\Delta/2<n<n+\Delta/2} V_{head}(n) \quad (8)$$

where Δ is T times the sampling rate, i.e., 10 Hz. *2*) The power spectrum $PS_n^T(f)$ of $e(n)$ (Fig. 3*B, left*), where f was the frequency varying over the range 0.3–5 Hz (for $T = 20$ s) and 0.12–5 Hz (for $T = 50$ s). In both cases, the lowest points of the power spectrum were discarded as unreliable. Power spectra $PS_n^T(f)$ were computed using the Welch's averaged, modified periodogram method (pwelch function, Matlab), with 50% overlap between successive Hamming-windowed segments, with a size equal to $T/4$. The Welch method splits a set of data into smaller sets and calculates the periodogram of each small set. Then the frequency domain coefficients arising from calculating the periodograms are averaged over the frequency components of each data set. This results in a power spectrum that is a smoothed version of the original but with less noise. *3*) The smoothed power spectrum $\langle PS_n^T(f)\rangle$, computed using a semi-octave centered on each f (as a spectral window) and defined as

$$\langle PS_n^T(f)\rangle = \sum_{F=f/\sqrt{2}}^{f\sqrt{2}} PS_n^T(F) \quad (9)$$

(Fig. 3*B, right*).

The power spectrum of the recorded time series was characterized by a $1/f^n$ noise, which was a typical component of the power spectra of no stationary stochastic processes (Kantz and Schreiber 1997), with n assuming values between 3/2 and 2. By smoothing such a power spectrum over a frequency-dependent window, noise was removed and the dominant frequencies of the signal were enhanced. Smoothing the power spectrum over an octave or a fraction of an octave is a common practice in acoustics (Miller et al. 2002).

The frequency $f_T^d(n)$ for which $\langle PS_n^T(f)\rangle$ was maximum was taken as the dominant frequency for the point n in a window of length T. In this way, two quantities $(V_T^{max}(n), f_T^d(n))$ were associated to every point n of the time series. Both $V_T^{max}(n)$ and $f_T^d(n)$ depended on the size of the time window T: with larger time windows, the computation of $PS_n^T(f)$ was more reliable but the time localization of the behavioral state was less precise. In fact, by using large windows, sequences of short-lived states could be considered as a single state. Therefore a time window T of only 20 s was used initially to localize precisely fast and short oscillations.

Figure 3*B* shows $PS_n^T(f)$ (*left*) and $\langle PS_n^T(f)\rangle$ (*right*) of two different intervals of the time series, one with $f_{20}^d(n)$ around 1.5 Hz (black line) and the other with $f_{20}^d(n)$ around 0.3 Hz (gray line).

The occurrences of the pair $(V_{20}^{max}(n), f_{20}^d(n))$ were represented in a three-dimensional histogram. These values were not homogeneously distributed: two well-resolved clusters or

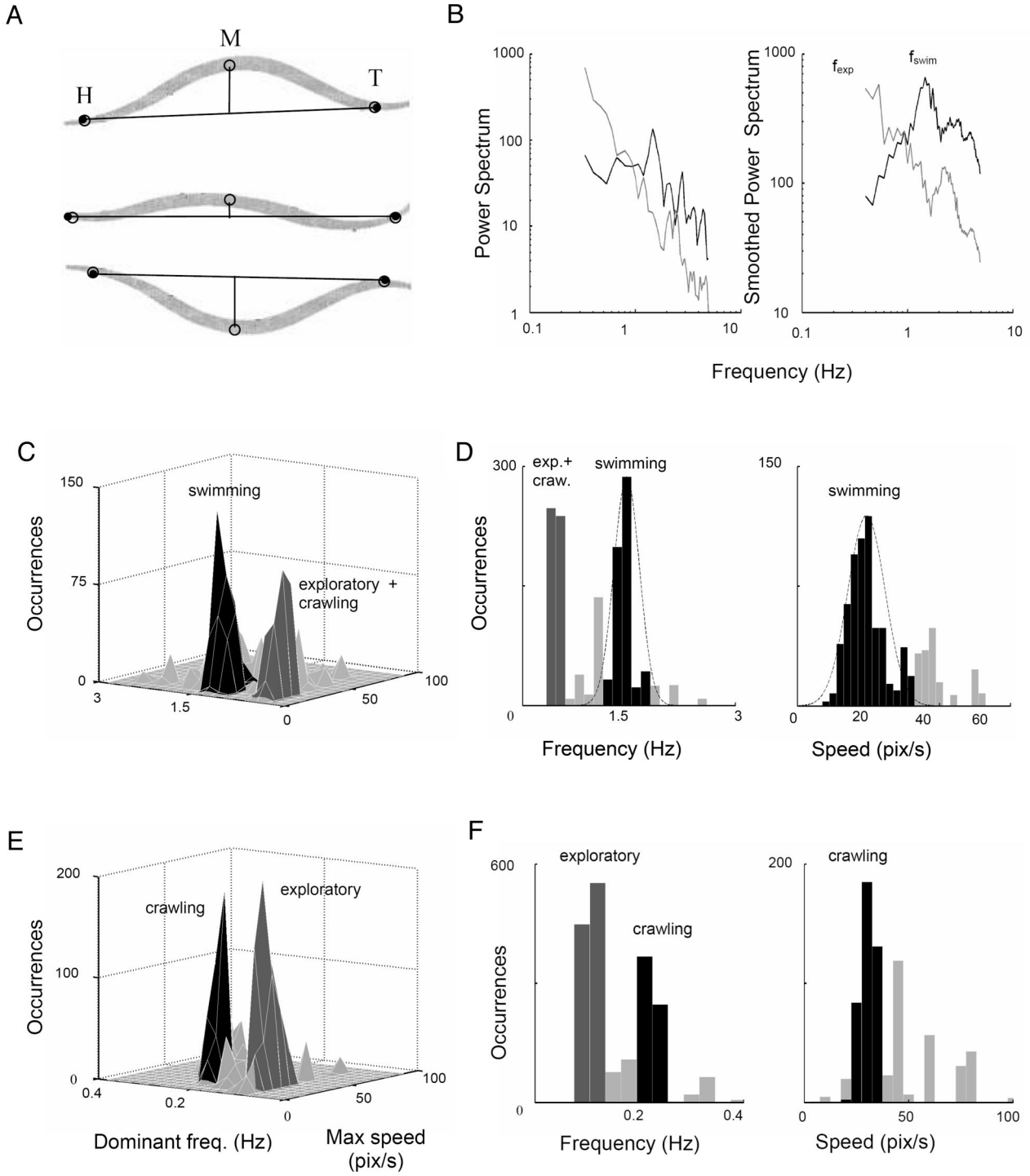

FIG. 3. *A*: 3 different positions of the leech during swimming. The projection P $[(x(n), y(n)]_{\text{midbody}}$ was the distance of the bead glued on the midbody (*M*) from the line joining the head to the tail bead. During swimming episodes, P$[x(n), y(n)]_{\text{midbody}}$ and $e(n)$ oscillated with the same frequency, ~1.5 Hz. *B*: power spectrum $PS(n)$ of $e(n)$ (*left*) and smoothed power spectrum $<PS(n)>$ of $PS(n)$ (*right*) for a swimming (black line), and an exploratory episode (gray line). The dominant frequency f_d for each window of length T was taken as the frequency for which $<PS(n)>$ was maximum. *C*: 3-dimensional histogram of the pair $[V_T^{\max}(n), f_T^d(n)]$ for a recording lasting 1 h showing 2 clear clusters posteriorly identified as swimming and exploratory + crawling, respectively. *D*: distribution of frequencies (*left*) and speeds (*right*) around the black peak of *C*. *E*: as in *C* but with $T = 50$ s. *F*: as in *D* but for the black and gray peaks of *E*.

peaks were observed—with different heights but always in similar positions—in all 30 examined leeches, indicating the existence of two different behavioral states.

Figure 3*C* illustrates a three dimensional histogram of the pair $(V_{20}^{\max}(n), f_{20}^{d}(n))$ for a recording lasting 1 h, where two clusters corresponding to these frequencies were clearly distinguishable.

A Gaussian fit (Fig. 3*D,* dotted line) of the occurrences with frequency >0.5 Hz was used to determine the center (μ_f) and the width ($2\sigma_f$) of the high-frequency cluster (Fig. 3*C,* black

peak) in the frequency domain. Lower frequencies were excluded on the assumption they probably belonged to the separate low frequency cluster. In Fig. 3*D* (*left*), the distribution of frequencies was represented (frequencies belonging to the black cluster). A second Gaussian fit was performed for the occurrences with speed corresponding to the domain of frequencies belonging to the cluster, thus determining μ_V and $2\sigma_V$ in the velocity domain. For the high-frequency cluster shown in Fig. 3*C,* the obtained values were $\mu_V = 20$ pixel/s, $\mu_f = 1.5$ Hz, $2\sigma_V = 10$ pixel, and $2\sigma_f = 0.2$ Hz, but both position and width were consistently similar for all experiments with free leeches (see Fig. 8*B*). The distribution of speeds belonging to the black cluster was represented in Fig. 3*D* (*right*). As a final step, all the pairs $(V_{20}^{\max}(n), f_{20}^{d}(n))$ having a speed

$$\mu_V - 2\sigma_V < V_{20}^{\max}(n) < \mu_V + 2\sigma_V \quad (10)$$

and a frequency

$$\mu_f - 2\sigma_f < f_{20}^{d}(n) < \mu_f + 2\sigma_f \quad (11)$$

were considered as belonging to the cluster centered in (μ_V, μ_f).

The state characterized by the $f_{20}^{d}(n)$ around 1.5 Hz can be clearly identified as swimming behavior. To verify that these events correspond to swimming occurrences, the videotape of the leech motion was analyzed visually to confirm that the events n located in the cluster around $f_{20}^{d}(n) = 1.5$ Hz and $V_{20}^{\max}(n) = 20$ pixel/s belonged always to swimming episodes and that every swimming episode belonged to this cluster. Swimming behavior, which involved a periodic movement of the whole body, could be identified also by analyzing the distance $P(x(n), y(n))_{\text{midbody}}$ of the bead glued on the midbody from the line joining the head to the tail bead (see shortest line in Fig. 3*A*). During swimming episodes, $P(x(n), y(n))_{\text{midbody}}$ also oscillated with a frequency of 1.45 ± 0.15 (SD) Hz.

The states identified as swimming behavior through the frequency analysis of $P(x(n), y(n))_{\text{midbody}}$ largely overlapped those identified analyzing the elongation (data not shown). The latter was nevertheless a more sensitive parameter because it varied considerably during crawling and exploratory motion, and therefore the classification was performed from the elongation time series.

For a free leech, all the points in the high-frequency cluster (which correspond in the histogram of Fig. 3*C* to the points located within 0.2 Hz from the dominant frequency $f_{20}^{d}(n)$ of 1.5 Hz and with speeds from 8 to 30 pixel/s) were taken as belonging to swimming events. Indeed the period of a swimming movement was ~0.6 s as reported before (Muller et al. 1981).

In the experiments in which the leech was restrained, the algorithm for the identification of periodic motion was applied only to the $\rho(n)_{\text{head}}$ time series because this variable corresponded to the elongation $e(n)$ of the leech. In the corresponding three-dimensional histograms of the pairs $(V_{20}^{\max}(n), f_{20}^{d}(n))$, two distinct clusters were observed centered on 1 and 0.3 Hz, indicating the presence of swimming also in the pinned leech (1 Hz) in addition to exploratory motion (0.3 Hz) but at a reduced frequency. Then, for a restrained leech, all the points located within the high-frequency cluster, defined with the same procedures used for the free leech, were classified as swimming episodes.

The cluster at the low-frequency end of the histogram of Fig. 3*C* was not well resolved, especially at lower frequencies. Therefore to obtain a better resolution at lower frequencies, the time series $e(n)$ was reanalyzed using a larger time window T of 50 s. The resulting histogram of the pairs $(V_{50}^{\max}(n), f_{50}^{d}(n))$ is shown in Fig. 3*E.* In this case, a well-resolved cluster centered on 0.2 Hz (in black) with $2\sigma_f = 0.04$ Hz and a remaining cluster (in dark gray) still centered at the lowest resolved frequencies (near 0.1 Hz), were observed (Fig. 3, *E* and *F, left*). The state corresponding to $f_{50}^{d}(n)$ around 0.2 Hz can be identified with the crawling behavior as confirmed by inspection of the videotape of the leech motion. Indeed the period of a crawling step ranges from 3 to >10 s (Eisenhart et al. 2000; Stern-Tomlison et al. 1986).

In the restrained leech, it was impossible to observe crawling because this behavior involves lifting of the tail. Even if some crawling attempts (elongation and contraction alternating with a frequency close to 0.2 Hz) were observed, no behavior of the restrained leech was classified as a crawling state.

The state corresponding to $f_{50}^{d}(n)$ around 0.1 Hz could be associated with the irregular motion observed during exploratory behavior (see next section). The two identified clusters were centered on approximately the same speed of ~30 pixel/s (see Fig. 3*F, right*). Points in the histograms of Fig. 3, *E* and *F,* in black and dark gray were identified as crawling and exploratory states, respectively.

Time windows centered on behavioral end points of periodic states also contained nonperiodic components. As a consequence, the power spectrum that was computed over the entire window often did not show a clear peak, and these points could not be classified as periodic. The classification of periodic movements was therefore completed with a prolongation procedure (see *Prolongation of periodic behaviors beyond the well-identified window*), necessary for an accurate determination of the onset and termination of the behavior.

SWIMMING AND PSEUDOSWIMMING. The identification of the swimming state was based on the analysis of the elongation $e(n)$, i.e., on the head to tail distance. As a consequence, the proposed identification procedure did not distinguish whether the entire leech was moving on the dish surface (swimming) or whether $e(n)$ oscillated but the leech had one sucker attached to the bottom of the dish. Figure 4, *A* and *B,* showed two time series of $e(n)$ obtained from two different free leeches. Both had a clear oscillatory component at ~1.5 Hz, the typical frequency of swimming.

When the trajectories of the leech head and tail, i.e., $[x(n)_{\text{head}}, y(n)_{\text{head}}]$ and $[x(n)_{\text{tail}}, y(n)_{\text{tail}}]$ were plotted on the (x, y) plane, it appeared that the time series of Fig. 4, *A* and *B,* corresponded to two different behaviors. In one case (Fig. 4, *A* and *C*), the leech was swimming around the dish, but in the other case (Fig. 4, *B* and *D*), the tail sucker was fixed to the bottom of the dish and the head was oscillating with a frequency of ~1.5 Hz. This second behavior was referred to as pseudo-swimming, characterized by an oscillation of the elongation $e(n)$ with a frequency identical to that observed during swimming, although with smaller amplitude and with the rear sucker attached to the bottom of the dish. The amplitude of the swimming movements of a free leech corresponded to approximately the 15–20% of the length of the full-extended leech, matching with previous evaluations (Stent et al. 1978). During pseudo-swimming, the average amplitude value was only the 10% of the length (data not

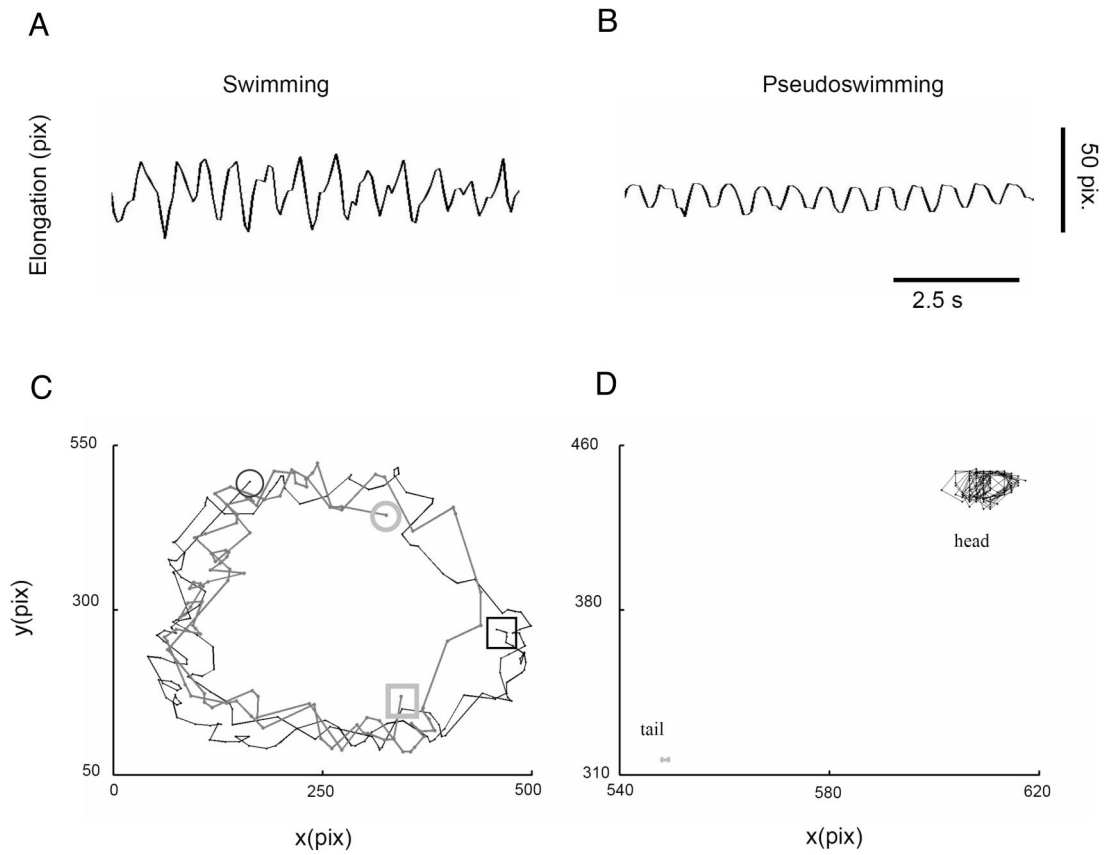

FIG. 4. Discrimination between swimming and pseudo-swimming. *A*: elongation $e(n)$ of a leech during a period of swimming. The frequency of the trace was ~1.5 Hz. *B*: elongation $e(n)$ of another leech during a period of pseudo-swimming, where the leech had the tail sucker attached to the dish and the head was oscillating with a frequency of 1.5 Hz. In this case, the amplitude of the oscillations was smaller than that observed in *A*. *C* and *D*: trajectories of the leech head and tail during a period of swimming and pseudo-swimming, respectively. While in *C,* the leech moves around the dish; in D, the leech was fixed in the same position. The circles in *C* show the initial position of the head (black circle) and tail (gray circle) and the squares represents their final position.

shown). These two states were distinguished easily by analyzing $V_{10}^{\text{tail}}(n)$ defined as

$$V_{10}^{\text{tail}}(n) = \max_{n-\Delta/2<n<n+\Delta/2} V_{\text{tail}}(n)$$

where Δ was 10 times the sampling rate. The states with $V_{10}^{\text{tail}}(n) < 3$ pixel/s were classified as pseudoswimming states because the tail was not moving quickly enough to allow real swimming. They can probably be associated with ventilation behavior, previously reported by some authors (Magni and Pellegrino 1978). Note that in the case of restrained leeches, swimming and pseudoswimming cannot be dissociated because the rear sucker of the animal was kept stationary by the pinning. In this case, the amplitude of the swimming movements was again the 10% of the full length of the leech. Moreover, as previously mentioned, the characteristic frequency of oscillation of pinned leeches during such swimming or swimming-like motion is slightly lower (~1 Hz) than for free leeches.

Exploratory states

Events belonging to the low-frequency cluster (Fig. 3, *E* and *F,* dark gray) in the histogram of the pairs $(V_{50}^{\max}(n), f_{50}^{d}(n))$ were identified as exploratory behavior. The videotape also confirmed this observation. In fact, the events with $f_{50}^{d}(n)$ at the lowest resolved frequencies correctly matched with the exploratory movements. These were irregular oscillations of the head and the anterior part of the body, while the rear sucker, which was stuck on the bottom of the recording chamber, kept the tail motionless. The power spectrum of time intervals containing substantial amounts of exploratory motion was not associated with sharp peaks of $PS(n)$ at any frequency (Fig. 2*B*).

Mixed states

When the front sucker of the leech was attached to the dish (V_{head} close to 0), the midbody usually was motionless (the peak in (0,0) of Fig. 2). However, in some cases, it was also observed to be moving (when V_{midbody} assumed values >0, see Fig. 2).

As the assumed threshold for a point to be stationary was <1 pixel/s, points of the time series in which V_{head} was smaller and V_{midbody} was larger than this threshold, and points in which they were both under threshold were classified as distinct states: head-attached states in the first condition and still in the second. Figure 5 shows the analysis of these states. In this experiment, the leech was pinned (its tail was fixed to the dish) and the ρ coordinates of the head and midbody were analyzed.

At the beginning of the trace in Fig. 5, a small episode of exploratory behavior is shown. Sometimes, it was observed (in 5/30 experiments) that during a stationary state (the front and the rear sucker were attached to the dish), the midbody had

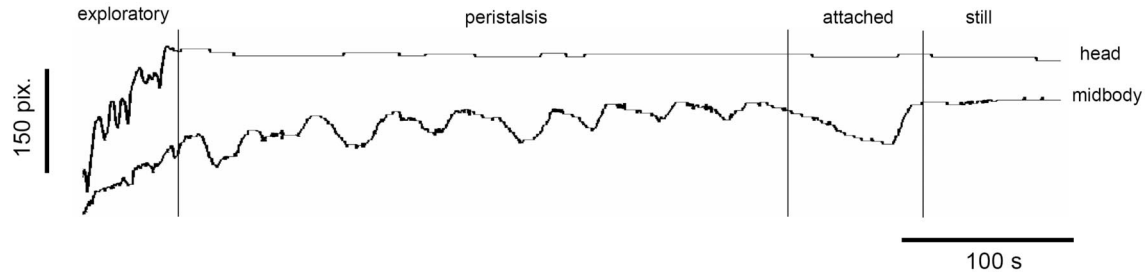

FIG. 5. Analysis of states in which the head was attached to the bottom of the petri dish. The leech was pinned and $\rho(n)$ was analyzed. In the 1st interval from the left, an exploratory episode was detected and the next intervals presented 3 different states where the head of the leech was found motionless. In the 1st, the midbody was oscillating regularly with a frequency of <0.1 Hz. The 2nd shows irregular oscillations of the midbody, and in the 3rd, the midbody is motionless.

low-frequency oscillations similar to peristalsis. The moving midbody was analyzed and a low periodic motion about 0.03 Hz was identified (see Fig. 5). A peristaltic state is usually composed of no more than 5 slow oscillations (i.e., not lasting >3 min), so this motion was not identified with Fourier analysis but by smoothing the time series (to eliminate high-frequency components) and finding consecutive maxima with <60% of relative difference in the period.

Despite the low frequency of the oscillations, this state was referred as "peristalsis-like" movement because the visual analysis of the videotape showed the same rostral-to-caudal and caudal-to-rostral waves reported for peristalsis (Lent et al. 1988) where the frequency had been reported to be ~0.16 Hz. The whole duration of the peristalsis-like movement in each experiment (lasting 12 h each) ranged from 0.5 to 12% of the total time and from 1 to 15% of the stationary time. The peristalsis was present only in experiments where the stationary state was prevalent (>50% of the time).

Stationary points of the time series where V_{midbody} was neither negligible nor periodic were referred as "head-attached" states (see Fig. 5). Stationary points of the time series where V_{midbody} was negligible were referred as "still" states (see Fig. 5).

In 1 case of 30 leeches observed, a double periodic motion was found with frequencies of ~0.02 and 0.7 Hz. As this motion was observed only in one leech, it was not considered as a typical behavior (data not shown).

Abrupt movements

The last identified behavior, characterized by a fast transition during which the leech changed its location on the dish was referred as "abrupt movement." To be classified as belonging to this group, transitions must be of ≥20 pixel and last <5 s. In Fig. 6*A*, abrupt movements indicated in gray, occur between different still states.

Unclassified behaviors

Previous criteria were not enough to classify every movement of the leech; therefore in the time series, there were some unclassified intervals. Some of them were eventually classified as belonging to one of the behaviors mentioned in the preceding text through a further analysis procedure (see *Prolongation of periodic behaviors beyond the well-identified window* and *Assembling of identical states and elimination of short states*) while the rest was left unclassified. Examples of behaviors—extending over several seconds—that were not classified are shown in Fig. 6, *B* and *C*. These behaviors were often characterized by a slow drift (see Fig. 6*B*) or by oscillations superimposed on an apparently exploratory event (see Fig. 6*C*). In this last case, there is no clear dominant frequency. As will be discussed later, these unclassified states represented usually <10% of the total leech behavior.

IDENTIFICATION OF DIFFERENT BEHAVIORS

In the previous, different states or behaviors were identified from the statistical analysis of the time series. Points belonging to these states could be identified from the plots shown in Figs. 2 and 3: points falling within 2σ from the identified peaks of Figs. 2*B* and 3, *C* and *E,* were unequivocally identified as part of a still, swimming, crawling, and exploratory behavior.

These well-identified points were matched into the original time series (see Figs. 5, 6*A,* and 7, *A* and *D*). After the matching of a sequence of consecutive points, all identified as belonging to the same behavioral state represented a well-identified behavioral window in the original time series. However, onset and termination of these windows were not precisely determined by the analysis described in the previous section. Indeed, a reliable computation of the power spectrum requires a large time window T (≤50 s). Thus for end points, the entire interval with different dominant frequency was included in the same window. As a result, no clear peaks appeared in the corresponding power spectrum, and a correct classification was not possible.

To obtain an exhaustive and full classification of all points n of the time series we adopted the following strategy: *1*) matching of well-identified points (see Fig. 7, *A* and *D*); *2*) prolongation of periodic points beyond the well-identified window (see Fig. 7, *B* and *E*); and *3*) assembling of close identical states and elimination of short isolated states (see Fig. 7, *C* and *E*).

Matching of well-identified points

The statistical analysis illustrated in CLASSIFICATION OF DIFFERENT BEHAVIORS identified six kinds of states.

1) Stationary states with a value of $V_{\text{head}}(n) < 1$ pixel/s, subdivided into "still" when $V_{\text{midbody}}(n)$ was also < 1 pixel/s, "peristaltic-like" when $V_{\text{midbody}}(n)$ was >1 pixel/s and the midbody was regularly oscillating at a frequency of ~0.03 Hz, and "head-attached" when $V_{\text{midbody}}(n)$ was >1 pixel/s and the midbody was moving with no regular oscillations.

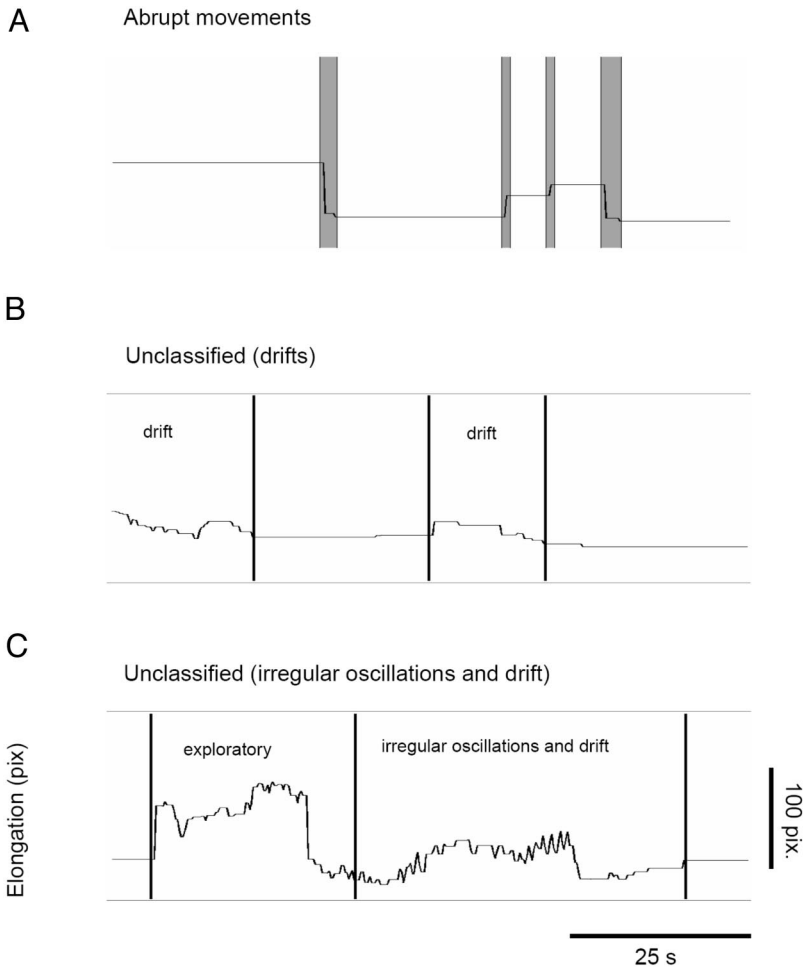

FIG. 6. Abrupt movements and unclassified states. *A*: in this panel, still states separated by brief transitions referred as abrupt movements (in gray) are shown. *B*: examples of unclassified states where a significant drift was observed. *C*: another example of an unclassified state characterized by oscillations superimposed to slow drifts.

2) Swimming states with a value of $V_{20}^{\max}(n)$ between 10 and 30 pixel/s, a value of $f_{20}^{d}(n)$ between 1.3 and 1.7 Hz, and a value of $V_{10}^{\text{tail}}(n)$ >3 pixel/s.

3) Pseudo-swimming states with a value of $V_{20}^{\max}(n)$ between 5 and 15 pixel/s, a value of $f_{20}^{d}(n)$ between 1.3 and 1.7 Hz, and a value of $V_{10}^{\text{tail}}(n)$ <3 pixel/s.

4) Crawling states with a value of $V_{50}^{\max}(n)$ between 20 and 40 pixel/s and a value of $f_{50}^{d}(n)$ between 0.16 and 0.24 Hz.

5) Exploratory states with a value of $V_{50}^{\max}(n)$ between 10 and 50 pixel/s and a value of $f_{50}^{d}(n)$ <0.12 Hz.

6) Abrupt movements, i.e., rapid transitions of ≥20 pixels between previously classified states occurring in <5 s.

These points, identified in the histograms of Figs. 2 and 3, were matched into the original time series. Figure 7, *A* and *D,* illustrates the leech elongation, i.e., $e(n)$, over a time window of ~5 min: swimming, still, and exploratory states were indicated in gray, yellow, and blue, respectively. White indicated unclassified behaviors. It was evident that these well-identified windows captures the central portion of corresponding behaviors but cannot properly identify the onset and termination of the behavioral state. This was particularly evident for swimming, crawling, and exploratory states, which were identified by computing the power spectrum and its smoothed version in time windows of 20 and 50 s. Stationary states, identified by convolving the time series with the time derivative of a Gaussian filter with $\sigma = 1$ s (see Fig. 2*B*) were localized with an accuracy of ~1 s.

Prolongation of periodic behaviors beyond the well-identified window

The end points of swimming and crawling states were identified by looking at the existence of periodic events at the boundaries of the well-identified windows.

First, all local maxima of the elongation time series were identified. Every interval between two consecutive maxima was tested as a potential periodic motion. The amplitude of this potential oscillation was defined as the difference between the maximum and the minimum in the interval. If the amplitude was <3 pixel, the oscillation was considered to be caused by noise. The oscillation was thus discarded, and the next interval between two consecutive maxima was considered. Otherwise (if the amplitude was >3 pixel) the interval was counted as a potential periodic interval. Second, for every potential oscillation, the period was taken as the distance between two successive maxima. If for more than four consecutive potential oscillations the difference between the periods is <60% of their average and the difference between the amplitudes was less than their average, the interval between the first and the last maximum was considered as a regular periodic motion with a period that was the average of the single periods.

If a regular periodic motion with period between 0.5 and 1 s bordered or partially overlapped with a state previously classified as swimming, then the swimming state was prolonged to the border of the motion. The same thing happened if a

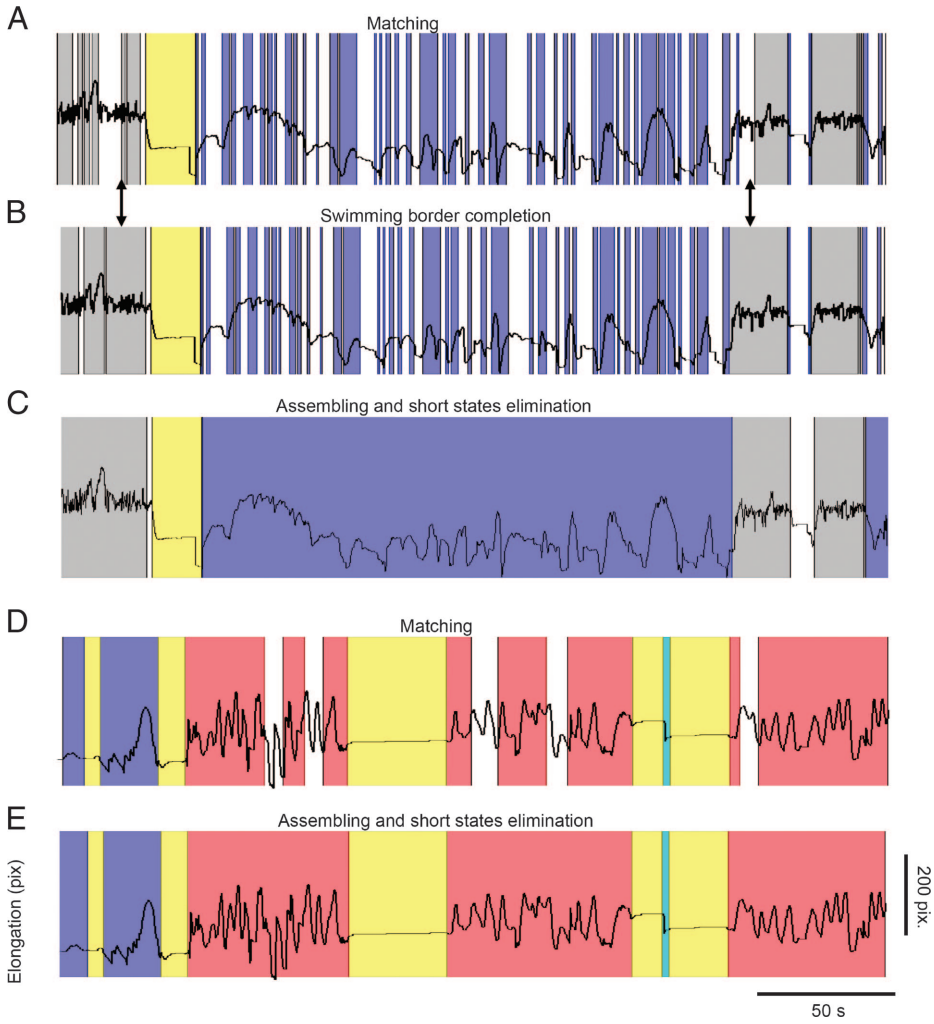

FIG. 7. Final identification of exploratory, swimming, and crawling episodes. In *A* and *D*, the points corresponding to the large peaks of Figs. 2 and 3 were identified in the original time series and classified as still (indicated in yellow), swimming (in gray), crawling (in red), abrupt movements (in cyan), and exploratory (in blue) states. In *B* and *D*, periodic states, i.e., swimming and crawling, were prolonged beyond boundaries detected in *A* and *D* by analyzing possible periodicity. In *C* and *E*, short unclassified states of duration <10 s between episodes of the same state were eliminated.

crawling state bordered or partially overlapped with a regular periodic motion with period between 3 and 10 s.

Because swimming and crawling prolongation were not allowed to be overlapped, a constraint was imposed on this procedure. Moreover, if the time interval of prolongation of a periodic (swimming or crawling) state overlapped with a state previously classified as exploratory or stationary (even if this was unlikely to happen), the time interval was classified as belonging to the periodic state.

This prolongation is showed in Fig. 7*B*, where the swimming behavior had been prolonged in correspondence to the two thick arrows. Swimming and pseudo-swimming were distinguished by analyzing the values of $V_{10}^{\text{tail}}(n)$.

Assembling of identical states and elimination of short states

Unclassified sections of events of duration <10 s separating two identical crawling, swimming, or exploratory states were considered as part of the surrounding behavior and therefore included in it. Unclassified states between two stationary states, instead, were also considered stationary if their duration was <10 s and the maximum displacement of the head in the time interval was <10 pixel. After this procedure, the remaining classified states lasting <5 s were eliminated avoiding positive classification of incomplete behaviors. Figure 7 shows these different steps leading to the final identification of swimming, crawling, and exploratory states.

With this procedure, the final behavior classification shown in Fig. 7, *C* and *E*, was obtained. At the end of the procedure in Fig. 7*C*, three swimming episodes (in gray), one still state (in yellow), and one exploratory episode (in blue) were correctly identified. In the same way, in Fig. 7*E*, five still states (in yellow), two exploratory (in blue), one abrupt movement (in cyan), and three crawling episodes (in red) were identified.

EVALUATION OF THE AUTOMATIC SYSTEM

The proposed method for the automatic classification of leech behaviors identifies the following states: stationary states subdivided into still, peristaltic-like, and head attached; swimming; pseudo-swimming; crawling; exploratory states; and abrupt movements.

The existence of these states was justified by visual inspection of the leech motion and behavior and by the vast ethological literature on the leech (Baader 1997; Brodfuehrer and Thorogood 2001; Cacciatore et al. 2000; Kristan 1992; Lent et al. 1988; Lewis and Kristan 1998; Muller et al. 1981; Wilson

and Kleinhaus 2000). The identification of these states was based on a simple statistical analysis of the speed and frequency content of the leech elongation $e(n)$ and of the head, midbody, and tail coordinates described by the time series.

The automatic identification of these states was based on the location of clusters and on their width in the histograms of $(V_{\text{head}}, V_{\text{midbody}})$, $(V_{20}^{\max}(n), f_{20}^{d}(n))$ and $(V_{50}^{\max}(n), f_{50}^{d}(n))$. Figure 8 illustrates the statistics of the cluster location and its width for free moving and pinned leeches. Figure 8*A* shows the SD σ of the stationary peak in $(V_{\text{head}}, V_{\text{midbody}})$ for five pinned leeches (on the left) and five free leeches (on the right). Figure 8*B* shows the central frequency and the relative σ of the swimming cluster in $(V_{20}^{\max}(n), f_{20}^{d}(n))$ for five pinned leeches (on the left) and seven free leeches (on the right). As seen before (in the *Pronlongation of periodic behaviors beyond the well-identified window*), pinned leeches swim at a reduced frequency. Figure 8*C* shows the central frequency and the relative σ of the crawling cluster in $(V_{50}^{\max}(n), f_{50}^{d}(n))$ for four free leeches (on the right). As explained in *Prolongation of periodic behaviors beyond the well-identified window,* pinned leeches cannot crawl. The number of analyzed leeches was different for different behaviors because very often a leech was swimming but never crawling or doing the opposite, mainly depending on the level of water in the dish. For every figure, data coming from experiments where the behavior shown was present for >1 h are displayed.

A small variability in the peak location and its width among different leeches is shown in Fig. 8, *A–D,* indicating that the proposed state identification captured fundamental properties of leech motion consistently identified across individuals.

The proposed identification was not only based on the statistical analysis described in CLASSIFICATION OF DIFFERENT BEHAVIORS but also on the procedures illustrated in IDENTIFICATION OF DIFFERENT BEHAVIORS. Figure 8*D* shows, for different leeches, the total fraction of the time series that had been identified as belonging to one of the states described before during the different steps used in the identification procedure: matching, prolongation, and assembling. States identified by the matching step were rather reliable as these points were those around the identified clusters in the histograms of Fig. 2 and 3, having a very stable position. They represent ~75% for different leeches. The fraction of identified states becomes 90% after border completion and assembling.

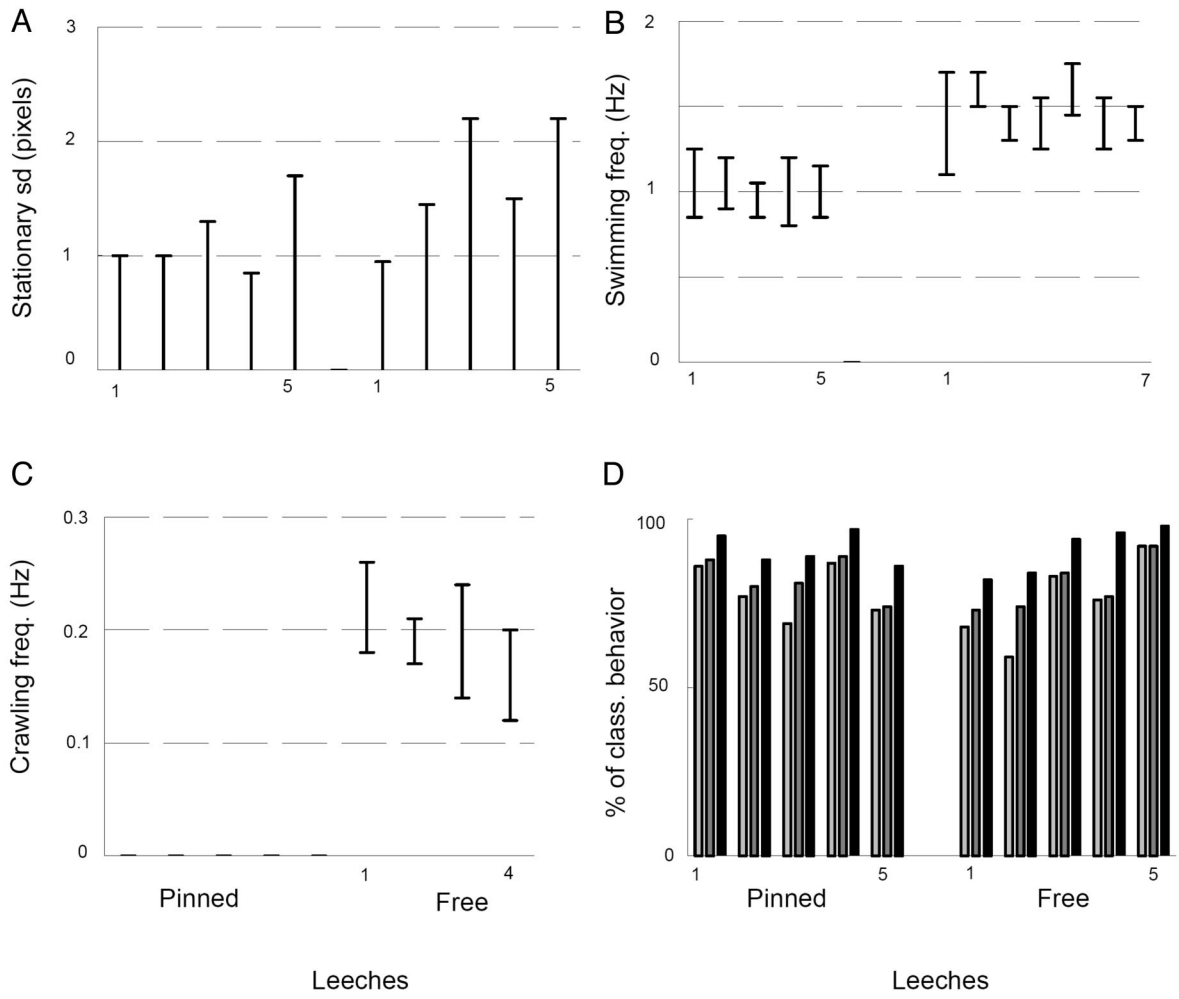

FIG. 8. Statistics on the properties of behaviors in different leeches. *A*: SD of the stationary peak for 5 pinned leeches (on the left) and 5 free leeches (on the right). *B*: central frequency of the swimming cluster for 5 pinned leeches (on the left) and 7 free leeches (on the right). *C*: central frequency of the crawling cluster for 4 free leeches (on the right). *D*: fraction of states identification during the different steps: matching, prolongation, and short states removal.

DISCUSSION

The objective of the present study was to provide a novel automatic method for the classification of the leech behavior. Automatic systems are the best way for analyzing animal behavior in natural or controlled conditions, offering the possibility to obtain some quantitative parameters as spatial and temporal activity, speed, duration of stops, etc., which are hard to calculate when are only based on the observer's subjective judgment. Our multiple marker approach was thought as a tool allowing precise and informative characterization of the leech motion in real time.

The proposed method was based on the tracking of colored beads glued to the dorsal side of the animal body. As a consequence of the glue, the segment where each bead was attached lost flexibility. Because our measurements were based on the whole body deformation, these local effects do not affect the characterization of the global behavior of the leech. At the end of the experimental session 6 time series

$$(x(n), y(n))_{\text{head}}; (x(n), y(n))_{\text{midbody}}; (x(n), y(n))_{\text{tail}} \quad \text{for } n = 1 \ldots\ldots N$$

were obtained. Therefore the determination of characteristic values was done from time series (x, y, and time series) and not from a video-aided recording system, which required the scanning and storing of each frame (Gharbawie et al. 2004; Orito et al. 2004). In fact, the possibility of recording only the time series of the tracked points allowed us to record long periods of locomotion (hours instead of minutes).

The obtained time series were analyzed off-line. Identification of leech behaviors was based primarily on a statistical analysis of time series and not on pattern-recognition methods. The proposed method provides an automatic classification for ~90% of the behavior observed in a leech freely moving in a petri dish and/or a small tank. These characteristics are discussed in the following text.

Reliability of the tracking state

Colored beads—usually, red, green and blue—glued on the back of the leech were tracked in real time by a simple processing of images acquired by a color CCD camera. For a reliably discrimination of the beads, it was necessary to match properly the spectral and sensitivity properties of the CCD camera to the illumination of the experimental set-up. There are some points to take in mind for selecting the colors of the beads. First is the color of the leech. By selecting light colors, this inconvenience could be avoided. In the case of the green bead, for example, the selection was done using a light green because by adjusting the source of light, the leech seems to be black, and the beads could be easily identified. Second is the water and the color of the dish. If the light is high, it is reflected by the water (or by the dish), and these reflexes could be taken as beads when the leech is in a stationary state. On the other hand, if the light is low, then everything is dark and tracking is not possible. Third is the volume of water displaced by the moving leech. This effect could also be avoided by adjusting the light because there is only a small quantity of water displaced. Then the tracking process only requires a proper illumination of the dish where the leech is moving.

The proposed scheme, at the moment, provides a useful classification of the leech motion when the animal moves mainly on a plane. In this case, however, the animal could rotate around its body and the CCD camera cannot track the colored beads. Using small colored rings surrounding the animal body, this problem could be circumvented. Likewise, by using an experimental set-up with two color CCD cameras, the complete three-dimensional motion of the animal could be reconstructed. Additionally, the CCD camera, software, and hardware used in the present work were low-cost components. By using more sophisticated and expensive components, it will be possible tracking and monitoring social interactions among multiple animals simultaneously. The only restriction of the system is the impossibility to track the locomotion of small animals, such as the *Caenorhabditis elegans,* where the attaching of beads is impossible, but perhaps this problem could be solved by staining the skin on the three required positions.

Statistical methods versus pattern recognition

Stationary states, swimming, crawling, and exploratory behaviors were not identified by recognizing a predefined pattern in the time series. Behavior classification was primarily based on statistical methods and not on pattern-recognition procedures. Indeed, systems using color-based tracking combined with movement-based tracking techniques (Balch et al. 2001) have limitations measuring immobility. If the animal remains immobile for some time, it cannot longer be tracked, and this represents a problem. There are different kinds of locomotion and certainly different kinds of immobility. Some periods of immobility or pauses could increase the capacity of the sensory systems to detect stimuli, and in this context, they should be measured. This segmentation into stops and progressions occurs in mammals (Drai et al. 2000; Kenagy 1973), insects (Collins et al. 1994), lizards (Pietruska 1986), etc. Our system has the possibility of measuring all these motionless periods, and detailed analyses of these observations, in the leech, will be published elsewhere (E. Garcia-Perez, A. Mazzoni, D. Zoccolan, H.P.C. Robinson, and V. Torre, unpublished data).

Analysis of speed and frequency provided enough information to discriminate between behaviors without introducing any ad hoc hypothesis on their characteristics. The prolongation of periodic behaviors beyond the well-identified window, described in *Prolongation of periodic behaviors beyond the well-identified window*, however, was based on the search of patterns of a priori known periods: 1.5 Hz for swimming and 0.2 Hz for crawling. The use of statistical methods was useful to avoid classification bias based on the experimenter expectations.

Reliability of state identification

Reliability of the identification of well-known behaviors, such as swimming, crawling, and peristalsis was checked by visual inspection of the videotape of the leech motion. This check was performed on randomly chosen episodes but was neither performed over the entire duration of the experiments—usually lasting several hours—nor for all leeches. These checks indicated correct behavior identification. Therefore we conclude that the system seems to be able to classify properly ~90% of the leech motion.

Besides swimming, crawling, peristalsis, and stationary states, we have identified another state, the exploratory state, which can account for ~30% of the leech motion. To analyze the complexity of the exploratory behavior, a visualization and analysis tool is needed. This tool should emphasize regularities, if they exist, and also should help generating new theories about the structure of this behavior. Our system characterized the exploratory state by a power spectrum of the elongation $e(n)$ with no clear peaks at any frequency. This exploratory behavior was likely to be composed by several substrates with distinct properties, which will be reported elsewhere (E. Garcia-Perez, A. Mazzoni, D. Zoccolan, H.P.C. Robinson, and V. Torre, unpublished results).

The proposed system for the automatic classification of the leech behavior has ~10% of unclassified states. The analysis of these unclassified states will be presented elsewhere.

Having validated the classification procedures for restrained leeches, the electrical activity of motoneurons was monitored with suction pipettes and/or intracellular sharp electrodes (unpublished observations) and its correlation with the behavior was analyzed.

Conclusion

A quantitative characterization of the behavior of the leech over extended intervals of time is an essential step for understanding its internal organization and how it is determined by interactions with the environment. This method for automatic characterization of the leech behavior is an important step toward understanding leech behavior and its properties (E. Garcia-Perez, A. Mazzoni, D. Zoccolan, H.P.C. Robinson, and V. Torre, unpublished observations). We believe that this system could be used also to characterize the behavior of other small invertebrates like worms and snails and possibly also some vertebrates such as snakes, lizards, frogs, and small fishes. Therefore this system could help to quantify and characterize abnormal patterns of locomotion of mutant animals contributing to understand the relationship between genetic disorders and behavior.

ACKNOWLEDGMENTS

We are indebted to H. Robison for reading the manuscript and useful comments and to W. Kristan for inspiring discussions and fruitful suggestions.

REFERENCES

Akaka WH and Houck BA. The use of an ultrasonic monitor for recording locomotor activity. *Behav Res Meth Instr Comp* 12: 514–516, 1980.

Averbeck BB and Lee D. Neural noise and movement-related codes in the macaque supplementary motor area. *J Neurosci* 23: 7630–7641, 2003.

Baader AP. Interneuronal and motor patterns during crawling behavior of semi-intact leeches. *J Exp Biol* 200: 1369–1381, 1997.

Baek JH, Cosman P, Feng Z, Silver J, and Schafer WR. Using machine vision to analyze and classify *Caenorhabditis elegans* behavioral phenotypes quantitatively. *J Neurosci Methods* 118: 9–21, 2002.

Balch T, Khan Z, and Veloso M. Automatically tracking and analyzing the behavior of live insect colonies. In: *Proceedings of the Fifth International Conference on Autonomous Agents,* edited by Mueller J, Andre E, Sen S, and Frasson C. Montreal: AA Press, 2001, p. 521–529.

Brodfuehrer PD and Thorogood MS. Identified neurons and leech swimming behavior. *Prog Neurobiol* 63: 371–381, 2001.

Bucher D, Akay T, DiCaprio RA, and Buschges A. Interjoint coordination in the stick insect leg-control system: the role of positional signaling. *J Neurophysiol* 89: 1245–1255, 2003.

Cacciatore TW, Rozenshteyn R, and Kristan WB Jr. Kinematics and modeling of leech crawling: evidence for an oscillatory behavior produced by propagating waves of excitation. *J Neurosci* 20: 1643–1655, 2000.

Cang J and Friesen WO. Model for intersegmental coordination of leech swimming: central and sensory mechanisms. *J Neurophysiol* 87: 2760–2769, 2002.

Chrásková J, Kaminsky Y, and Krekule I. An automatic 3D tracking system with a PC and a single TV camera. *J Neurosci Methods* 88: 195–200, 1999.

Collins RD, Gargesh RN, Maltby AD, Roggero RJ, Tourtellot MK, and Bell WJ. Innate control of local search behavior in the house fly, Musca domestica. *Physiol Entomol* 19: 165–172, 1994.

Drai D, Benjamini Y, and Golani I. Statistical discrimination of natural modes of motion in rat exploratory behavior. *J Neurosci Methods* 96: 119–131, 2000.

Eisenhart FJ, Cacciatore TW, and Kristan WB Jr.. A central pattern generator underlies crawling in the medicinal leech. *J Comp Physiol [A]* 186: 631–643, 2000.

Esch T, Mesce KA, and Kristan WB. Evidence for sequential decision making in the medicinal leech. *J Neurosci* 22: 11045–11054, 2002.

Friesen WO and Hocker CG. Functional analyses of the leech swim oscillator. *J Neurophysiol* 86: 824–835, 2001.

Friesen WO, Poon M, and Stent GS. An oscillatory neuronal circuit generating a locomotory rhythm. *Proc Natl Acad Sci USA* 73: 3734–3738, 1976.

Gharbawie OA, Whishaw PA, and Whishaw IQ. The topography of three-dimensional exploration: a new quantification of vertical and horizontal exploration, postural support, and exploratory bouts in the cylinder test. *Behav Brain Res* 151: 125–135, 2004.

Gray J, Lissmann HW, and Pumphrey RJ. The mechanism of locomotion in the leech (*Hirudo medicinalis ray*). *J Exp Biol* 15: 408–430, 1938.

Hoy JB, Koehler PG, and Patterson RS. A microcomputer-based system for real-time analysis of animal movement. *J Neurosci Methods* 64: 157–161, 1996.

Hoy JB, Porter SD, and Koehler PG. A microcomputer-based activity meter for multiple animals. *J Neurosci Methods* 72: 183–188, 1997.

Kantz H and Schreiber T. *Nonlinear Time Series Analysis.* Cambridge, UK: Cambridge Univ. Press, 1997.

Kenagy GJ. Daily and seasonal patterns of activity and energetics in a heteromyid rodent community. *Ecology* 54: 1201–1219, 1973.

Kristan WB Jr. Neuronal basis of behavior. *Curr Opin Neurobiol* 2: 781–787, 1992.

Kruk M. Measuring behavior into the twenty-first century. *Trends Neurosci* 20: 187–189, 1997.

Lent CM, Fliegner KH, Freedman E, and Dickinson MH. Ingestive behavior and physiology of the medicinal leech. *J Exp Biol* 137: 513–527, 1988.

Lewis JE and Kristan WB Jr. Quantitative analysis of a directed behavior in the medicinal leech: implications for organizing motor output. *J Neurosci* 18: 1571–1582, 1998.

Magni F and Pellegrino M. Patterns of activity and the effects of activation of the fast conducting system on the behaviour of unrestrained leeches. *J Exp Biol* 76: 123–135, 1978.

Martin PH and Unwin DM. A microwave Doppler radar activity monitor. *Behav Res Meth Instr Comp* 12: 517–520, 1980.

McIver MA and Nelson EM. Body modeling and model-based tracking for neuroethology. *J Neurosci Methods* 95: 133–143, 2000.

Miller LM, Escabi MA, Read HL, and Schreiner CE. Spectrotemporal receptive fields in the lemniscal auditory thalamus and cortex. *J Neurophysiol* 87: 516–527, 2002.

Muller KJ, Nicholls JG, and Stent GS. *Neurobiology of the Leech.* New York: Cold Spring Harbor Laboratory, 1981.

Oppenheim AV and Schafer RW. *Discrete-Time Signal Processing.* Englewood Cliffs, NJ: Prentice-Hall, 1989.

Orito K, Chida Y, Fujisawa C, Arkwright PD, and Matsuda H. A new analytical system for quantification scratching behavior in mice. *Br J Dermatol* 150: 33–38, 2004.

Pietruska RD. Search tactics of desert lizards: how polarized are they? *Anim Behav* 34: 1742–58, 1986.

Prut Y and Perlmutter SI. Firing properties of spinal interneurons during voluntary movement. I. State-dependent regularity of firing. *J Neurosci* 23: 9600–9610, 2003a.

Prut Y and Perlmutter SI. Firing properties of spinal interneurons during voluntary movement. II. Interactions between spinal neurons. *J Neurosci* 23: 9611–9619, 2003b.

Reichardt W. Autocorrelation, a principle for evaluation of sensory information by the central nervous system. In: *Principles of Sensory Communications,* edited by Rosenblith WA. New York: Wiley, 1961, p. 303–317.

Reichardt W. Nervous processing of sensory information. In: *Theoretical and Mathematical Biology*, edited by Morowitz HJ. New York: Blaisdell, 1965, p. 344–470.

Sommer S and Wehner R. The ant's estimation of distance travelled: experiments with desert ants, *Cataglyphis fortis. J Comp Physiol [A]* 190: 1–6, 2004.

Stange G and Hengstenberg R. Tri-axial, real-time logging of fly head movements. *J Neurosci Methods* 64: 209–218, 1996.

Stent GS, Kristan WB Jr, Friesen WO, Ort CA, Poon M, and Calabrese RL. Neuronal generation of the leech swimming movement. *Science* 200: 1348–1357, 1978.

Stern-Tomlinson W, Nusbaum MP, Perez LE, and Kristan WB, Jr. A kinematic study of crawling behavior in the leech, *Hirudo medicinalis. J Comp Physiol [A]* 158: 593–603, 1986.

Wehner R. Desert ant navigation: how miniature brains solve complex tasks. *J Comp Physiol [A]* 189: 579–588, 2003.

Wilson RJ and Kleinhaus AL. Segmental control of midbody peristalsis during the consummatory phase of feeding in the medicinal leech, *Hirudo medicinalis. Behav Neurosci* 114: 635–646, 2000.

Zakotnik J, Matheson T, and Durr V. A posture optimization algorithm for model-based motion capture of movement sequences. J Neurosci Methods 135: 43–54, 2004.

Zoccolan D and Torre V. Using optical flow to characterize sensory-motor interactions in a segment of the medicinal leech. *J Neurosci* 22: 2283–2298, 2002.

Zoccolan D, Giachetti A, and Torre V. The use of optical flow to characterize muscle contraction. *J Neurosci Methods* 110: 65–80, 2001.

Behavioral/Systems/Cognitive

Statistics of Decision Making in the Leech

Elizabeth Garcia-Perez,[1]* Alberto Mazzoni,[1]* Davide Zoccolan,[1]* Hugh P. C. Robinson,[2] and Vincent Torre[1]

[1]Scuola Internazionale Superiore di Studi Avanzati, 34014 Trieste, Italy, and [2]Physiological Laboratory, University of Cambridge, Cambridge CB2 3EG, United Kingdom

Animals continuously decide among different behaviors, but, even in invertebrates, the mechanisms underlying choice and decision are unknown. In this article, leech spontaneous behavior was tracked and quantified for up to 12 h. We obtained a statistical characterization, in space and time domains, of the decision processes underlying selection of behavior in the leech. We found that the spatial distribution of leech position in a uniform environment is isotropic (the same in all directions), but this isotropy is broken in the presence of localized external stimuli. In the time domain, transitions among behaviors can be described by a Markov process, the structure of which (allowed states and transitions) is highly conserved across individuals. Finally, a wide range of recurrent, deterministic motifs was identified in the apparently irregular and unstructured exploratory behavior. These results provide a rigorous description of the inner dynamics that control the spontaneous and continuous flow of behavioral decisions in the leech.

Key words: **leech behavior; dynamics; recurrence plot; periodic motion; exploratory motion; Markov process**

Introduction

Animals react to changes of the environment by responding with an appropriate behavior (Tinbergen, 1951; Drewes, 1984), from simple escape responses in invertebrates (Furshpan and Potter, 1959; Zucker, 1972; Bennett, 1997, 2000) to decision strategies in primates (Barraclough et al., 2004). An understanding of the decision process and the neuronal mechanisms underlying the selection of a specific behavior is a fascinating problem of contemporary neuroscience (Glimcher, 2002; Montague and Berns, 2002). As the pioneering work of sensory psychology and psychophysics (Green and Swets, 1966), decision making has been investigated primarily by looking at the behavioral responses of human subjects. More recently, neural correlates underlying decision processes have been investigated in primates performing visual recognition tasks (Freedman et al., 2001; Gold and Shadlen, 2002; Barraclough et al., 2004) and by using microstimulation of cortex areas involved in the representation of sensory stimuli (Salzman et al., 1990; Britten and Van Wezel, 1998; Ditterich et al., 2003). Similar experimental paradigms in simple invertebrates, such as the leech, revealed the existence of nontrivial interactions between different sensory modalities and trigger-like command neurons (Brodfuehrer and Friesen, 1986a,b,c; Brodfuehrer and Burns, 1995; Esch et al., 2002).

Approaches based on detection/decision tasks provide a solid framework for investigating the decision process in response to external sensory stimuli but are less suitable for understanding the inner neural dynamics that control spontaneous transitions from one behavioral category to another when animals are in an almost uniform and stable environment. This issue needs an alternative approach based on the analysis of the temporal structure of unconstrained animal behavior, which has been applied successfully in the analysis of behavior of different species (Bressers et al., 1995; Haccou and Meelis, 1992; Chen et al., 2002); however, this requires a reliable classification of all behavioral categories and continuous measurement of all possible transitions between these categories over a period of many hours.

In our work, we tried to overcome such difficulties by quantifying the behavior of the medicinal leech, the sensory capabilities and neuronal circuitry of which are relatively well understood (Baader and Kristan, 1992; Brodfuehrer and Thorogood, 2001; Esch et al., 2002). The animal was positioned in an almost homogeneous, stable, and isotropic environment: a large dish filled with dechlorinated water at a constant temperature and illuminated by dim, diffused light. An automatic system based on imaging with a CCD camera tracked three colored beads attached to the back of the leech and recorded its motion for up to 12 h. Statistical analysis based on the kinematic and spectral content of the leech motion (Mazzoni et al., 2005) allowed unambiguous classification of >90% of the leech motion into characteristic behavioral categories. We found that the mechanism by which the leech decides its behavior is adequately described by a Markov process, the transition rates of which are probably controlled by the firing of command-like neurons found in the leech head ganglion (Brodfuehrer and Burns, 1995; O'Gara and Friesen, 1995; Shaw and Kristan, 1997; Esch et al., 2002).

Materials and Methods

Animals and preparations

Adult leeches (*Hirudo medicinalis*) were obtained from Ricarimpex (Eysines, France) and kept at 5°C in tap water dechlorinated by aeration for 24 h. Two different kinds of preparations were used. The first preparation consisted of an intact leech free to move on a dish. The second prepara-

Received Sept. 14, 2004; revised Jan. 16, 2005; accepted Jan. 18, 2005.

We thank Dr. William Kristan for valuable scientific suggestions and helpful comments on this manuscript.

*E.G.-P., A.M., and D.Z. contributed equally to this work.

Correspondence should be addressed to Vincent Torre, Scuola Internazionale Superiore de Studi Avanzati, Via Beirut 2, 34014 Trieste, Italy. E-mail: torre@sissa.it.

D. Zoccolan's present address: McGovern Institute for Brain Research, Massachusetts Institute of Technology, Cambridge, MA 02139.

DOI:10.1523/JNEUROSCI.3808-04.2005

 0270-6474/05/252597-12$15.00/0

Table 1. Summary of the behaviors of the leech and criteria used for their identification

Behaviors	Description	Behavior identification
Stationary	Anterior and posterior sucker attached to the dish	Speed of the head $V_{head}(n)$ and $V_{tail}(n) < 1$ pixel/s
Still	Midbody still	Speed of the midbody $V_{midbody}(n) < 1$ pixel/s
Peristaltic-like	Midbody oscillating in a regular way	$V_{midbody}(n) > 1$ pixel/s, oscillating with a frequency of ~0.03 Hz
Head attached	Midbody oscillating in an irregular way	$V_{midbody}(n) > 1$ pixel/s with no regular oscillations
Swimming	Undulatory movement of the entire body	Maximal speed of the head $V_T^{max}(n)$ between 10 and 30 pixels/s; dominant frequency $f_T^d(n)$ of elongation (head to tail distance) between 1.3 and 1.7 Hz; and speed of the tail $V_T^{tail}(n) > 3$ pixels/s
Pseudo-swimming (ventilation)	Undulatory movement of the body and posterior sucker attached to the dish	$V_T^{max}(n)$ between 10 and 30 pixels/s; $f_T^d(n)$ of elongation between 1.3 and 1.7 Hz; and $V_T^{tail}(n) < 3$ pixels/s
Crawling	Alternating steps of elongation (posterior sucker attached) and contraction (anterior sucker attached)	$V_T^{max}(n)$ between 20 and 40 pixels/s; $f_T^d(n)$ of elongation between 0.16 and 0.24 Hz
Exploratory	Irregular oscillations of the head and anterior part of the body with the posterior sucker attached	$V_T^{max}(n)$ between 10 and 50 pixels/s; $f_T^d(n)$ of elongation <0.12 Hz
Abrupt movements	Rapid transitions between two states	Changes in position of at least 20 pixels in <5 s

tion consisted of an intact leech restrained by fixing the rear sucker of the animal to the center of the dish with one pin. Pins were carefully inserted through the animal's body, avoiding the penetration of the connective fibers running along the animal. When one pin was used, the leech was able to fully rotate around the pin and could explore the surrounding space.

All preparations were kept either in a round dish (15 cm diameter) or a square tank (15 × 15 cm) filled with dechlorinated water at constant temperature (20–24°C) and illuminated by dim, diffused light, with no abrupt spatial and/or temporal gradients of sensory stimuli, such as chemical or olfactory anisotropies, isolated visual cues, or abrupt illumination changes. The dechlorinated water in the dish was changed every 2 h to avoid the effects of serotonin and ions released by the leech (Schnizler and Clauss, 1998; Schnizler et al., 2002). In every preparation, three colored plastic beads (red, green, and blue) of a diameter of ~2 mm were glued on the back of the leech with Superglue (World Precision Instruments, Berlin, Germany). The red, green, and blue beads were attached near the head, the middle, and the tail of the leech.

Imaging

A color CCD camera (640 × 480 pixels of image size; model 231S; Watec, Tsuruoka, Japan) was used to view the leech from above. The camera was connected via the S-video-output to a frame grabber (PCI-1411; National Instruments, Milan, Italy) installed on a personal computer, which processed the images in real time. The colored beads placed on the back of the leech were tracked at 10 Hz by using a software program developed by Sergio Graziosi in our laboratory (Mazzoni et al., 2005) with LabVIEW 6.1 (National Instruments). Briefly, the software acquires images directly in the hue/saturation/lightness color space, and the tracking algorithm works in real time with no frequency constraints. A user-customized color matching is performed to convert each acquired frame into three binary images, one for each bead, in which the ON bit represents a pixel that fit in the expected color subspace. This software did not require saving all of the processed images but only the coordinates of the selected beads. In this way, it was possible to monitor the leech behavior for several hours without filling hard disk space. The positions of the beads on the image plane were acquired as Cartesian coordinates, and six time series were obtained as follows:

$$\begin{matrix} [x(n),\ y(n)]_{\text{head/red}}; \\ [x(n),\ y(n)]_{\text{midbody/green}}; \\ [x(n),\ y(n)]_{\text{tail/blue}} \end{matrix} \quad \text{for } n = 1 \ldots N \quad \text{steps},$$

where every step corresponds to 100 ms.

Some analysis required the motion to be studied in a polar system centered on the middle of the dish. In this way, Cartesian coordinates $(x,y)_{color}$ were transformed into a pair of planar polar coordinates $(\rho,\theta)_{color}$. When the leech was restrained from moving around by a pin inserted in its tail, the polar system had a clear geometrical and physiological meaning: ρ_{color} is the elongation of the leech body at the position marked by the bead (color), and θ_{color} is the angle between this position and a reference axis.

Sensory stimulation

In one series of experiments, a small pulsating light-emitting diode (LED) (at 0.5 Hz) was put above the water but near the edge of the dish. The behavior of the leech was first monitored for 3 h in control conditions of low and diffused light (without light stimulation). The animal was allowed to rest for 30 min, and then the light stimulation (LED) was initiated. In some experiments, two LEDs were placed diametrically opposite each other and flashed alternately at 1 s intervals. These experiments were done with restrained leeches, and the residence time distributions, in both light and control (no light) preparations, were analyzed.

Behavior classification

Often the leech moved in the dish for >12 h. The marker coordinate time series thus often comprised >100,000 samples, which had to be analyzed consistently. We therefore developed an automatic classification method for identifying the leech behavior, which is based on analyzing the kinematics and spectral content of the recorded time series and is described in detail in a previous work (Mazzoni et al., 2005).

Briefly, leech movements were classified into six different categories (Table 1): stationary (including still, peristaltic-like, and head-attached states), swimming, pseudo-swimming (or ventilation states), crawling, and exploratory and abrupt movements. At each time step n of the recorded time series, different criteria were used to discriminate one behavioral category from the others. For example, given the set of coordinates describing the leech dynamics at time step n, to test whether the current behavioral state was a stationary state, the speed of the head $[V_{head}(n)]$ and tail $[V_{tail}(n)]$ beads at time n was calculated. If the speed was less than 1 pixel per second (pixel/s), then the state was considered stationary. Additionally, to distinguish between the three different stationary states, the speed of the midbody $[V_{midbody}(n)]$ bead and its frequency were computed. If $V_{midbody}(n)$ was <1 pixel/s, then the state was classified as still; however, if $V_{midbody}(n)$ was >1 pixel/s, then the frequency of oscillation was computed, and, depending on this result, the stationary state was classified as peristaltic like (with a frequency of ~0.03 Hz) or head attached, during which the midbody oscillated in an irregular way.

The other behavioral categories were identified by computing the following parameters: (1) elongation $e(n)$, that is, the distance from head to tail beads; (2) maximal speed $V_T^{max}(n)$ of the head over a time window of width T centered in n (with T ranging from 20 to 50 s); (3) dominant frequencies $f_T^d(n)$ of the power spectrum $PS_n^T(f)$ of $e(n)$, computed over the same time window of width T. More specifically, oscillatory behaviors (such as swimming, pseudo-swimming, and crawling) could be reliably identified by the pairs of values $[V_T^{max}(n), f_T^d(n)]$. For instance, swimming episodes were consistently characterized by $f_{20}^d(n) \sim 1.5$ Hz and $V_{20}^{max}(n) \sim 20$ pixels/s, whereas crawling was characterized by $f_{50}^d(n)$

~0.2 Hz and $V_{50}^{max}(n)$ ~30 pixels/s. The spectral analysis of $e(n)$ also allowed identification of the exploratory states, because events with $f_{50}^{d}(n)$ at the lowest resolved frequencies (~0.1 Hz) matched correctly with the exploratory movements (i.e., slow and irregular oscillations of the head and the anterior part of the body). An exhaustive inventory of all identified leech behaviors and the criteria used to classify them is given in Table 1. Note that all definitions of behavior are based on units of pixels, in which 1 pixel = 0.4 mm.

Statistical analysis of stationary, swimming, and exploratory states

Space distribution. Once a specific behavior was identified across the whole time series, the mean values of the polar coordinates for the head $[\rho_{behav}(i), \theta_{behav}(i)]$ in each time interval $i = 1, \ldots, N_{behav}$ in which the leech was performing that behavior were computed (N_{behav} is the total number of episodes found for that behavior). The distributions of angles $\theta_{behav}(i)$ were plotted as polar histograms (see Fig. 2*B*,*D*), with an angular bin size of 18°. If the analyzed behavior is isotropic, then the number of recorded states with $\theta_{behav}(i)$ belonging to a given angular sector must be distributed according to a Poisson distribution with mean $\mu =$ (number of occurrences N_{behav})/(number of sectors S). A χ^2 test was used to check whether the obtained distributions were Poisson distributions ($p > 0.05$) and therefore whether the behavior was isotropic. If the behavior was found to be significantly anisotropic, then a *post hoc* test was used to specifically test whether such anisotropy was caused by one or more sectors that were overpopulated and to find out the orientation of such sectors (i.e., the preferred direction for that behavior). The *post hoc* test was based on the null hypothesis that the distribution of states per sector is not significantly different from a Poisson distribution and that therefore the probability of having Z states or less in a sector is the following:

$$P_{\mu}(n \leq Z) = \sum_{i=0}^{Z} P_{\mu}(i) .$$

Then, the probability Q that n exceeds Z, at least in one sector, is the following:

$$Q(Z) = 1 - \left(\sum_{i=0}^{Z} P_{\mu}(i) \right)^{S} .$$

In Figure 2*B–D*, the magenta circle indicates the value of Z associated with $Q = 0.05$. Note that this value depends only on the number of states and the number of sectors.

Time series correlation. To study the linear properties of the sequence of identified states, series of average angles $\theta_{behav}(i)$ and lengths $\rho_{behav}(i)$, with $i = 1, \ldots, N_{behav}$, were considered as the outcome of two stochastic processes $\Theta_{behav}(i)$ and $P_{behav}(i)$. First, we assessed whether these stochastic processes were stationary, testing the stability of the mean and variance on the first and second half of the series (ANOVA test).

The correlation between consecutive values $\theta_{behav}(i)$ [and consecutive values $\rho_{behav}(i)$] was then evaluated by computing the autocovariance of the process $\Theta_{behav}(i)$ [and of the process $P_{behav}(i)$]. Similarly, the correlation between consecutive pairs of values $\theta_{behav}(i)$ and $\rho_{behav}(i)$ was evaluated by computing the covariance between the processes $\Theta_{behav}(i)$ and $P_{behav}(i)$. Statistical significances of autocorrelation and cross-correlation values were evaluated by a two-tailed normal test under the assumption that correlation values for uncorrelated time series are normally distributed with mean zero and variance $1/(N - l - 3)$, where N is the number of samples in the two series, and l is the lag number. Correlation values were considered significant at $p < 0.05$. The number of consecutive significantly correlated states around $n = 0$ gives the size of the central peak of the autocorrelation. The width of the central peak of the autocovariance function gives a measure of the "memory" of the stochastic process and indicates on how many previous states the identity of the state depends (Priestley, 1981). To compare the processes $\Theta_{behav}(i)$ and $P_{behav}(i)$ with random processes of the same statistical properties but without any correlation ("no memory"), the original series $\rho_{behav}(i)$ and $\theta_{behav}(i)$ were scrambled before the autocovariance was computed.

Time structure of the sequence of behaviors. The time structure of the sequence of behavioral states was studied by computing, for any identified behavior, the distribution of the duration Δt of the time intervals (residence times) during which that behavior was performed. In every experiment and for every behavior, this distribution had a high and narrow peak centered on a small Δt (usually <10 s), which decayed to 0 with increasing Δt. This suggested that the sequence of behaviors could be modeled as a Markov process in which the residence time for each behavior is distributed as an exponential or a mixture of exponentials (Haccou and Meelis, 1992). Therefore, for each behavior, the observed residence time distribution was fit by an exponential function, $f(\Delta t) = A\exp(-\Delta t/\tau)$, or by the sum of two exponential functions. To determine whether two exponentials were required, goodness of fit was tested with a χ^2 test, and a one-exponential fit was accepted only if there was no significant difference ($p > 0.05$) between the data and the fit. When one exponential was insufficient, two exponentials were always found to be sufficient by the χ^2 criterion.

Power spectral analysis. An informative parameter about the motion of the leech is the elongation $e(n)$, i.e., the distance between the head and the tail, which varies during every oscillatory behavior. As mentioned previously, during the classification procedure (Mazzoni et al., 2005), for every nonstationary point in the time series, a power spectrum PS(f) of the elongation over the portion of the time series centered on that point and having a half-size of 10 s was computed to accurately detect high-frequency oscillations. A second power spectrum with a half-size of 25 s was then computed to discriminate low-frequency oscillations. Sometimes, power spectra were computed even for much larger windows to analyze global properties of the behavior (see Fig. 4*A*,*B*). Welch's averaged modified periodogram method was used (*pwelch* function in Matlab; MathWorks, Natick, MA), with 50% overlap between successive time windows, each one being one-fourth the size of the analyzed interval. Points of the resulting power spectra were averaged within logarithmically spaced frequency bins to smooth the power spectrum at high frequencies. Power spectra were further smoothed by averaging every spectral point PS(f) over a semi-octave centered on each frequency f to enhance detection of any peaks (Mazzoni et al., 2005).

Recurrence analysis of exploratory states. Complex exploratory motion was investigated using the recurrence plot technique (Eckmann et al., 1987). The advantage of this approach is its capability of detecting deterministic or repeated component patterns even in highly nonlinear and irregular time series, which would be lost through averaging in linear measures such as the power spectrum (or equivalently, the autocorrelation function). First, an m-dimensional delay representation (Kantz and Schreiber, 1997) is constructed for a 1000 s segment of motion time series. The delay coordinate vectors $\mathbf{d}_n$ are given by the following:

$$\mathbf{d}_n = (y_{n-(m-1)v}, y_{n-(m-2)v}, \ldots, y_{n-v}, y_n)$$

These represent successive short pieces of the waveform history preceding each point y_n in the time series. We used $m = 20$ and lag $v = 2$. A 4000×4000 diagonally symmetric matrix $\mathbf{c}$ is then plotted in which the point at row i, column j is color coded (in gray scale) according to the Euclidean distance between $\mathbf{d}_i$ and $\mathbf{d}_j$ as follows:

$$c_{ij} = \sqrt{(d_{i1} - d_{j1})^2 + (d_{i2} - d_{j2})^2 + \cdots + (d_{im} - d_{jm})^2} .$$

Within this plot (see Fig. 5), dark colors represent similarity, or low distance, between delay vectors. A sequence of intensely dark points along a line of slope −1 represents a flow in which history repeats itself. We visually scanned the recurrence matrix for diagonal lines satisfying a threshold similarity condition of length at least twice the duration of the delay vector (>19 s). Having identified one diagonal, all similar repeats within the time series are easily extracted as those diagonal lines that intersect a horizontal (or vertical) line drawn through the center of the first line. The repetition frequency of the pattern is quantified by the number of such sister diagonals (for a diagram of this process, see Fig. 5). Repeats that follow the same trajectory but with a different timescale appear as diagonal lines with different slopes.

Estimation of transition probabilities and test of sequential dependences. Once every point of the time series has been classified, the behavior of the leech can be seen as a sequence of identified behavioral states. To estimate the transition probabilities between pairs and triplets of behaviors, we computed, for each behavior A, the following quantities: the number of occurrences N_A of behavior A; the number of times N_{AB} that behavior A was followed by behavior B (i.e., the number of transitions $A \rightarrow B$), for all possible following behaviors B; the number of times N_{XA} that behavior A was preceded by behavior X (i.e., the number of transitions $X \rightarrow A$), for all possible preceding behaviors X; the number N_{XAB} of transitions $X \rightarrow A \rightarrow B$, for all possible preceding behaviors X and following behaviors B. Then, the probabilities of first-order transitions $A \rightarrow B$ were estimated as $P(B/A) = N_{AB}/N_A$. Similarly, the probabilities of second-order transitions $X \rightarrow A \rightarrow B$ were estimated as $P(B/A,X) = N_{XAB}/N_{XA}$. Values of these transition probabilities during the first and second half of the experiments were compared with a χ^2 test to check whether the process was stationary. Differences between the two sets were considered significant at $p < 0.05$.

To test whether the sequence of behavioral states could be modeled as a first-order Markov chain, we used the χ^2 test for first- against second-order dependences in the sequences of identified states (Haccou and Meelis, 1992). Given the null hypothesis that $P(B/A) = P(B/A,X)$, for all triplets $X \rightarrow A \rightarrow B$, we first computed the χ^2 test statistics for each behavior A: $\chi^2_A = \Sigma_X \Sigma_B [N_{XAB} - N_{XA}P(B/A)]^2/N_{XA}P(B/A)$, where the summation is taken over all behaviors X and B, preceding and following A. Then, a global χ^2 test statistics was computed as $\chi^2 = \Sigma_A \chi^2_A$, i.e., taking into account all possible intermediate behaviors A. The degrees of freedom of the global χ^2 test statistics are $k = b(b-2)^2$, where b is the number of different behaviors identified in the analyzed experiments; however, if some of the transitions toward or from A occur rarely or not at all (i.e., with almost zero probability), this number is overestimated. In this case, the correct number of degrees of freedom becomes $k = \Sigma_A (b - v_A - 1)(b - w_A - 1)$, where v_A and w_A are the number of transitions toward A and from A, respectively, that cannot occur (Haccou and Meelis, 1992). Deviations from the null hypothesis of a first-order-dependent Markov chain were considered significant at $p < 0.05$.

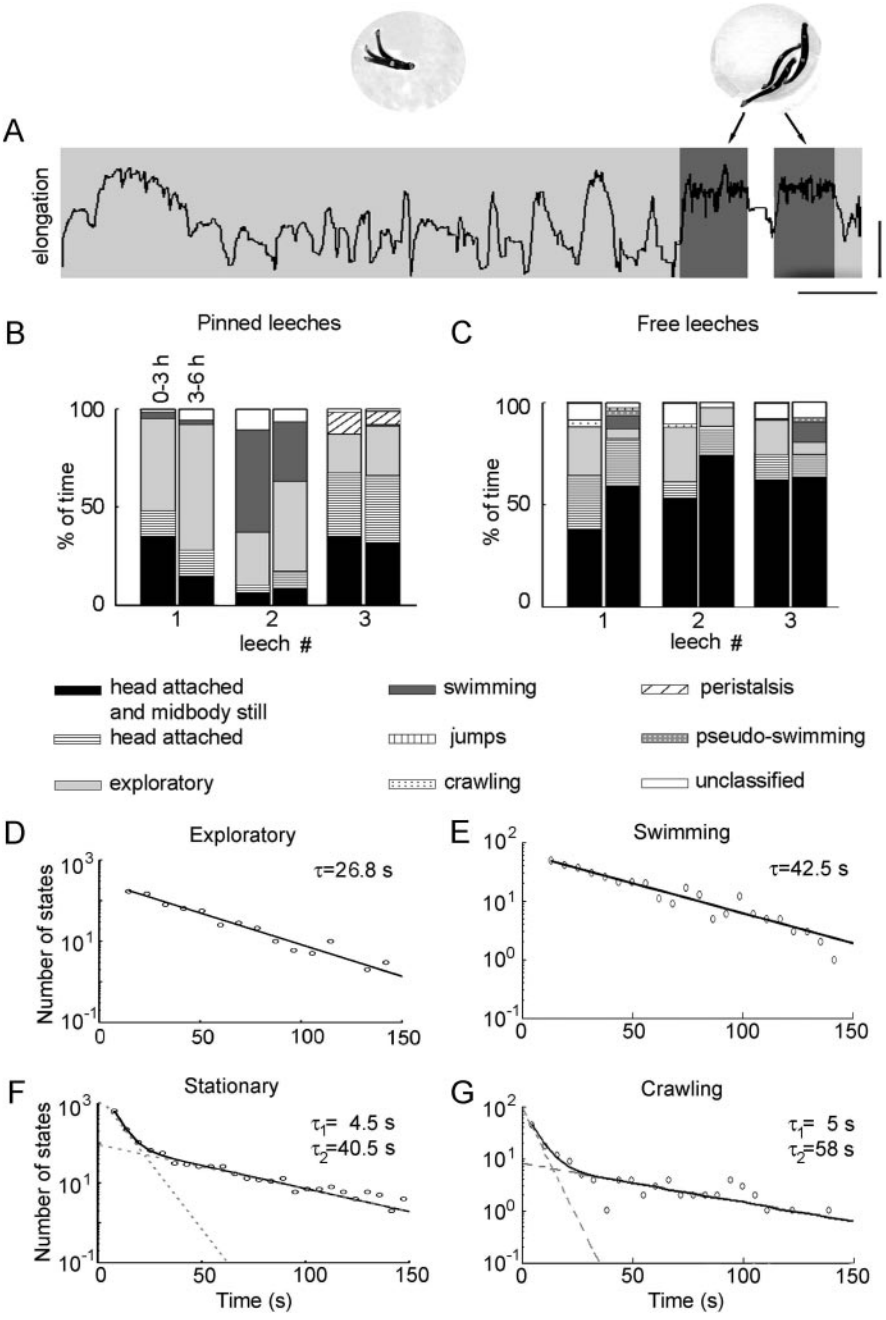

Figure 1. Behaviors of the leech. ***A***, Elongation $e(n)$ of a freely moving leech tracked over time. Exploratory behaviors are shown in light gray, and swimming behaviors are shown in dark gray. Photos show three superimposed pictures of the leech exploring (left) and three superimposed pictures of the leech swimming (right). Scale bars, 3.5 cm. ***B***, Time distribution of behaviors for three pinned leeches for the first 3 h of recording and for the following 3 h. Behaviors are coded as shown at the bottom of ***B***. ***C***, As in ***B***, but for three free leeches. ***D–G***, Distribution of residence time for exploratory (***D***; pooled data obtained from 7 leeches), swimming (***E***; 4 leeches), stationary (***F***; 11 leeches), and crawling (***G***; 4 leeches) states. Duration for each distribution is shown in a semilog plot. Continuous lines represent single- and double-exponential fits for distributions; time constants are indicated.

Results

Leech behavior was studied by observing leech motion in a dish with a color CCD camera. Leeches that were completely free to move exhibited their usual behavior, i.e., they crawled, swam, explored, and stayed stationary. Leeches restrained by having one pin inserted in the tail moved and explored the dish for several hours before showing any sign of weakness such as, for instance, small responses to touch, low erection of the annulus, or total immobility. The behavior of the leech was monitored, often for up to 12 h, by imaging and tracking three colored beads attached to its back. In total, 25 freely moving leeches and 27 restrained leeches were observed, and their behavior was quantified. Because of the high variability of behaviors from leech to leech (Fig. 1*B*,*C*), only some of these observations were suitable for each particular kind of analysis. For instance, the properties of swimming were quantified from experiments during which the leech was swimming most of the time. As a consequence, the total number of experiments (i.e., leeches) included in each behavioral analysis depends on that particular behavior and analysis. This number is reported in the text and in the legend of each figure.

Behavior inventory and distribution of the durations of each state

Figure 1*A* illustrates the time evolution of the elongation $e(n)$, i.e., distance between the head and tail bead, while the leech moved freely in a covered dish. The analysis of $e(n)$ (Mazzoni et al., 2005) allowed us to identify well known leech behaviors such as crawling and swimming, which are shown in Figure 1*A* (example of swimming, dark gray, and three superimposed snapshots, right).

By analyzing the motion of the head, midbody, and tail, some other behavioral categories were identified (Mazzoni et al., 2005) and are summarized in Materials and Methods and Table 1. Additionally, there were some unclassified states, characterized by slow drifts or by oscillations superimposed on an apparently exploratory event. One example of this is shown between two swimming states in Figure 1*A* (white). Unclassified states comprised, on average, ~10% of the observation time.

Leeches not only show stationary and periodic states, but they also exhibit a more complex behavior, referred to here as exploratory (Fig. 1*A*, light gray). This behavioral category is characterized primarily by the absence of any evident regularity (Table 1). Three superimposed snapshots of exploratory behavior are shown in the left inset of Figure 1*A*. Figure 1*B* shows the relative occurrence of different behavioral categories observed over 6 h of continuous recording of leech motion (three restrained leeches). For each leech, statistics were obtained from 0 to 3 h (left bar) and from 3 to 6 h (right bar), respectively. Figure 1*C* shows the same statistics but for three freely moving leeches. These data indicate a degree of variability among individuals, but the repertoire of behaviors identified for a given animal as well as the percentage of time spent in each behavior were well preserved during the first and second 3 h of observation.

The distribution of the residence times of exploratory, swimming, stationary, and crawling states is shown in Figure 1*D–G*. The distributions for exploratory and swimming states could be reliably fitted (χ^2 test; $p > 0.05$) by a single-exponential function with time constants $\tau = 26.8$ s and $\tau = 42.5$ s, respectively (Fig. 1*D*,*E*). On the other hand, the distributions of the residence time for stationary and crawling states were significantly different (χ^2 test; $p < 0.05$) from the best fit achieved with a single-exponential function; however, in both cases, the sum of two exponential functions gave a best fit that did not significantly differ from the observed distribution (χ^2 test; $p > 0.05$). The time constants found were $\tau_1 = 4.5$ s and $\tau_2 = 40.5$ s for stationary states and $\tau_1 = 5$ s and $\tau_2 = 58$ s for crawling states (Fig. 1*F*,*G*). All of these fits have been calculated on distributions of pooled states from many leeches (7 for exploratory, 4 for swimming, 11 for stationary, and 4 for crawling) because single experiments did not have enough data to provide a reliable evaluation of the time constants; however, after the best fit for each pooled distribution was found, we tested whether individual distributions were consistent with that fit. The results of this second test are as follows: six of seven residence time distributions of exploratory states, four of four distributions of swimming states, 11 of 11 of stationary states, and four of four distributions of crawling states were not significantly different (χ^2 test; $p > 0.05$) from the corresponding fitting functions obtained with the pooled data.

Spatial distribution

Leeches appear to wander around uniformly. Indeed, when the tail is pinned to the center of a round or square dish, the leech explores uniformly in every direction (Fig. 2*A*), and the orientation of its body during stationary states is evenly distributed over all θ coordinates. To test the isotropy of leech orientation during stationary states, the area of the dishes was divided into 20 sectors of 18° each (Fig. 2*B*). To have expected frequencies of at least five states per sector, seven experiments were done with pinned leeches, with at least 100 stationary states each, were analyzed. In seven of seven leeches, the distribution of the number of states per sector was not significantly different from a Poisson distribution (χ^2 test; $p > 0.05$), as expected for an isotropic behavior. As an example, four superimposed representative polar plot distributions (a different color for each leech) are shown in Figure 2*B*. These distributions show the leech orientation for the first 100 stationary states. The magenta circle indicates the confidence threshold for each sector, with $p < 0.05$ of being exceeded (see Materials and Methods), given the null hypothesis of isotropic behavior. The radius of this circle depends only on the number of states analyzed and on the number of sectors and therefore is the same for every data set analyzed in the figure. If one sector exceeds this confidence threshold, then the distribution of states is anisotropic, because the animal visited that sector a significantly higher number of times than the others. For the experiments shown in Figure 2, because no sector exceeded this threshold, there was no significant deviation from isotropy. Similar distributions were obtained for all experiments ($n = 7$).

Free leeches spent most of the time near the dish edges (Fig. 2*C*), but again the θ distribution of stationary states did not have any statistically privileged direction. For this analysis, five experiments with free leeches with at least 80 stationary states were analyzed (just three of them having >100 states). The number of occurrences per sector followed a Poisson distribution in five of five leeches ($p > 0.05$). As an example, the superimposed polar distributions for the first 50 stationary states observed in four different leeches (to simplify the plot) are shown in Figure 2*D* with their confidence threshold.

Temporal distribution

Elongations ρ and orientations θ during stationary states were ordered according to their temporal occurrence, and their temporal statistics were evaluated. Autocorrelation analysis for both ρ and θ (Fig. 2*E*,*F*, black line) exhibited a small but significant bump (normal test; $p < 0.01$) flanking the central peak, with a width corresponding to two to eight successive states that were significantly correlated. This bump was not observed when the original time series was scrambled (Fig. 2*E*,*F*, gray line). This phenomenon was observed and was significant in seven of seven free leeches and in seven of seven pinned leeches, with an average central peak width for ρ series (Fig. 2*G*, black bars) of 5 ± 2 states for pinned leeches and 4 ± 2 states for free leeches. The same results were obtained for θ series (Fig. 2*G*, white bars), with a central width of 6 ± 2 and 3 ± 1 states, respectively, indicating the existence of a correlation between positions of successive stationary states. Values of ρ and θ were not significantly cross-correlated.

Effects of sensory stimulation

We further tested how the spatial distribution of leech locations changed as a consequence of localized sensory stimulation. For this purpose, we used seven pinned leeches (different leeches from those in Fig. 2). Five of them were monitored when one light was flickering, and the other two were monitored when two lights were flickering. Figure 3 shows some representative polar plots in which the angular distribution of the position of the leech during stationary states is reported. Without sensory stimulation, the distribution of stationary states for all tested leeches was isotropic

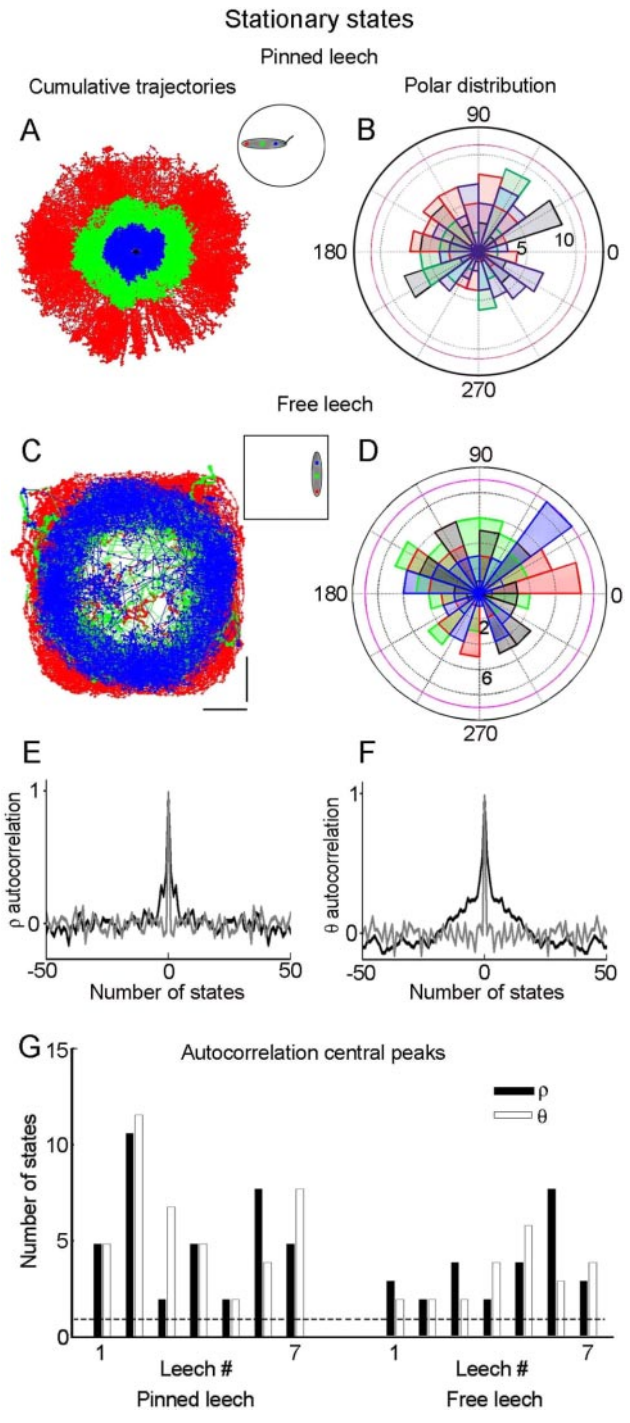

Figure 2. Analysis of stationary states. ***A***, Displacement of a restrained leech (the position of the pin is marked with a black circle). The trajectories of the head, midbody, and tail, shown in red, green, and blue, respectively, show that the leech uniformly explores the surface of the dish. The inset shows a scheme of the restrained leech preparation. ***B***, Polar plot distribution of stationary states of four different restrained leeches (different color for each leech). The polar plot represents the number of stationary states for every direction, and the magenta circle shows that the distribution of stationary states does not have any statistically privileged direction ($p > 0.05$). ***C***, As in ***B***, but for a freely moving leech in a square dish. Scale bars, 3.5 cm. ***D***, Polar plot distribution of stationary states of four freely moving leeches, which also demonstrates the spatial uniformity of exploration ($p > 0.05$). ***E***, ***F***, Superimposed plots of the autocorrelation of ρ and θ, respectively, for stationary states (black) and of the same series scrambled (gray). Black traces show a small but significant bump flanking the central peak, with a width corresponding to 5–10 successive states. ***G***, Width of the autocorrelation central peaks for seven pinned (left) and seven free (right) leeches, representing the mean number of significantly correlated successive states for ρ (black) and θ (white). The horizontal dotted line indicates the central spike expected even in the absence of any correlation.

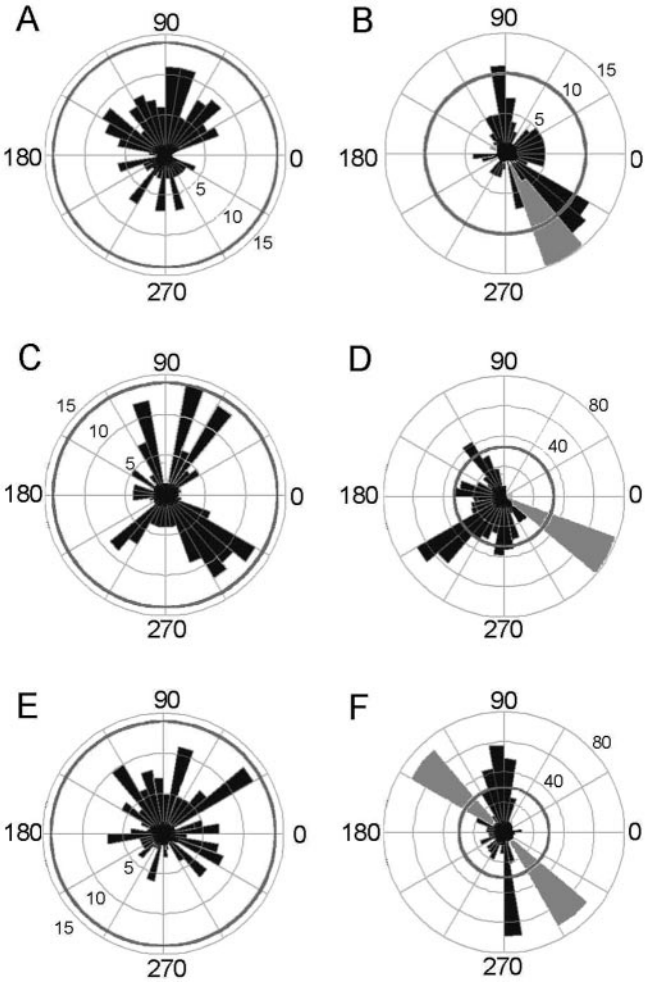

Figure 3. Effects of external stimulation. ***A***, ***C***, ***E***, Polar plots with the distribution of the leech body orientations during stationary states in three different experiments using the pinned leech, showing that, in absence of any stimulation, the leech explores the dish uniformly with no preferential direction. ***B***, ***D***, ***F***, Polar plots of three different experiments using pinned leeches, showing the angular distribution of the position of the leech during stationary states in the presence of an external stimulation (light is represented as gray triangles). ***F***, Two (almost opposite) lights were used. Dark gray circles indicate 5% confidence circle for the Poisson distribution of states per sector, as required by an isotropic behavior.

(the number of occurrences per sector followed a Poisson distribution; $p > 0.05$). As an example, the distribution of stationary states for three leeches is shown in Figure 3, *A*, *C*, and *E*, in which no sector exceeds the significance threshold (dark gray circle) for anisotropy; however, in four of five cases with one light and in two of two cases with two lights, the presence of the light broke this isotropy. Figure 3, *B*, *D*, and *F*, shows the angular distributions during stationary states for these same three leeches when the lights were switched on (the gray triangles indicates the orientation of the lights). In all three cases, some sectors were more populated than the statistical threshold for acceptance of isotropy ($p < 0.05$) (dark gray circle). Although a systematic relationship between orientation of light and preferred resting orientation of the leeches could not be found, in general the leeches avoided spending time under the light sources (Fig. 3*D*). Their preferred direction was often close to but not coincident with the light source, as if leeches moving toward the light source were constrained to proceed along a nearby direction (Fig. 3*B*).

Analysis of exploratory states

Well resolved peaks characterized the smoothed power spectrum of swimming and crawling episodes, at 1.5 and 0.2 Hz, respectively (Mazzoni et al., 2005). On the other hand, exploratory states were characterized by a $1/f^S$ distributed power spectrum (where S is the slope of the power spectrum when plotted on a logarithmic scale), with no resolvable peaks. Furthermore, the shape of the smoothed power spectrum of $e(n)$ during exploratory episodes was very similar across different free and pinned leeches. Examples showing a superposition of four power spectra corresponding to different exploratory episodes observed in four pinned (reddish curves) and four free (bluish curves) leeches are reported in Figure 4, *A* and *B*, respectively. Similarity among exploratory power spectra was better quantified by computing their $1/f^S$ fit (Fig. 4*A*,*B*, black lines). The slope S of the power spectrum was very similar across different pinned (red bars) and free (blue bars) leeches, as shown by the slope distributions reported in Figure 4*C*. The value of the slope S is highly indicative of the kind of process analyzed and can be considered, in this case, as a measure of the correlation of the different movements composing the behavior (Berg, 1993; Szendro et al., 2001). The observed similarity suggests that, although very different and very irregular, all exploratory episodes belong to the same dynamics. For instance, the average slope of the power spectrum was 1.8 ± 0.2 for free (blue bars) and 2.0 ± 0.2 for pinned (red bars) leeches. Although small, the difference between average slopes in the two sets was significant (ANOVA test; $p < 0.05$). The slope of the power spectrum is close to $1/f^2$, indicating that exploratory movements approximately follow random walk dynamics (Berg, 1993).

Despite the quasi-periodic appearance of exploratory motion (Fig. 1*A*, first light gray patch), its power spectrum was not associated with peaks at any frequency. Such a broadband spectrum is indicative of noise or nonlinear deterministic chaos. As a test for low-dimensional nonlinear deterministic chaos, which could be caused by, for example, the interactions of a few underlying motor oscillators, we examined whether exploratory time series could be predicted better by linear prediction, by nonlinear prediction, or by nonlinear prediction of the phase-randomized time series (Kantz and Schreiber, 1997); however, the best result was obtained using linear prediction (data not shown). Thus, we were not able to find evidence for simple low-dimensional chaos in exploratory time series.

We also verified that, during exploratory events, the leech visited the entire surrounding environment (Fig. 4*D*), with no preferential direction or location, and that the distribution of the head speed V_{head} was Gaussian (Fig. 4*E*), as it was for the other behaviors (Mazzoni et al., 2005). Even if there was a characteristic speed for this behavior ($\mu = 35$ pixels per second) that was similar for pinned and free leeches, the distribution was broad ($\sigma = 13$ pixels per second) compared with other behaviors (Mazzoni et al., 2005), as shown by the statistics for seven pinned and seven free leeches presented in Figure 4*F*. This broad distribution suggested heterogeneity of activated motor patterns, as expected for the highly irregular motion characterizing the exploratory behavior. Indeed, using the recurrence plot technique, it was possible to identify qualitatively various repeated, effectively deterministic motifs within the exploratory motion. Figure 5*A* shows an example of a recurrence plot of a 1000 s section of exploratory behavior. A pattern of similar behavior repeated at two different points in the time series was observed as a diagonal line segment of slope -1. All other similar patterns within the time series could be picked out as those diagonal line segments, which intersect the same horizontal as the first identified diagonal. An example of this is shown in the inset; this pattern was found several times along the recurrent plot, and some of these are shown superimposed in Figure 5*C* as pattern 4. This pattern and some other recurrent patterns (Fig. 5*C*, patterns 1, 11) are superimposed in black on a piece of the original time series in Figure 5*B*. These patterns show that the evolution of the exploratory behavior is similar at different times over periods lasting tens of seconds.

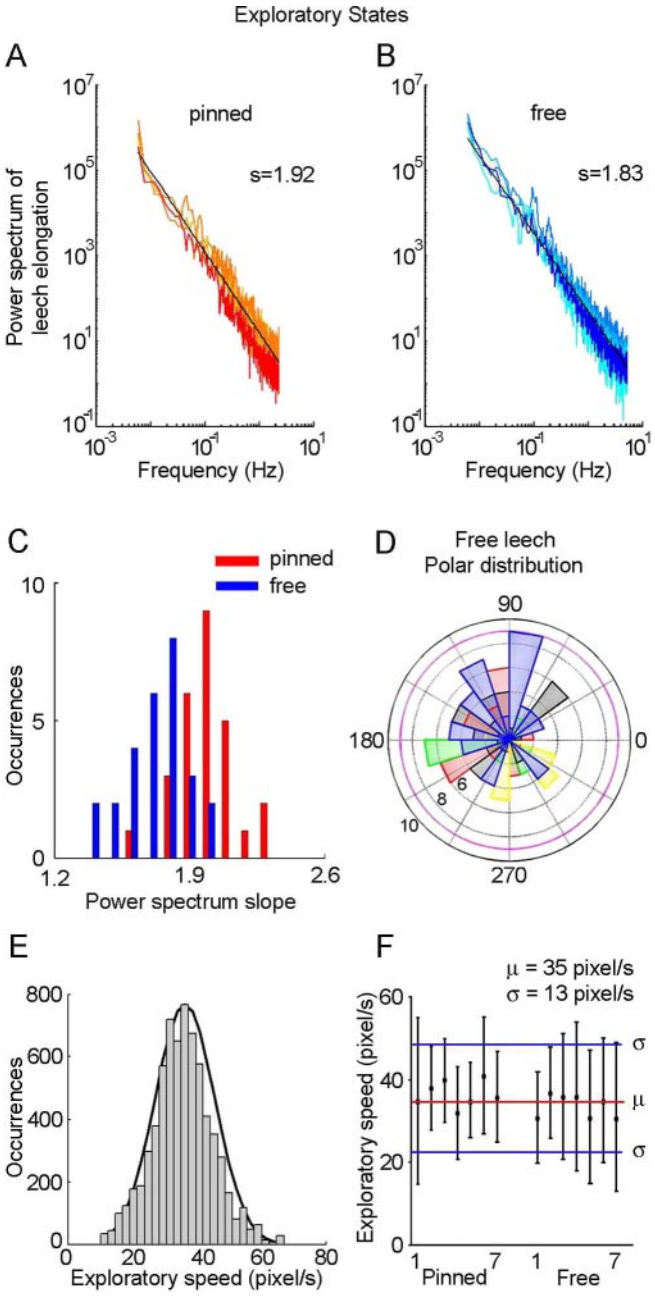

Figure 4. Spectral analysis for exploratory states. ***A***, Superposition of four smoothed power spectrums for $e(n)$ during four episodes (lasting 100 s each) of exploratory behavior observed in different leeches. The black line represents the $1/f^S$ fit to one of the power spectra. The slope S is indicated. ***B***, As in ***A***, but for four free leeches. ***C***, Distribution of the power spectrum slope S during exploratory episodes observed in 54 leeches, 27 pinned (in red) and 27 free (in blue). ***D***, Polar plot distribution of the position of the leech during exploratory states observed in five free leeches. Confidence interval is shown in magenta. ***E***, Maximum speed distribution during exploratory behavior (calculated for 10 s) of one leech. This plot is well fit by a Gaussian distribution (black). ***F***, Mean and SD of the Gaussian fits for exploratory speeds of seven pinned leeches and seven free leeches.

We also performed the same analysis after Fourier transforming, randomizing the phase information, and taking the inverse transform. This phase-randomized surrogate series (Kantz and Schreiber, 1997) has the same power spectrum and autocorrelation as the original time series and therefore should give the same results if a linear stochastic process produced the data; however, there were in the original time series a number of recurrent patterns that were not observed in the phase-randomized surrogate. The 12 most common of these are shown in Figure 5*C*. They could be separated into several groups: (1) abrupt movements, as patterns 1 and 4, indicated in the original trace shown in Figure 5*B*, and (2) quasi-periodic fragments and oscillating extensions sandwiched by smooth oscillations, such as patterns 7–12.

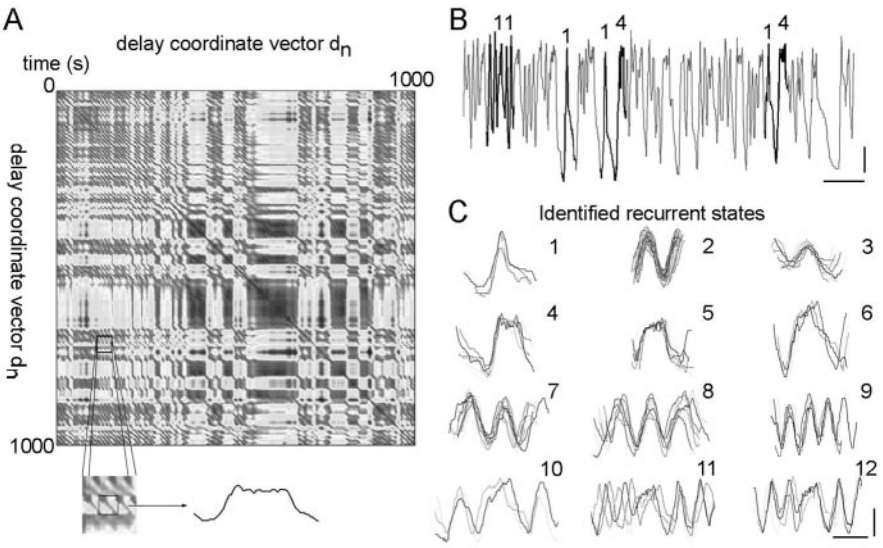

Figure 5. Analysis of the complex exploratory motion. ***A***, Recurrence plot obtained for 1000 s of exploratory behavior. Dark colors represent similarity or low distance (see Materials and Methods). Patterns of similar behavior repeated in the time series are represented by diagonal line segments (slope of −1), as shown in the inset. ***B***, Original time series (gray) for an exploratory period with some repeated patterns (black) superimposed. Calibration: 50 s, 1.2 cm. ***C***, Some repeated patterns obtained for the time series analyzed in ***A*** and ***B***. All of these patterns were absent from the phase-randomized surrogate of the time series. Calibration: 10 s, 2 cm.

Transitions between behaviors

A process in which the probability of transition between different states is determined only by the identity of the most recent state is said to be markovian. The exponential distribution of duration of exploratory, swimming, crawling, and stationary states (Fig. 1*D*,*G*) shows that every behavior or subcategory of behavior had a probability of ending per unit of time equal to $1/\tau$ (where τ is its characteristic time constant). This is highly suggestive of a Markov process underlying the decision mechanisms that control transitions among different behaviors. To verify this possibility, transitions between different behavioral categories were analyzed. The probability $P(B/A)$ of the first-order (or one step) transition $A \rightarrow B$, i.e., the probability of state $k+1$ belonging to behavior B if state k belongs to A, was estimated for each pair of behaviors (A, B), as described in Materials and Methods. The corresponding transition rate, i.e., the probability per unit of time for the leech of switching to behavior B when it is in a state belonging to the behavior A, is then given by $P(B/A)/\tau_A$.

Figure 6*A* shows, for a pinned leech, one-step transition probabilities between five different behaviors, for the first (0–3 h) and second (3–6 h) half of the experiment (black and white bars, respectively). In each panel, the transition probabilities in the first half of the recording session were not significantly different from those of the second half (χ^2 test for homogeneity of distributions; $p > 0.05$), and the same result was obtained for four of five leeches examined. This indicates that the decision process was stationary in time.

Transition probabilities varied from leech to leech, but some properties of the Markov process were present in all leeches. For instance, peristalsis was always followed by stationary states (Fig. 6*A*, fourth panel), and transitions usually occurred among stationary, exploratory, and stationary states (Fig. 6*A*, first three panels). Some transitions, like swimming to crawling and crawling to swimming, were never observed in free leeches (six experiments); however, when the water level was not sufficient to fully cover the leech body, hybrid behaviors such as swimming-like oscillations superimposed on the elongation phase of crawling (Fig. 7) (Esch et al., 2002) and elongation followed by a swimming behavior were sometimes observed (data not shown). Figure 7*A* shows the time displacement of the x and y coordinates of the head (red), midbody (green), and tail (blue). Four crawling steps are shown during which the body was oscillating. In Figure 7*B*, the space displacement of the same hybrid behavior is shown. As can be seen, the leech was crawling from the middle to the bottom of the plot (y direction) with oscillatory movements (x direction) superimposed on the elongation step. Note the difference between the x and y scales.

To verify that the sequence of behavioral states could be modeled as a first-order Markov process, we tested whether transitions between different states satisfied the Markov first-order dependence conditions, i.e., $P(B/A,X) = P(B/A)$, for every triplet $X \rightarrow A \rightarrow B$, where $P(B/A,X)$ is the probability of state $k+1$ belonging to behavior B if the current state k belongs to A and the previous state $k-1$ belonged to X.

A χ^2 test (see Materials and Methods) was used to test whether the set of two-step transition probabilities $P(B/A,X)$ was significantly different from the set of one-step transition probabilities $P(B/A)$. The χ^2 statistics were computed taking into account all possible transitions between the three most frequent behaviors (stationary states, exploratory, and swimming) (Fig. 6*A*) in the five experiments that had an appreciable number of transitions ($n > 5$) expected for every triplet of states (for instance, Sw → Exp → Stat or Exp → Sw → Exp, in which Sw is swimming, Exp is exploratory, and Stat is stationary). The result of the test was that, for five of five experiments, the two-step probabilities were significantly different ($p < 0.05$) from the one-step probabilities, and therefore the sequences of identified behaviors could not be considered as first-order Markov processes; however, a comparison among the different terms in the χ^2 statistics revealed that deviations from first-order dependence were attributable mainly to the transitions Exp → Stat → Exp (Fig. 6*B*, first panel). This finding, together with the previous result that the distribution of the residence time for stationary states could be fit by a sum of two exponentials (Fig. 1*F*), strongly suggested that states identified as stationary were actually divided into two distinct subcat-

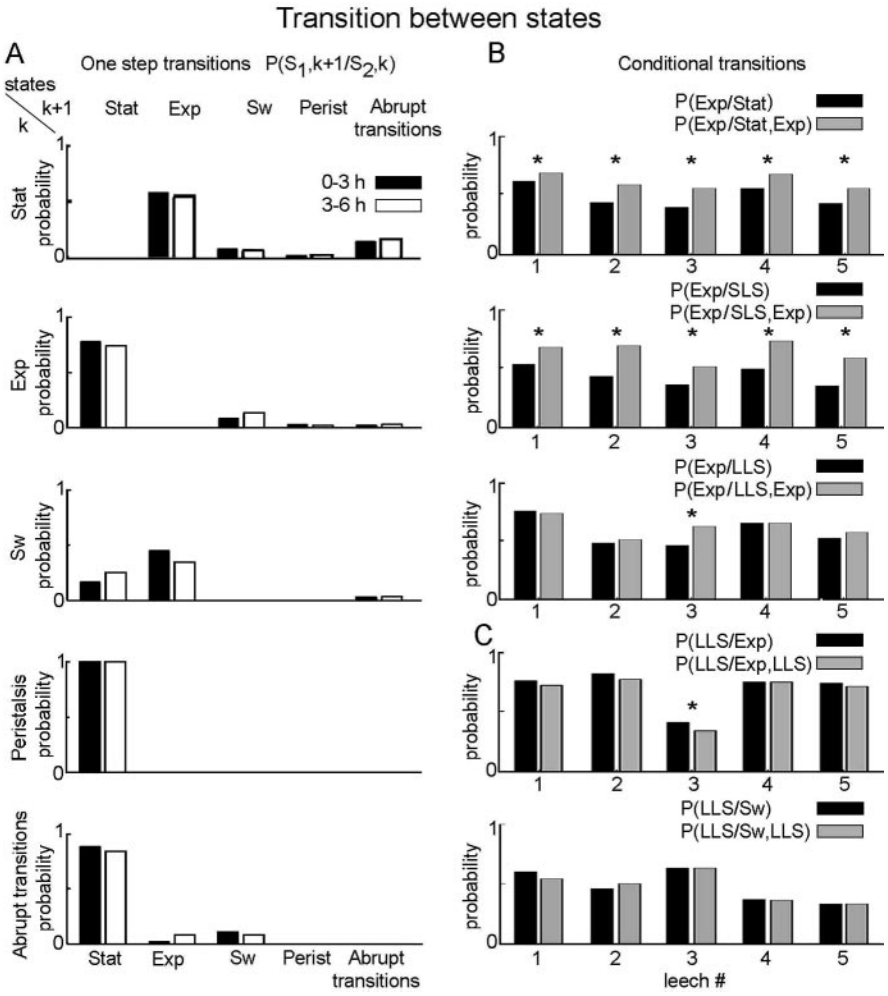

Figure 6. Analysis of transitions. ***A***, Transition probabilities between different behaviors observed in one leech. Each row represents the transition probability between a starting state (k, on the left) and the following state ($k + 1$, on top). Transition probabilities have been calculated for the first half (black) and second half of the experiment (white). Data were collected from a pinned leech preparation lasting 12 h. ***B***, The first panel shows probability of transition for state $k + 1$ being exploratory if state k was stationary (black) and probability of the same transition conditional on state $k - 1$ being exploratory (gray). This second two-step probability was always higher, and the overall transition rates were significantly different ($*p < 0.05$) from the one-step conditional probabilities. The second and third panels show the same analysis but for SLS states (middle) and LLS states (bottom). For SLS states, the conditional probability was always higher, and the overall transition rates were again significantly different ($*p < 0.05$) from the one-step conditional probabilities. For LLS states, however, the one- and two-step conditional probabilities were not significantly different for four of five experiments ($*p < 0.05$). ***C***, Top, Two-step transitions to LLS states from exploratory states (black) and from exploratory states after an LLS state (gray). The absence of significant difference (χ^2 test for homogeneity of distributions; $*p < 0.05$) between the one- and two-step conditional probabilities shows that transition probabilities do not depend on the previous behavioral history. Bottom, The same comparison is done for swimming transition probabilities, obtaining the same result ($*p < 0.05$). Stat, Stationary; Exp, exploratory; Sw, swimming.

egories. Therefore, based on the residence time distribution, we divided stationary states into two subcategories: short-lived stationary (SLS) states (duration <10 s) (Fig. 1*F*, first data point) and LLS states (duration >10 s).

The χ^2 test was then repeated to include those transitions involving only SLS states or those involving LLS states. When only short stationary states were included, the two-step probabilities were still significantly different (χ^2 test; $p < 0.05$; five of five experiments) from one-step probabilities. This again was because *P*(Exp/SLS,Exp) was always higher than *P*(Exp/SLS) (Fig. 6*B*, second panel). On the other hand, when only long stationary states were included in the statistics, conditioned one-step and two-step probabilities were not significantly different in four of five experiments (χ^2 test; $p > 0.05$). A comparison between *P*(Exp/LLS,Exp) and *P*(Exp/LLS) is shown in Figure 6*B* (third panel).

Overall, this analysis suggested that LLS and SLS states had very different properties. Long stationary states behaved like exploratory and swimming behaviors, and the transition probabilities were not affected by the previous behavior. On the contrary, during a short stationary state, the leech remembered the previous behavior and had the tendency to repeat it. This happened mainly when the leech was exploring. In fact, many of the short pauses were between two exploratory states, and most of them adjoin at least one exploratory state (32 and 74%, respectively, of SLS states for nine leeches in which both SLS and exploratory states had an appreciable number of occurrences). This suggests that SLS states are pauses that do not have to be considered as independent from the exploratory states. Therefore, we repeated the statistical test for first-order Markov dependence by absorbing each SLS state that bordered an exploratory state into the exploratory state itself. Such paired states contributed, on average, 15% of the total number of stationary states and 24% of the number of exploratory states (nine leeches). Figure 6*C* shows some of the resulting two-step and one-step transition probabilities after this adjustment in the classification of behaviors. Here, transitions from exploratory (Fig. 6*C*, top) and from swimming (bottom) to LLS states are compared, when the state preceding the swimming or exploratory state is either arbitrary (black) or LLS (gray). For four of five experiments, two-step probabilities were not significantly different ($p > 0.05$) from the one-step probability set, indicating that the underlying transition dynamics behaves, in essence, as a first-order Markov process.

Discussion

The aim of the present work was to establish a basis for the quantitative understanding of leech behavior and decision processes. The proposed automatic classification is able to recognize and classify most of the motions; only a small fraction, ~10%, of leech motion remains unclassified. This percentage appears to be a combination of different behaviors, drifts, and oscillations of body parts. In addition to the well characterized behaviors such as swimming and crawling, it was possible to identify and study a more complex category of movements, the exploratory behavior, which has never been investigated quantitatively before.

Flow of leech behavioral decisions as a first-order Markov process

The results shown in this study (Figs. 1, 6) suggest that the time structure of leech behavior is well described as a first-order

Markov process with transitions among various different behavioral categories, as illustrated in Figure 8*A*. Transition probabilities among different behavioral categories are likely to depend on the spontaneous neural activity of the animal brain as well on proprioceptive and sensory information. The discovery of many command interneurons in the subesophageal ganglion of the leech, the locations of which are indicated in the diagram in Figure 8*B*, offers a neurobiological basis for the scheme of Figure 8*A*.

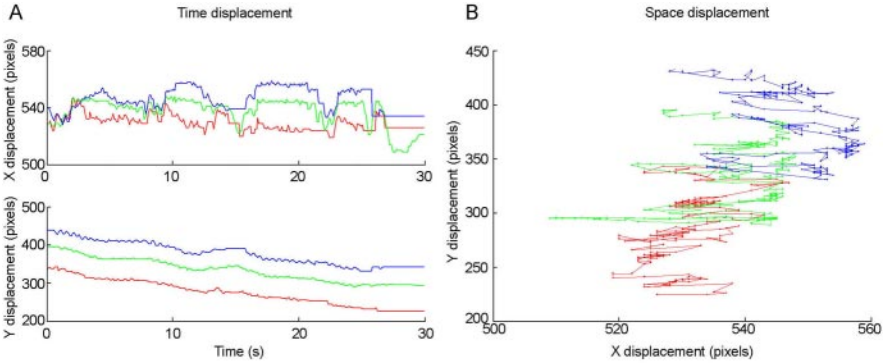

Figure 7. Hybrid behavior. ***A***, Temporal *x* and *y* displacement (top and bottom, respectively) of a hybrid behavior. In this case, the leech shows swimming-like oscillations superimposed on the elongation phase of crawling. Note the difference between both displacement scales. ***B***, Spatial displacement of the same behavior shown in ***A***.

Neurons Tr1, SE1, and R3b1 initiate swimming (Brodfuehrer and Friesen, 1986a,b,c; Brodfuehrer et al., 1995; Thorogood and Brodfuehrer 1995; Shaw and Kristan, 1997; Esch et al., 2002), whereas neurons SIN1 and Tr2 terminate swimming (Brodfuehrer and Burns, 1995; O'Gara and Friesen, 1995). The firing of neuron R3b1 (Esch et al., 2002) elicits both swimming and crawling or a hybrid behavior (similar to that shown in Fig. 7), depending on the sensory environment (the depth of the fluid surrounding the leech); however, leech behavioral decisions are likely to depend on a much more distributed neural dynamics than just the activity of this set of neurons. In fact, behavioral choice experiments have shown that most of these neurons are multifunctional, i.e., they are activated during different behaviors such as swimming and whole-body shortening (Tr1 and SE1) (Shaw and Kristan, 1997) or swimming and crawling (R3b1) (Esch et al., 2002). Moreover, recordings of the neural activity descending from the head ganglion in the connective have shown a massive coactivation of many unidentified interneurons during swimming episodes (Brodfuehrer and Burns, 1995). Finally, direct stimulation of identified command neurons produces highly variable behavioral responses and often does not elicit any kind of behavior (Brodfuehrer and Friesen, 1986b). The same variability is encountered when strong mechanosensory stimuli are used to elicit swimming (Grobstein, 1994; Brodfuehrer and Burns, 1995). As a consequence, the resulting stimulus–response curves do not have a clear stimulus level threshold for reproducible initiation of swimming. Overall, these findings suggest that leech behavioral decisions are controlled by the dynamics of a distributed neural network that defines the internal state of the leech CNS. This dynamics, because of its distributed nature and the intrinsic variability of leech interneuron and motoneuron firing (Zoccolan et al., 2002), can be regarded as a temporally structured probabilistic process. Therefore, we believe that the approach presented here (i.e., modeling leech behavioral data as a first-order Markov process) is at present the most effective for quantifying and characterizing the complexity of decision making in the leech CNS.

A future challenge in the study of leech behavioral decisions will be to compare transition probabilities in leeches moving in an unstructured sensory environment (as done in this work) and in leeches exposed to specific sensory stimuli or during selective intracellular stimulation of command neurons (or extracellular stimulation of the connective fibers). Another challenge will be to correlate the spontaneous activity of the identified command neurons with the overall Markov process controlling the transitions among different behaviors. The biophysical properties of these neurons and of their synapses are likely to take part in establishing the duration of different behaviors and transitions from one behavior to another. Because the duration distribution of long stationary states, swimming, and crawling episodes is on the order of tens of seconds, the dynamics of activation and deactivation of these command neurons should occur on a time scale much longer than the usual synaptic delays. Unraveling the biophysical and neurobiological mechanisms underlying such long-term neuronal modulations appears to be the key to understanding the process of behavioral decision making in the leech.

Spatial distribution during stationary states

Although the transitions among different behavioral states satisfied the Markov property of "no memory," a significant correlation between the orientations (as well as the elongations) of the leech body in consecutive stationary states has been found (Fig. 2*E–G*). This may be partially accounted for by a sort of "biomechanical memory" or inertia of the leech body that, in between two close stationary states, does not have time to change its location fully; however, because the correlation has been estimated by taking into account all identified stationary states, the existence of neural circuits that effectively implement a short-term spatial memory cannot be excluded. This possibility is also supported by the fact that, in the absence of directional sensory stimuli, the distribution of leech body orientations during stationary states is isotropic (Fig. 2*A–D*). Therefore, the correlation between consecutive stationary orientations cannot be attributed to the tendency of the leech to rest along some preferred direction(s). On the other hand, the finding that bright flashing lights located at specific orientations can destroy the isotropy of the leech resting orientations (Fig. 3) is easily explained as the direct and continuous effect of the sensory stimuli on the decision process, without the need to hypothesize any short-term spatial memory.

Exploratory behavior

The exploratory behavior is a highly irregular, apparently unpredictable motion, however, in which we were able to identify various recurring patterns or motifs, suggestive of a deterministic dynamics (Fig. 5). Although a test for a deterministic dynamic attractor failed when applied to a long piece (1000 s) of exploratory time series, these recurrent motifs were consistently found only in the original time series but not in its phase-randomized surrogate. This suggests that nonlinear neural pattern generators could actually produce deterministic pieces of exploratory motion embedded in an overall effectively random explorative behavior. Also, the exploratory motion could simply be continuously broken by the sensory feedback provided by the external environment (which is likely to be maximal during exploration),

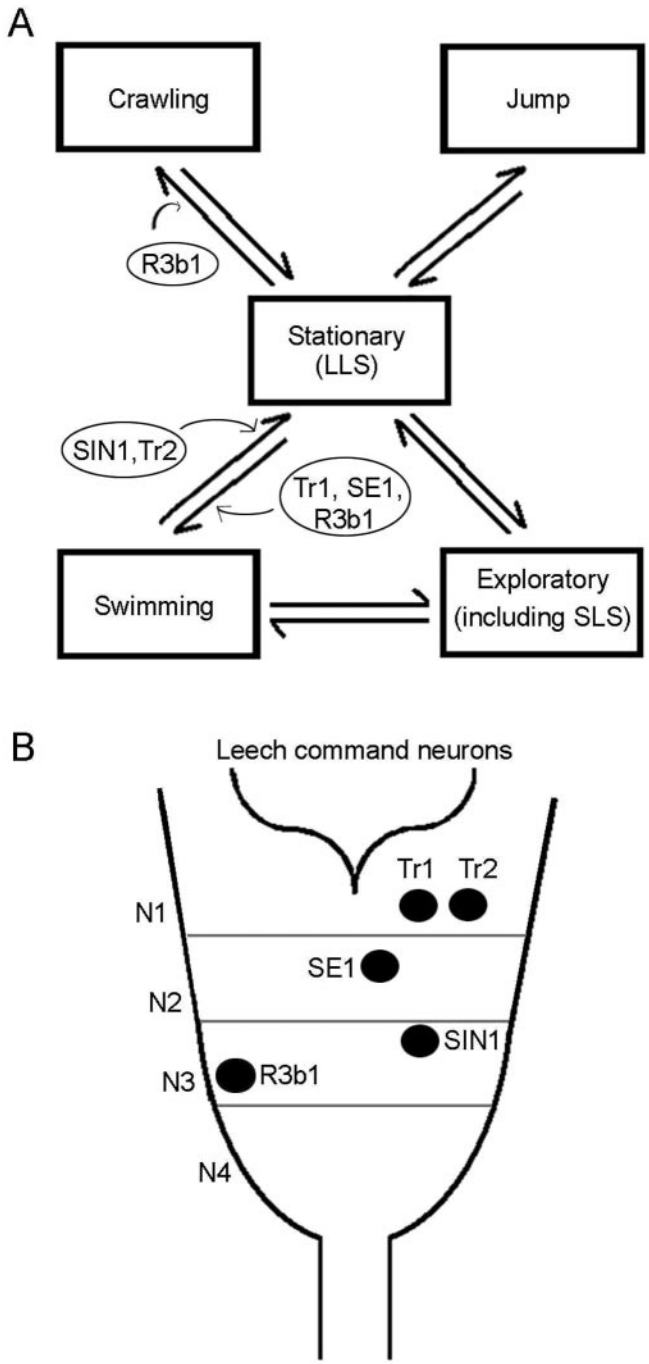

Figure 8. Behavior of the leech and transitions among behavioral categories. ***A***, Five behaviors and the transitions between them are shown. Stationary states (LLS) are those with a duration of $\geq$10 s. The exploratory states included the SLS, with a duration of $<$10 s. The transitions among behavioral categories are probably controlled by the firing of the command neurons. The known command neurons and their location in the head subesophageal ganglia are shown in ***B***. N1–N4 represent the four neuromeres of the head ganglion.

thereby preventing the existence of a global dynamic attractor. In any case, the existence of such motifs is likely to have a deep physiological and behavioral relevance.

Despite the heterogeneity of the activated motor patterns, as suggested by the broad distribution of the head velocity (Fig. 4*E*,*F*) and by the variety of identified recurrent motifs (Fig. 5), the residence time distribution of exploratory states could be fit by a single exponential (Fig. 1*D*). Moreover, transition probabilities involving exploratory states satisfied the Markov first-order dependence conditions as well as stationary and swimming states (Fig. 6*C*). This strongly suggests that the decision process underlying initiation and termination of the exploratory behavior should share the same neural architecture that triggers or inhibits more stereotyped behaviors such as swimming or crawling. Therefore, we are tempted to speculate that a network of "exploratory" command neurons should exist in the leech head ganglion. Similar to what was found for swimming, this high-level network could simply decide when to start and stop an exploratory episode, whereas more specialized intra-ganglia and inter-ganglia circuits could work as nonlinear pattern generators of the exploratory patterns. These speculations will be the subject of future investigations.

Short pauses that adjoined exploratory states were included in the exploratory states themselves, because their statistics were clearly distinct from that of longer stationary states (Figs. 1*F*, 6*B*). Therefore, short pauses could be considered a special kind of exploratory pattern. They could represent "intermittent locomotion," in which an animal uses brief pauses to improve the quality of sensory information to guide its behavior in response to external stimuli. This behavior has been observed in animals ranging from protozoans to mammals (Kramer and McLaughlin, 2001).

Final remarks

This work shows that the spontaneous behavior of the leech can be quantitatively analyzed and characterized for long periods of time, providing enough data for an adequate statistical analysis. Formal schemes for the behavior can then be compared with experimental data, and mathematical models can be obtained. Such an approach has already been applied successfully to the analysis of behavior of different species, from invertebrates to primates (Bressers et al., 1995; Haccou and Meelis, 1992; Chen et al., 2002); however, the leech offers the great advantage of accessibility of the nervous system to intracellular and extracellular recordings and a growing knowledge of the command interneurons responsible for shaping its behavior. Revealing the neural correlates of the Markov process and of the exploratory patterns found in the present investigation could lead to a better general quantitative theory of animal behavior relating to neuroeconomics (Glimcher, 2003) and game theory (Schultz, 2004).

References

Baader AP, Kristan Jr WB (1992) Monitoring neuronal activity during discrete behaviors: a crawling, swimming and shortening device for tethered leeches. J Neurosci Methods 43:215–223.

Barraclough DJ, Conroy ML, Lee D (2004) Prefrontal cortex and decision making in a mixed-strategy game. Nat Neurosci 7:404–410.

Bennett MV (1997) Gap junctions as electrical synapses. J Neurocytol 26:349–366.

Bennett MV (2000) Electrical synapses, a personal perspective (or history). Brain Res Brain Res Rev 32:16–28.

Berg HC (1993) Random walks in biology. Princeton: Princeton UP.

Bressers WM, Kruk MR, Van Erp AM, Willekens-Bramer DC, Haccou P, Meelis E (1995) A time-structured analysis of hypothalamically induced increases in self-grooming and activity in the rat. Behav Neurosci 109:1158–1171.

Britten KH, Van Wezel RJ (1998) Electrical microstimulation of cortical area MST biases heading perception in monkeys. Nat Neurosci 1:59–63.

Brodfuehrer PD, Burns A (1995) Neuronal factors influencing the decision to swim in the medicinal leech. Neurobiol Learn Mem 63:192–199.

Brodfuehrer PD, Friesen WO (1986a) Initiation of swimming activity by trigger neurons in the leech subesophageal ganglion. I. Output connections of Tr1 and Tr2. J Comp Physiol [A] 159:489–502.

Brodfuehrer PD, Friesen WO (1986b) Initiation of swimming activity by

trigger neurons in the leech subesophageal ganglion. II. Role of segmental swim-initiating interneurons. J Comp Physiol [A] 159:503–510.

Brodfuehrer PD, Friesen WO (1986c) Initiation of swimming activity by trigger neurons in the leech subesophageal ganglion. III. Sensory inputs to Tr1 and Tr2. J Comp Physiol [A] 159:511–519.

Brodfuehrer PD, Thorogood MS (2001) Identified neurons and leech swimming behavior. Prog Neurobiol 63:371–381.

Brodfuehrer PD, Parker HJ, Burns A, Berg M (1995) Regulation of the segmental swim-generating system by a pair of identified interneurons in the leech head ganglion. J Neurophysiol 73:983–992.

Chen S, Lee AY, Bowens NM, Huber R, Kravitz EA (2002) Fighting fruit flies: a model system for the study of aggression. Proc Natl Acad Sci USA 99:5664–5668.

Ditterich J, Mazurek ME, Shadlen MN (2003) Microstimulation of visual cortex affects the speed of perceptual decisions. Nat Neurosci 6:891–898.

Drewes CD (1984) Escape reflexes in earthworms and other annelids. In: Neural mechanisms of the startle response (Eaton RC, ed), pp 43–91. New York: Plenum.

Eckmann JP, Oliffson-Kamphorst S, Ruelle D (1987) Recurrence plots of dynamical systems. Europhys Lett 4:973–977.

Esch T, Mesce KA, Kristan WB (2002) Evidence for sequential decision making in the medicinal leech. J Neurosci 22:11045–11054.

Freedman DJ, Riesenhuber M, Poggio T, Miller EK (2001) Categorical representation of visual stimuli in the primate prefrontal cortex. Science 291:312–316.

Furshpan EJ, Potter DD (1959) Transmission at the giant motor synapses of the crayfish. J Physiol (Lond) 145:289–325.

Glimcher P (2002) Decisions, decisions, decisions: choosing a biological science of choice. Neuron 36:323–332.

Glimcher P (2003) Decisions, uncertainty, and the brain: the science of neuroeconomics. Cambridge, MA: MIT.

Gold JI, Shadlen MN (2002) Banburismus and the brain: decoding the relationship between sensory stimuli, decisions, and reward. Neuron 36:299–308.

Green DM, Swets JA (1966) Signal detection theory and psychophysics. New York: Wiley.

Grobstein P (1994) Variability in brain function and behavior. In: Encyclopedia of human behavior (Ramachandran VS, ed), pp 447–458. New York: Academic.

Haccou P, Meelis E (1992) Statistical analysis of behavioural data: an approach based on time-structured models. Oxford: Oxford UP.

Kantz H, Schreiber T (1997) Nonlinear time series analysis. Cambridge, UK: Cambridge UP.

Kramer DL, McLaughlin RL (2001) The behavioral ecology of intermittent locomotion. Am Zool 41:137–153.

Mazzoni A, Garcia-Perez E, Zoccolan D, Graziosi S, Torre V (2005) Quantitative characterization and classification of leech behavior. J Neurophysiol 93:580–593.

Montague PR, Berns GS (2002) Neural economics and the biological substrates of valuation. Neuron 36:265–284.

O'Gara BA, Friesen WO (1995) Termination of leech swimming activity by a previously identified swim trigger neuron. J Comp Physiol [A] 177:627–636.

Priestley MB (1981) Spectral analysis and time series. London: Academic.

Salzman CD, Britten KH, Newsome WT (1990) Cortical microstimulation influences perceptual judgments of motion direction. Nature 346:174–177.

Schnizler M, Clauss W (1998) Characterization of a voltage-dependent conductance in the basolateral membrane of leech skin epithelium. J Comp Physiol [B] 168:295–302.

Schnizler M, Buss M, Clauss W (2002) Effects of extracellular purines on ion transport across the integument of *Hirudo medicinalis*. J Exp Biol 205:2705–2713.

Schultz W (2004) Neural coding of basic reward terms of animal learning theory, game theory, microeconomics and behavioural ecology. Curr Opin Neurobiol 14:139–147.

Shaw BK, Kristan Jr WB (1997) The neuronal basis of the behavioral choice between swimming and shortening in the leech: control is not selectively exercised at higher circuit levels. J Neurosci 17:786–795.

Szendro P, Vincze G, Szasz G (2001) Pink-noise behavior of biosystems. Eur Biophys J 30:227–231.

Thorogood MS, Brodfuehrer PD (1995) The role of glutamate in swim initiation in the medicinal leech. Invert Neurosci 1:223–233.

Tinbergen N (1951) The study of instinct. Oxford: Clarendon.

Zoccolan D, Pinato G, Torre V (2002) Highly variable spike trains underlie reproducible sensorimotor responses in the medicinal leech. J Neurosci 15:10790–10800.

Zucker RS (1972) Crayfish escape behavior and central synapses. I. Neural circuit exciting lateral giant fiber. J Neurophysiol 35:599–620.

3

Dynamics of spontaneous activity

in neuronal networks

Alberto Mazzoni, Frederic Broccard, Elizabeth Garcia-Perez,
Paolo Bonifazi, Maria Elisabetta Ruaro and Vincent Torre

Paper submitted

Neuronal networks exhibit a spontaneous activity characterized by bursts of spikes, the origin and functional role of which are still unclear. In the present manuscript we show that during their spontaneous activity two very different networks -leech ganglia and dissociated rat hippocampal neurons cultures- share several properties despite the dissimilar underlying structure. We analysed the spontaneous activity of single identifed neurons, and how from tonic firing they switch to bursting firing according to the activity of the network. In the absence of stimuli both networks present temporal correlations on multiple timescales and a broad distribution of bursts size. Modulations in the coupling between neurons lead the networks into regimes in which large bursts and long-term temporal correlations are dominant or absent. Reliability of evoked activity in hippocampal cultures depends on the dynamical regime. We propose a statistical model for the interaction among neurons during spontaneous activity able to give a coherent description of all these phenomena.

Introduction

Spontaneous bursting activity in the nervous system of vertebrates and invertebrates has been studied primarily in rhythm-generating networks (Connors 1984, Marder and Calabrese 1996).

The origin, functional significance and intrinsic dynamics of arrhythmic bursts are still less understood. When neuronal networks are investigated from the point of view of information processing, arrhythmic spontaneous bursts have usually been considered as noise (Zohary et al. 1994, Krahe and Gabbiani 2004), hence it is important to determine their statistical properties, since they contribute to the trial-to-trial variability in stimuli driven experiments (Arieli et al. 1996, Fiser et al. 2004). Arrhythmic burst have been mainly studied in neuronal networks during development (O'Donovan 1999, Jones and Jones 2000, Baker et al. 2006): large and synchronized bursts of spikes during the early phase of development have a role in determining the structure and function of the networks (Leinekugel et al. 2002, van Pelt et al. 2004, Gonzales and Wenner 2006). In fully developed animals, arrhythmic spontaneous bursts may have an important functional role in movement initiation (Lee and Assad, 2003). Previous studies on the activity of in vitro neuronal networks (Segev et al. 2002) described the presence of scale-invariant distributions and long range correlations in spontaneous bursting activity.

In order to identify general dynamical properties of the arrhythmic spontaneous firing, we analysed and compared the spontaneous electrical activity of two very different networks: intact leech ganglia and dissociated neuronal cultures from hippocampal rat neurons.

In the present manuscript we show that despite their diversity in origin and function, the spontaneous activity of both networks has similar dynamical features. Neurons switch from tonic to bursting firing according to network activity. Neurons activity is strongly correlated and displays correlation on a broad range of low frequencies time scales. Burst size and duration follow power law distributions with the same slope in both preparations.

When excitatory synaptic pathways mediated by NMDA receptors are blocked, both neuronal networks are driven into a regime where large bursts are absent. In contrast, blockage of inhibitory synaptic pathways mediated by GABAergic receptors drives both networks into a regime characterized by large and highly synchronous bursts.

In hippocampal cultures in the non-bursting regime the responses to external stimuli become more reproducible but the activity is localized, while in the highly bursting regime the responses are more intense but less reliable.

Materials and Methods

Physiology

Adult leeches *Hirudo medicinalis* were obtained from Ricarimpex and kept at 5º C in tap water dechlorinated by aeration for 24 hours. Leech ganglia were isolated as previously described (Muller et al. 1981), and the roots emerging from the exposed ganglion were cleaned for suction pipette recordings (Arisi et al. 2001). Hippocampal neurons were obtained from Wistar rats (P0-P2) and plated on 60-channel multielectrode array (MEA) enabling extracellular recordings as previously described (Bonifazi et al. 2005). The age of the cultures varied from 22 to 35 days *in vitro*. Extracellular recordings were digitized at 10 or 25 kHz, recorded with MCRack (MultiChannelSystem) and analysed using the Matlab environment (Mathworks).
Electrodes of MEA were stimulated with bipolar voltage pulses lasting 100 μs at each polarity injected through the STG2008 stimulus generator. Voltage pulses were applied in parallel to a set of selected electrodes. The amplitude of the voltage pulse was 600 mV. Trials consisted in 50 identical trains of 20 pulses, with a fixed inter-pulse interval (IPI) followed by a 10 sec inter-train pause. For every preparation the same procedure was repeated for IPIs corresponding to 10, 20, 40 and 80 ms.
For studying spontaneous and evoked activity under reduced excitation, the non-competitive NMDA receptor antagonist 2-amino-5-phosphonopentanoic acid (APV) (final concentration, 20μM; TOCRIS) was bath-applied. For studying spontaneous and evoked activity under reduced inhibition, the ionotropic GABA receptors antagonists picrotoxin (PTX) (final concentration, 10μM; Sigma) and Bicuculline (final concentration, 10μM; Sigma) were bath-applied in the leech ganglia and in the hippocampal dissociated culture, respectively.

Data Analysis

Spike sorting was carried out for leech networks by using a software developed in our laboratory (Arisi et al. 2001).

The duration of the recording was divided into bins of constant width. Different widths were used to compare properties at different time scales. In leech networks, for each single neuron the number of spikes occurring in each bin was counted and the resulting discrete time series represented the *neuron firing rate*. Similarly, in the hippocampal network, given the sequence of spike times of a

single electrode, the *electrode firing rate* was computed. The *network firing rate* was defined as the sum of all neuron/electrode firing rates (i.e. the number of all spikes recorded in the network from each bin).

The probability distribution *P(S)* of the number of spikes S per bin of the network firing rate was fitted by a lognormal function:

$$P(S) = \frac{1}{S\sqrt{2\pi}\sigma}\exp\left[-\frac{(\ln S - \mu)^2}{2\sigma^2}\right]$$

where μ and σ are the mean and the variance of the distribution of the logarithm of *S*.

The skewness of a distribution, a measure of the degree of asymmetry, is defined as:

$\gamma_1 = \frac{\overline{\mu}_3}{\overline{\mu}_2^{3/2}}$ where $\overline{\mu}_i$ is the i-*th* central moment of the distribution (Papoulis, 1984).

The power spectral density of the network firing rate, obtained with a bin width of 10 ms, was computed by using Welch's averaged modified periodogram method (*pwelch* function in Matlab), after a low pass filtering with a cut off frequency of 25 Hz to prevent aliasing.

For each pair (i,j) of neurons or electrodes the correlation coefficient (Papoulis, 1984) $\rho_{i,j}$

$$\rho_{ij} = \frac{\sum_n (FR_i(n) - < FR_i >)(FR_j(n) - < FR_j >)}{\sqrt{(< (FR_i(n) - < FR_i >)^2 >)(< (FR_j(n) - < FR_j >)^2 >)}}$$

of the neuron or electrode firing rates *FR(n)* was computed in a bin width varying from 20 to 1000 ms. $\rho_{i,j}$ was then averaged for each bin width over all pairs to obtain the *network correlation coefficient* $\overline{\rho}$.

As there is not a unique definition of *burst*, we considered three alternative definitions.
Definition A: The distribution of inter-spike intervals (ISI) between successive spikes in the network was computed and fitted by a bi-exponential function:

$$P(ISI = t) = C_1 e^{-t/\tau_{long}} + C_2 e^{-t/\tau_{short}}$$

where C_1 and C_2 are two constants and τ_{short} and τ_{long} are a fast and a slow time constant, respectively. The network firing rate with a bin width equal to τ_{long} was calculated, and strips of adjacent bins, each counting more than two spikes, were considered as bursts.

For each experiment, we computed the average inter-spike interval ($\overline{ISI}$) between successive spikes in the network. $\overline{ISI}$ varied from 2 to 20 ms for hippocampal networks and from 10 to 50 ms for leech networks. Two additional definitions of bursts were also considered:

Definition B: a burst was identified as an ensemble of consecutive spikes separated by a time interval smaller than $\overline{ISI}$.

Definition C: the network firing rate with a bin width equal to $\overline{ISI}$ was calculated, as well as its average value. A burst was identified in the network firing rate as the strip of adjacent bins in which each bin has a number of spikes higher than the average firing rate.

In all these definitions of *burst*, only bursts containing more than three spikes were considered. The *burst size* is the total number of spikes within the burst, and its *duration* is the time interval between the first and the last spike of the burst.

The amount or degree of spontaneous bursting was quantified by analysing the dispersion of the firing statistics. The *Burst index* is defined as the interquartile relative range of the spike per bin distribution.

The response R evoked by a stimulus in the hippocampal network was measured as the value of the network firing rate in the 5 ms following the application of the stimulus. For every trial we calculated the coefficient of variation (CV) of the response, i.e. the ratio between the standard deviation of the set of the obtained responses and its mean value. To measure the reproducibility of the response of the network we averaged the CV over all trials.

We measured the background activity B_i associated to every evoked response as the value of the network firing rate in a 5 ms time window before the stimulus, similarly to the definition of Initial State of the ongoing activity in Arieli et al. (1996). The signal-to-noise ratio (SNR) (Rieke et al. 1997) for the network response to a train of pulses was calculated as

$$SNR = \left\langle 20 * \log_{10}\left(\frac{R_i}{B_i}\right)\right\rangle$$

The result was then averaged over all trials.

Results

We investigated the spontaneous firing of spikes in neuronal networks from the leech nervous system and from cultures of rat dissociated hippocampal neurons. Leech ganglia were isolated, and 6 to 8 emerging roots were dissected and inserted into suction pipettes, from which extracellular voltage recordings were obtained (Fig. 1A, *left*, see Methods). Dissociated cultures from neonatal hippocampal neurons were grown (Ruaro et al. 2005) on 60-channel multielectrode arrays (MEA) (Fig. 1B, *left*, see Methods).

We will refer to leech ganglia and hippocampal neuronal cultures as leech and hippocampal networks, respectively. In both preparations spontaneous activity was recorded for periods that ranged from 30 minutes to 2 hours (Arisi et al. 2001, Ruaro et al. 2005).

The single electrode firing pattern was characterized in both networks by intermittent bursts of activity with a broad variety of size, separated by episodes of low activity (Fig. 1A-B, *right*).

The network firing rate (see Methods) fluctuated significantly, showing large peaks corresponding to bursts of concerted electrical activity (Fig. 1C-D). Synchronous firing was observed also in electrical recordings obtained from spatially distant extracellular electrodes of the MEA, and from pipettes sucking roots emerging from opposite sides of leech ganglia.

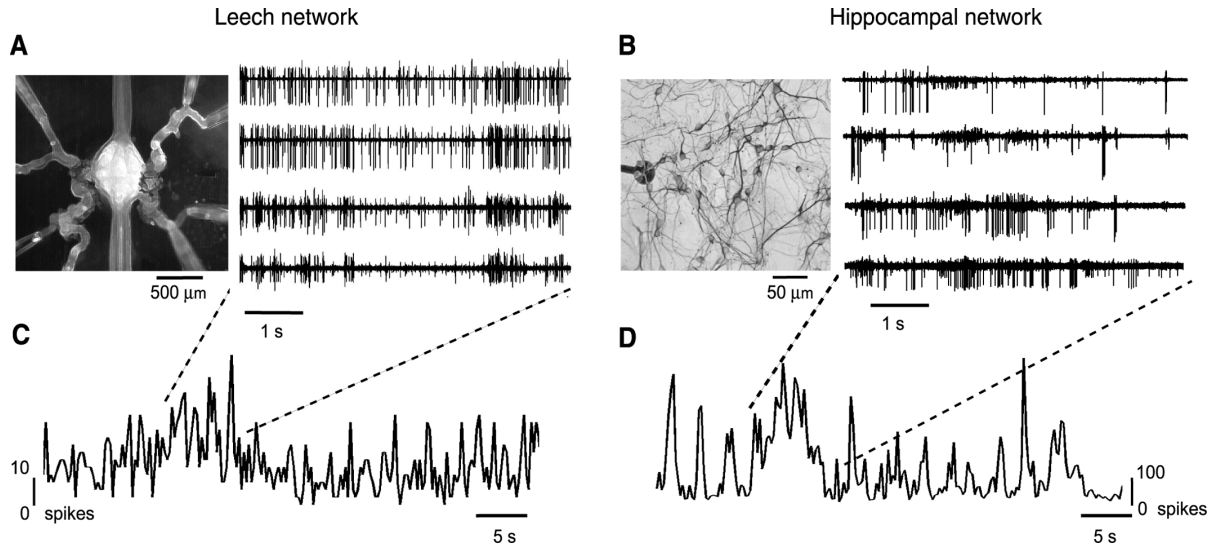

Figure 1. Spontaneous activity and burst dynamics ***A****, Left, Isolated leech ganglion with eight suction pipettes recording from different roots. Right, Extracellular recordings showing the spontaneous electrical activity monitored from four different roots.* ***B****, Left, close-up of dissociated hippocampal neurons grown on a MEA. The black dot is an individual electrode. Right, spontaneous activity recorded from four extracellular electrodes.* ***C-D****, Network firing rate, binned at 500 ms, of a representative leech network (****C****) and a representative hippocampal network (****D****). Note the presence of large peaks corresponding to concerted bursts of electrical activity and the difference between the two spike scales. 0 represents absence of spikes in network firing rates.*

Network correlation at short and long time scales

In both networks, the shape of the spike per bin distribution of the network firing rate depended on the bin width. When the activity was binned in time windows of 20 ms, the spike per bin distribution was fitted by a Poisson function in all the leech networks (n=15, χ^2 test, p>0.05, Fig. 2A), and in most hippocampal networks (7/10, χ^2 test, p>0.05, Fig. 2B). In a Poisson process, leading to Poisson distribution, the occurrence probability of a spike does not depend on the occurrence of other spikes. These results are consistent with an independent firing (Rieke et al. 1997) among neurons/electrodes. By contrast, when the activity was binned in time windows of 500 ms, the spike per bin distribution was fitted by a lognormal function for both networks (Fig. 2A-B, leech, n=15, hippocampal network, n=10; χ^2 test p>0.05), suggesting that the networks activity is – at this scale- regulated by interactions leading to a correlated firing (Crow and Shimitzu 1997, Limpert et al. 2001).

As different functions fit the spike per bin distribution when data were binned with different bin widths, the degree of correlation observed in the network could depend on the timescale in which spikes are counted. We measured the degree of correlation present in the entire network averaging the cross-correlation at lag 0 over all pairs of neurons (see Methods), thus obtaining the network correlation coefficient $\overline{\rho}$. As shown in Fig. 2C-D, $\overline{\rho}$ grew with the bin width for most leech (14/15, χ^2 test, p>0.05) and hippocampal networks (9/10, χ^2 test, p>0.05). At a bin width of 20 ms, for leech networks (n=15), $\overline{\rho}$ was less than 0.05, and increased by 3±1 times at a bin width of 500 ms, reaching a mean value of 0.14±0.04. In hippocampal networks (n=10), $\overline{\rho}$ was less than 0.3 at a bin width of 20 ms, and similarly to leech networks, it increased by 3.5±1 times at a bin width of 500 ms, reaching a mean value of 0.45±0.15.

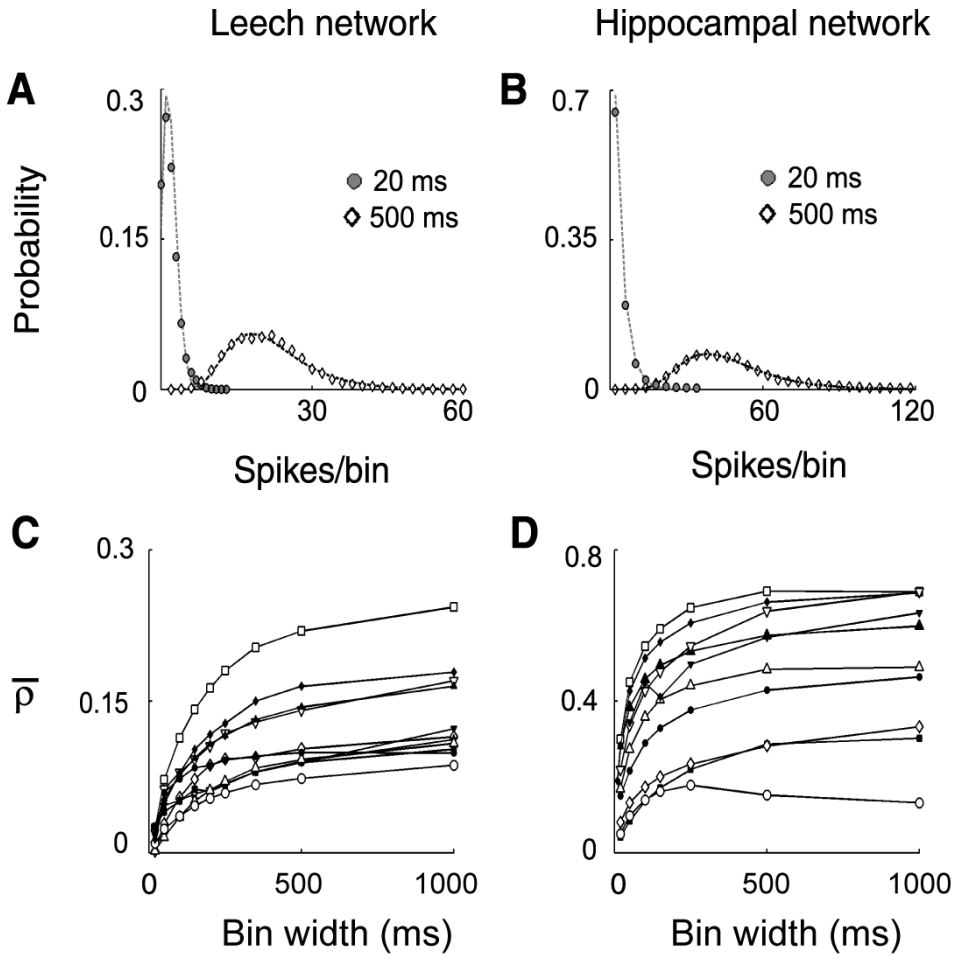

Figure 2. Network firing correlation ***A-B***, *Spikes per bin distribution of the network firing rate binned at 20 ms (filled symbols) and 500 ms (open symbols), in leech (**A**) and hippocampal networks (**B**). Data binned at 20 ms were fitted with a Poisson distribution, corresponding to an independent firing among neurons, for leech networks (15/15, χ^2 test, p>0.05) and for most hippocampal networks (7/10, χ^2 test, p>0.05), included the experiment shown in figure. Data binned at 500 ms were fitted by a lognormal distribution (leech: 15/15, hippocampal network: 10/10, χ^2 test, p>0.05), indicating the presence of strong interactions at this time scale.* ***C-D***, *Network correlation coefficient $\bar{\rho}$ as a function of the bin width for leech (**C**) and hippocampal networks (**D**) showing a bin width-dependent growth. Each symbol corresponds to a different experiment.*

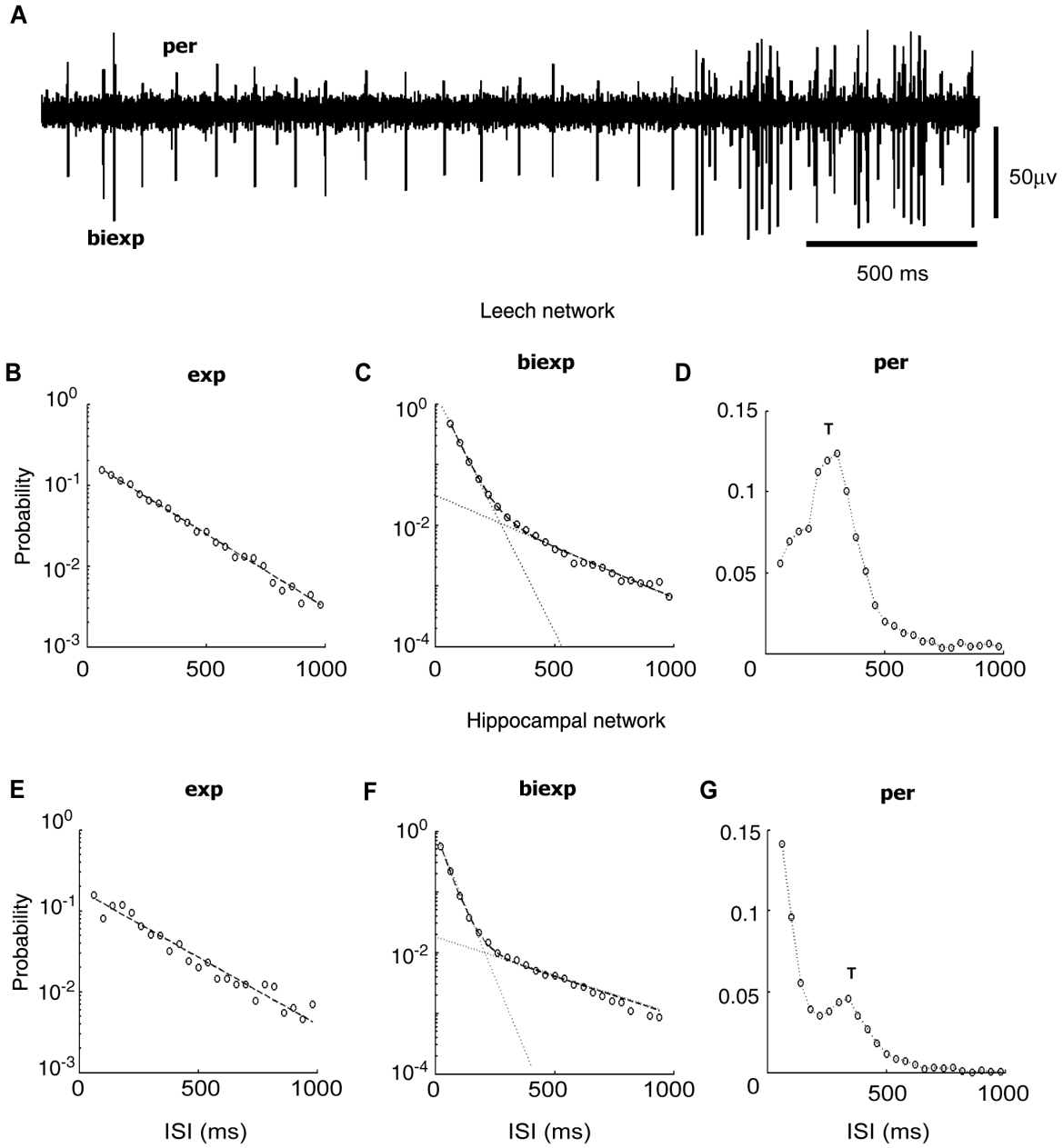

Figure 3 Single neurons dynamics: ***A****, extracellular recording from a leech root showing the activity of two identified neurons, one displaying a bursting dynamics leading to bi-exponential ISI distribution, and the other displaying a periodic behavior.* ***B,E,*** *ISI distribution of identified neurons with exponential dynamics for leech (****B****) and hippocampal (****E****) network. Black dashed lines indicate exponential fit.* ***C,F,*** *ISI distribution of identified neurons with bi-exponential dynamics for leech (****C****) and hippocampal (****F****) network. Black dashed lines indicate bi-exponential fit.* ***D,G,*** *ISI distribution of identified neurons with periodic dynamics for leech (****D****) and hippocampal (****G****) network. Label T indicates the position of the peak, corresponding to the period of the firing.*

The spontaneous activity of single neurons

We have studied the spontaneous activity of single neurons in both networks. From the extracellular recordings it was possible to sort single neurons activity according to the procedure described in the Methods section. The extracellular recording shown in Fig. 3A was obtained from the left PP root emerging from the 12th ganglion of the leech. The spike sorting procedure (see Methods section) identified two distinct spike shapes, one with a large and the other with an intermediate amplitude, each one corresponding to a different neuron. Different neurons do not differ only for their average firing rate, but also for their firing statistics, which can be regular (tonic firing) or irregular (bursting firing). As evident by visual inspection, in the trace shown in Fig. 3A one motor neuron fired in a periodic fashion, while the other fired in a more irregular way, with occasional bursts of spikes.

The ISI of the spontaneous firing of the neurons of both networks had three stereotyped distributions: i- exponentially distributed (Fig. 3B,E) as expected form Poissonian firing; ii - bi-exponentially distributed (Fig. 3C,F) when the ISI probability is given by the sum of two exponential functions $P(ISI = t) = C_1 e^{-t/\tau_1} + C_2 e^{-t/\tau_2}$; iii **-** periodic, i.e. with a large peak at a time T superimposed to either an exponential or a biexponential distribution (Fig. 3D,G), indicating an almost periodic firing with an average period between successive spikes equal to T. Characteristic times of each dynamics and fraction of neurons belonging to it for the two preparations are summarized in Table 1.

	Leech network		**Hipp. Network**	
	char. time	**% neurons**	**char. time**	**% neurons**
Exponential	175 ± 76 ms	37% (27%-56%)	290 ± 90 ms	15% (5%-22%)
Bi-exponential	42 ± 24 ms 331 ± 117 ms	35% (18%-54%)	47 ± 19 ms 378 ± 194 ms	70% (53%-88%)
Periodic	167 ± 91 ms	27% (18%-33%)	280 ± 74 ms	15% (0%-33%)

Table 1 Single neurons dynamics: *Characteristic times of different single neuron dynamics and fraction of neurons displaying each dynamics (numbers in between commas indicate the range of the values across different experiments) for the two networks.*

Since the activity of the neurons is correlated (see Fig. 2) the high firing frequency corresponding to small ISI intervals could occur in different neurons in an almost synchronous way. In order to test this possibility we divided the electrical recordings in binwidth of 1 second and we calculated the average ISI of every neuron inside the bins. As shown in Fig. 4A and B for leech and hippocampal networks the average ISI in pairs of neurons was highly correlated (n=15, r=0.7 leech, n=10 r=0.85 hippocampal networks, see Fig. 4A-B). Therefore the occurrence of ISI with a short time occurs almost simultaneously in a large portion of both networks.

We identified some leech motor neurons with the procedure described in the Methods section. In this way we found that the dynamics of a neuron can change across different experiments. Every leech motor neuron has a characteristic dynamics of tonic firing: whether Poissonian or periodic, indicated respectively by an exponential decay or by a sharp peak in the ISI distribution; moreover every neuron is able to display bursting dynamics. The switch from tonic to bursting firing can depend on the network activity (Turrigiano et al. 1994). We defined a burst index (see Methods) to measure the dispersion of the activity of the network. Briefly, the higher the burst index, the more the activity is divided into quiet intervals and intense bursts. The fraction of neurons displaying bi-exponential ISI distributions is indeed growing with the burst index in both leech (r=0.98, Fig. 4B) and hippocampal network (r=0.96, Fig. 4C).

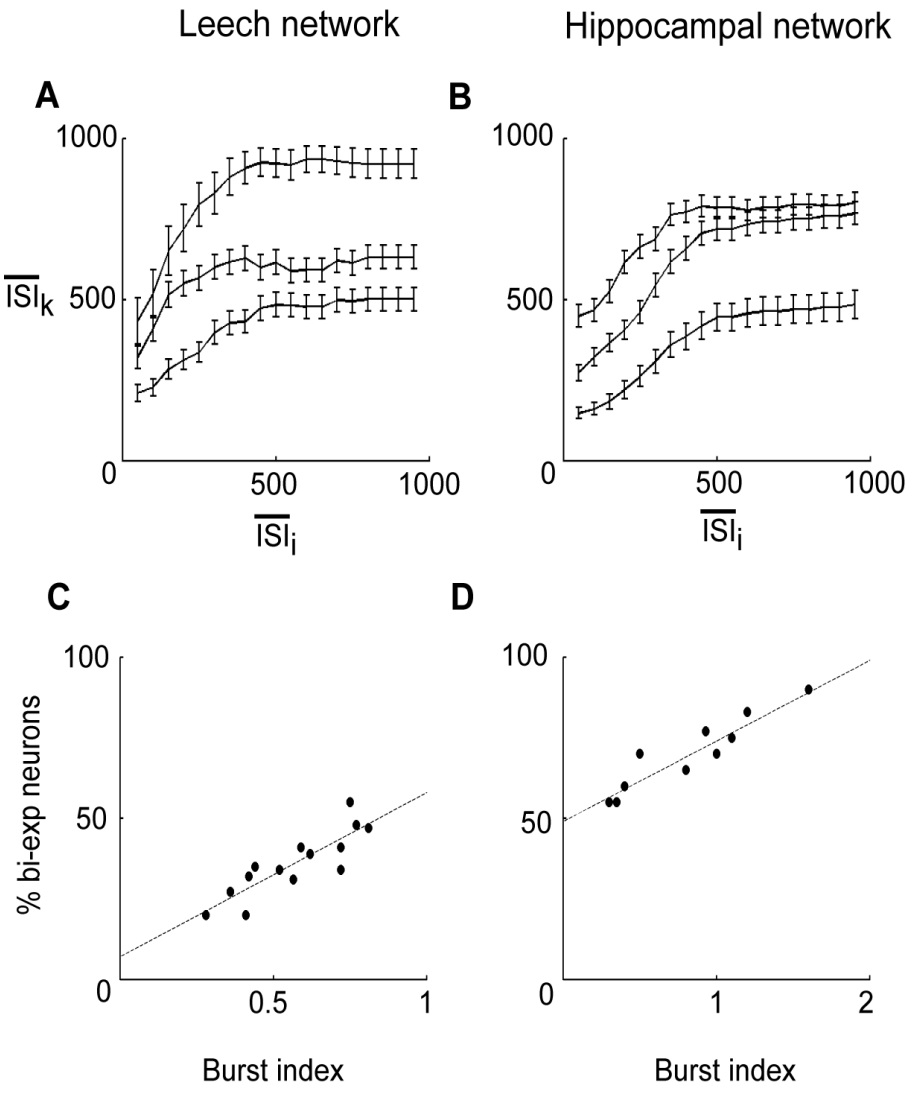

Figure 4 Single neurons dynamics and network bursts: ***A*** *Relationship between ISI of different neurons in the leech (**A**) and hippocampal (**B**) network. For three representative pairs of neurons (i,j) for each preparation, the average ISI of the neuron j calculated over 1 s long bins is displayed as a function of the average ISI of the neuron i .* ***C-D,*** *Fraction of neurons displaying bi-exponential ISI distribution as a function of a burst index for leech networks (**C**) and hippocampal networks (**D**). Black dashed lines linear regression.*

Single neurons correlations

The three kind of dynamics reflect in different auto-correlation function for the activity of single neurons. Poisson firing neurons have an almost flat autocorrelation except for the peak at zero lag, while bi-exponential neurons display an exponential decay of the autocorrelation with time constants ranging from 2 to 10 seconds, indicating that the presence of bursts produces long range temporal correlations. Periodic neurons have peaks in the autocorrelation, superimposed to one of the two described functions. As a result, the spectral analysis reveals a broad range of behaviors, going from flat to Lorentzian-like spectra (see Fig. 5A-B).

We analysed the correlations of pairs of neurons identified in both networks (see Methods). At short time scales every neuron is correlated (Pearson test for independence, $p>0.05$) just with a small fraction of the network. For both networks at a bin width of 20 ms every neuron is correlated with less than 10% of the network (0.046±0.015 for the leech, n=15; 0.08±0.04 for hippocampal network n=10). At this time scale every neuron of the leech network is then correlated to just 1 or 0 other neurons, and hippocampal network neurons are correlated just to the neighbours or to few not-neighbouring neurons. The number of correlated neurons is growing with the bin width, and at a time scale of 500 ms every neuron is instead correlated to approximately 60% of the neurons in both cases (0.57±0.06 for the leech, n=15; 0.64±0.06 for hippocampal network, n=10), indicating the presence of a coherent activity in the network. These values are in both cases not significantly different from the values obtained with a bin width of 1000 ms (0.60±0.05 for the leech, n=15, t-test p=0.4; 0.64±0.07 for hippocampal network, n=10, t-test p=0.9). Even if the extent of the spatial correlation is similar in the two networks the sinchronyzation is more precise among hippocampal neurons (data not shown) so the resulting network correlation coefficient is higher.

A change in dynamics for timescales between 1 and 2 Hz is evident also from frequency analyis. The power spectrum of the network firing rate of both networks was flat for frequencies above 2 Hz and was decreasing as f^{-slope}, with slope close to 1, (leech, n=15, mean slope= 0.97±0.3; hippocampal, n=10, mean slope= 1.15±0.2), for frequencies ranging from 0.1 to 1 Hzm (Fig. 5C-D). This indicates long range temporal correlations in the network activity, as a result of the structure of the activity of the single neurons and of their correlation. These results show that in both cases neurons are neither independently firing nor precisely synchronized during spontaneous activity, but they are rather correlated through processes acting on the hundreds of ms timescale. A bin width of 500 ms was used thereafter, since it was large enough to capture the cooperative behavior in both networks.

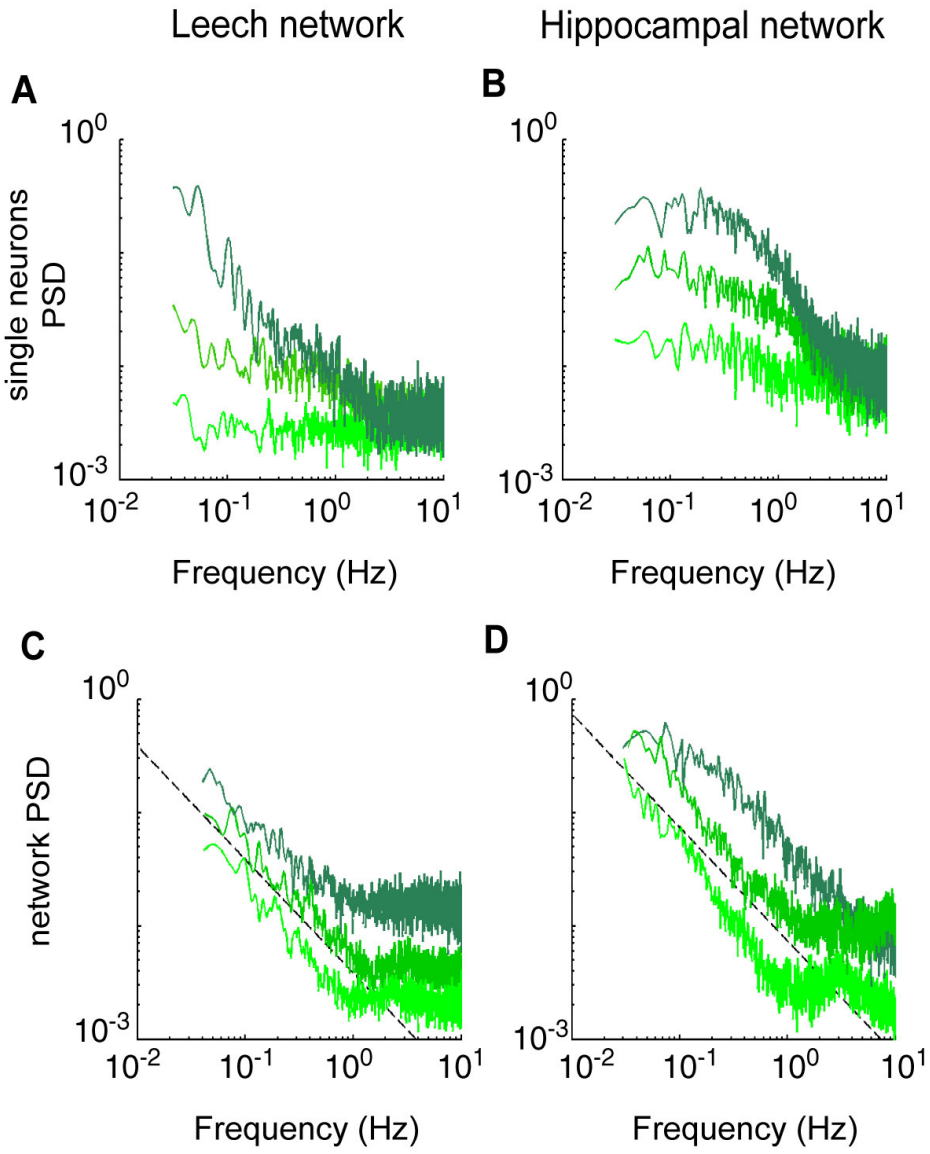

Figure 5 Single neurons and network frequency analysis ***A-B,*** *Power spectral density (PSD) of representative neurons from leech (**A**) and hippocampal networks (**B**). Notice that the range goes from almost flat PSD to PSD displaying high values associated to low frequencies.* ***C-D,*** *PSD of representative experiments from leech (**C**) and hippocampal networks (**D**). Black dashed lines correspond to 1/f slope, describing the PSD for frequencies smaller tan 1 Hz.*

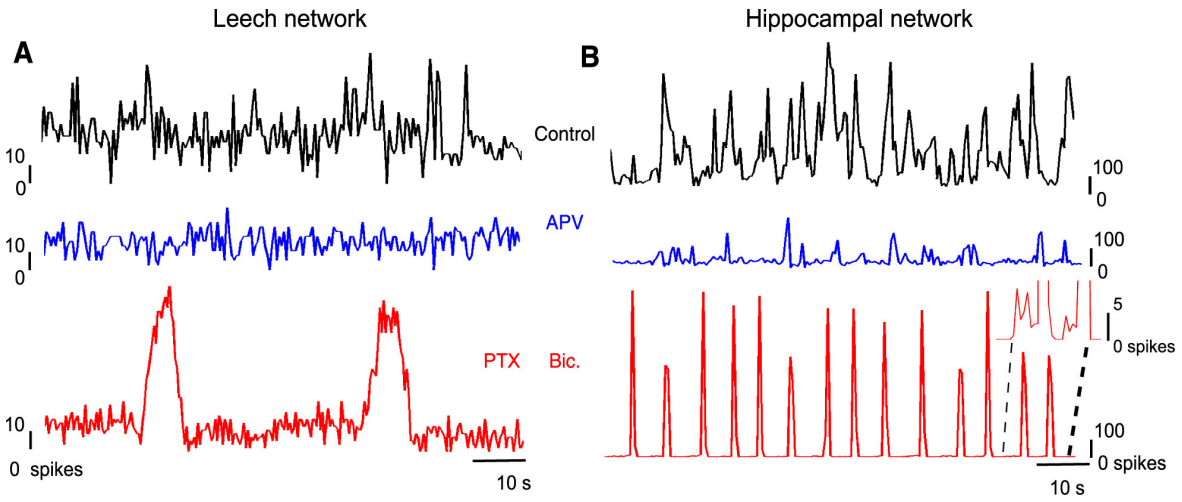

Figure 6. Modulation of NMDA and GABA synaptic pathways ***A-B***, *Changes in the network firing rates binned at 500 ms for leech (**A**) and hippocampal (**B**) networks, in control (black trace), in the presence of 20μM APV (blue trace) and 10μM PTX (red trace, panel **A**) or Bicuculline (red trace, panel **B**). Note the residual spiking activity between periods of synchronous activity in the hippocampal network (inset, right red trace; large peaks have been truncated for clarity).*

Blockage of excitatory and inhibitory synaptic pathways

To assess more accurately the role of neurons interactions in the spontaneous activity in both networks we investigated the action of antagonists of excitatory and inhibitory transmission.

The role of GABA receptors in the leech nervous system is well known (Cline 1986) and blocking them with PTX (see Methods) resulted in an increase of the bursting activity (Fig. 6A, red trace). The presence of NMDA receptors was instead debated (Wu 2002, Burrell and Sahley 2004) but when we applied the selective antagonist APV (see Methods) we always obtained a clear reduction of the bursting activity (Fig. 6*A*, blue trace), thus proving that NMDA receptors are present in the leech ganglion.

In dissociated hippocampal cultures approximately 90% of the neurons are Glutamate-ergic and the remaining 10% is GABA-ergic. Blocking the excitatory transmission mediated by NMDA receptors with APV (see Methods) decreased the bursting activity (Fig. 6B, blue trace), while when inhibitory pathways mediated by GABA receptors were blocked with Bicuculline (see Methods), the bursting activity increased (Fig. 6B, red trace).

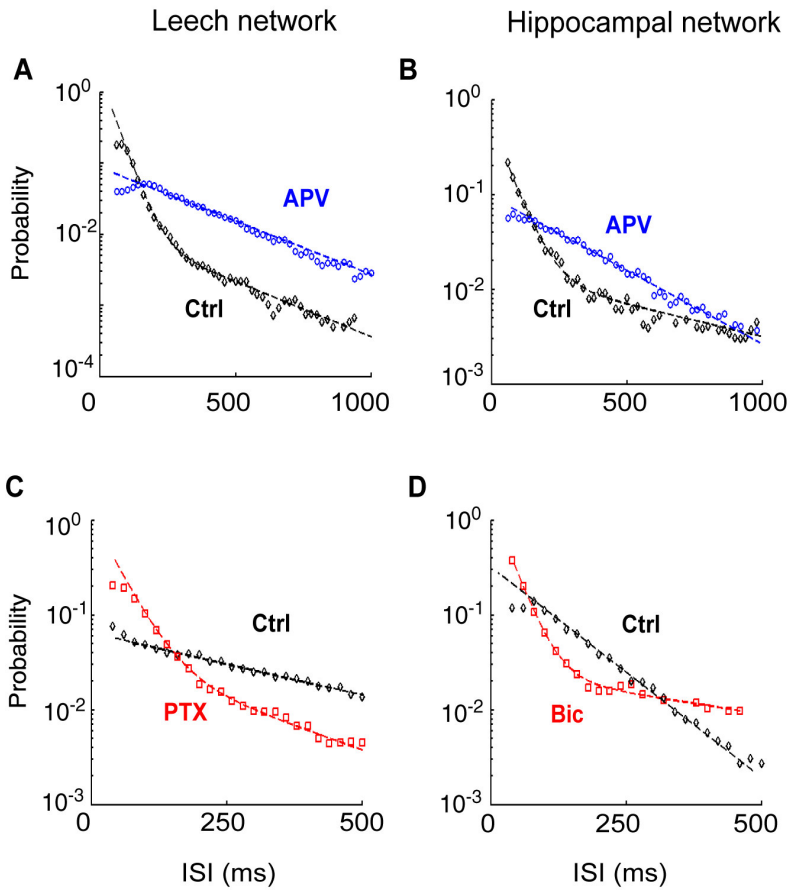

Figure 7. Effects of modulation of NMDA and GABA synaptic pathways on single neurons dynamics ***A-B***, *Neurons from leech (**A**) and hippocampal (**B**) networks, having a bi-exponential ISI distribution in control (black trace), and an exponential ISI distribution in the presence of 20μM APV (blue trace)* ***C-D***, *Neurons from leech (**C**) and hippocampal (**D**) networks, having an exponential ISI distribution in control (black trace), and a bi-exponential ISI distribution in the presence of 10μM PTX (red trace, panel **C**) or Bicuculline (red trace, panel **D**).*

It was possible to monitor the activity of identified neurons before and after the application of receptor blockers in both preparations and to see that modulating the interactions among neurons affected the dynamics of single neurons.

In both networks the presence of APV lead to an increase of the fraction of neurons displaying an exponential ISI distribution (leech: from 37% to 56% n=6; hipp. culture: from 15% to 28% n=5). ISI distributions of neurons of both preparations switching from bursting to tonic firing in presence of APV are displayed in Fig. 7A-B.

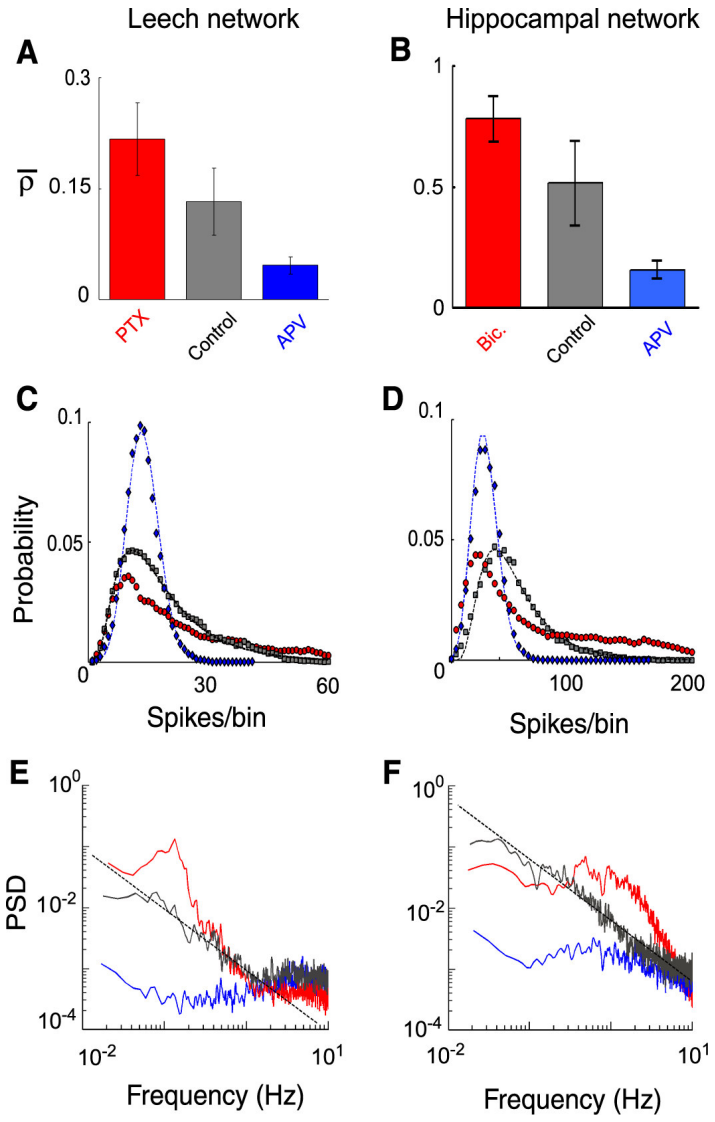

Figure 8. Effects of modulation of NMDA and GABA synaptic pathways on network correlation, ***A-B,*** *Network correlation coefficient rate in leech (**A**) and hippocampal (**B**) networks in the different pharmacological conditions.* ***C-D,*** *Spikes per bin distribution of the network firing rate in leech (**C**) and hippocampal (**D**) networks. Data were fitted by a lognormal function in normal conditions (gray symbols). In the presence of APV (blue symbols) data were fitted by a Poisson distribution for the leech network and a lognormal distribution for the hippocampal network. Note the reduction of skewness in the presence of APV in both preparations (see text).* ***E-F****, Power spectrum of the network firing rate in control (black trace), in the presence of APV (blue trace), PTX (**E**, red trace) or Bicuculline (**F**, red trace). Black broken lines have 1/f slope.*

In both networks the blocking of GABA receptors had opposite effects. The fraction of neurons displaying an exponential ISI decreased (leech: from 37% to 14% n=6; hipp. culture: from 15% to 8% n=5). ISI distributions of neurons switching from tonic to bursting firing in both preparations are displayed in Fig. 7C-D.

The cooperative behavior observed in both networks at longer bin width is likely to be mediated by synaptic pathways. Therefore, we investigated the action of antagonists of excitatory and inhibitory transmission on the degree of correlation in both networks. As the power spectral density of the network firing rate (see Methods) characterizes also the temporal structure of correlated activity we analysed in detail their effect on the spike per bin distribution, the power spectrum of the firing rate and $\bar{\rho}$ of both networks.

Blocking the excitatory transmission mediated by NMDA receptors with APV (see Methods) considerably diminished the degree of correlated firing (leech: n=6, $\bar{\rho}$=0.05±0.01, hippocampal: n=5, $\bar{\rho}$=0.14±0.03; Fig. 8A-B). In both networks the two values were significantly different (t test, $p<0.05$), meaning that there is a decrease of correlation in the presence of APV. In leech networks, the spike per bin distribution, which was fitted by a lognormal distribution in normal conditions (Fig. 8C, black trace), became either a Poisson distribution (Fig. 8C, blue trace; 3/6, χ^2 test, $p>0.05$), or a lognormal distribution (3/6, χ^2 test, $p>0.05$) with a reduced skewness (between 40% and 60% of the control values, see Methods), as expected from a decreased correlated firing. Similarly, in hippocampal networks, the skewness of the lognormal function decreased significantly (between 5% and 20% of the control values; black and blue trace in Fig. 8D).

In normal conditions, the firing rate power spectrum decreased as 1/f for frequencies between 0.1 and 2 Hz (leech, n=15, mean slope= -0.97±0.3; hippocampal, n=10, mean slope= -1.15±0.2), consistently with the presence of correlations at time scales larger than 500 ms (Fig. 8E and F, black trace). In the presence of APV, the power spectrum was almost flat (Fig. 8E and F, blue trace) at all analysed frequencies (leech, n=6, slope between 0 and -0.2; hippocampal, n=5, slope between 0 and -0.4), just as expected in the absence of correlation (Papoulis, 1984). By contrast, when inhibitory pathways mediated by GABA receptors were blocked (see Methods), a correlation increase was observed in both networks (leech: n=5, $\bar{\rho}$=0.22±0.05, hippocampal: n=5, $\bar{\rho}$=0.7±0.1 see Fig. 8A-B). The increase of correlation was significant in both networks (t test, $p<0.05$) and modified also the shape of the power spectrum, leading to a broad peak at low frequencies (Fig. 8E and F, red trace; leech, n=5; hipp., n=5). In the presence of Bicuculline the firing rate power spectrum of hippocampal networks exhibited a pronounced peak at frequencies

between 0.2 and 0.6 Hz, while PTX in leech networks increased the power associated to frequencies between 0.1 and 0.3 Hz.

These results show that excitatory synaptic pathways mediated by NMDA receptors contribute to the correlated firing of the spontaneous activity of both networks and that inhibitory synaptic pathways mediated by GABA receptors have an opposite effect.

Spontaneous bursting activity

Previous results have shown that long range interactions lead to power law dynamics in *in vitro* cultures (Segev et al. 2002). The distribution of size and duration of spontaneous bursts in cortical slices (Beggs and Plenz 2003, Beggs and Plenz 2004, Haldeman and Beggs 2005, Stewart and Plenz 2006) has been shown to follow power law distributions with characteristic slopes. We checked then whether size and duration of spontaneous burst in leech and hippocampal networks followed power law distributions. Since there is no standard way to define a burst, we have used three different definitions (A, B and C) to identify it (see Methods). The definition of a burst is based on the analysis of ISI and of the network average firing rate. In Definition A, we discriminated a fast and a slow dynamics, and we identified bursts by grouping together spikes occurring during the fast dynamics. Definition B identifies bursts as collections of spikes with an value of ISI lower than the average, and definition C as strips of bins where the network firing rate is higher than the average value. These definitions are described in detail in the Methods section.

For leech networks and for the three definitions of burst, the distribution of the bursts size and duration (see shades of red in Fig. 9) followed a power law over two log units. In hippocampal networks (see shades of blue in Fig. 9) approximately 10 times more neurons than in leech networks were recorded, and therefore we could observe power law behavior over an extended range: as shown by the blue shaded lines, the distribution of burst size and duration had a power law distribution over three log units for the three definitions.

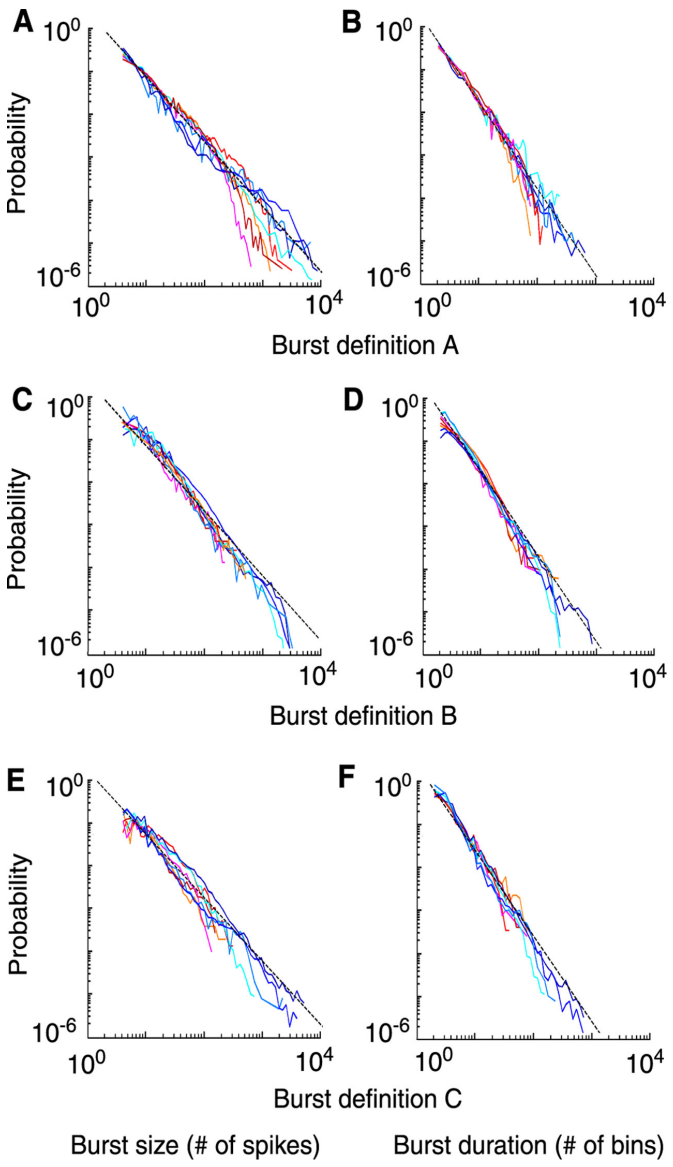

Figure 9. Bursts statistics. *Probability distribution of bursts size and duration, computed according to three different definitions of burst. Data from representative experiments obtained in leech (reddish lines) and hippocampal networks (bluish lines).* ***A-B****, Bursts size (****A****) and duration (****B****) distributions calculated according to definition A.* ***C-D****, Burst size (****C****) and duration (****D****) distributions calculated according to definition B.* ***E-F,*** *Burst size (****E****) and duration (****F****) distributions calculated according to definition C. Black broken lines are power laws with a slope of –1.5 in the left column and –2 in the right column. Note the power law behavior of bursts size distribution of hippocampal networks for more than 3 log units.*

The average slope of the bursts size distribution (Fig. 9A, C and E) was –1.6±0.2 (Def. A), –1.55±0.2 (Def B.), –1.6±0.2 (Def. C) for leech networks (n=15), and –1.55±0.2 (Def. A), –1.65±0.2 (Def. B), –1.6±0.2 (Def. C) for hippocampal networks (n=10). We also observed that the duration distribution of the bursts followed a power law distribution (Fig. 9B, D and F), with an average slope of –2.1±0.2 (Def. A), -2.2±0.2 (Def B.), –2.1±0.2 (Def. C) for leech networks (n=15), and –2.1±0.1 (Def. A), -2.15±0.2 (Def B.), –2.1±0.2 (Def. C) for hippocampal networks (n=10). The statistics of bursts obtained with the three definitions were not significantly different (t test, $p>0.1$). However, definition A is able to characterize bursts over a more extended range, therefore it was used for later analysis.

As changing the balance of inhibition and excitation affected significantly the degree of correlated firing among neurons in both networks, we analysed how pharmacological modulations of excitation and inhibition modified the distribution of bursts size and duration. In the presence of APV, the distributions of bursts size and duration (Fig. 10 A-B) of leech (shades of red) and hippocampal (shades of blue) networks were concave and decaying faster than a power law (black dashed line in the figures). In contrast, in the presence of PTX or Bicuculline, very large bursts were more frequent than in control conditions, as indicated by the presence of a secondary peak (marked with an arrow) in the burst size and duration distribution (Fig. 10 C-D). These results show that when excitatory synaptic pathways mediated by NMDA receptors are blocked, and the interaction among neurons is reduced, both networks enter into a non-bursting regime. In contrast, blockage of inhibitory GABAergic synaptic pathways drives the networks towards a regime characterized by large and highly synchronous bursts.

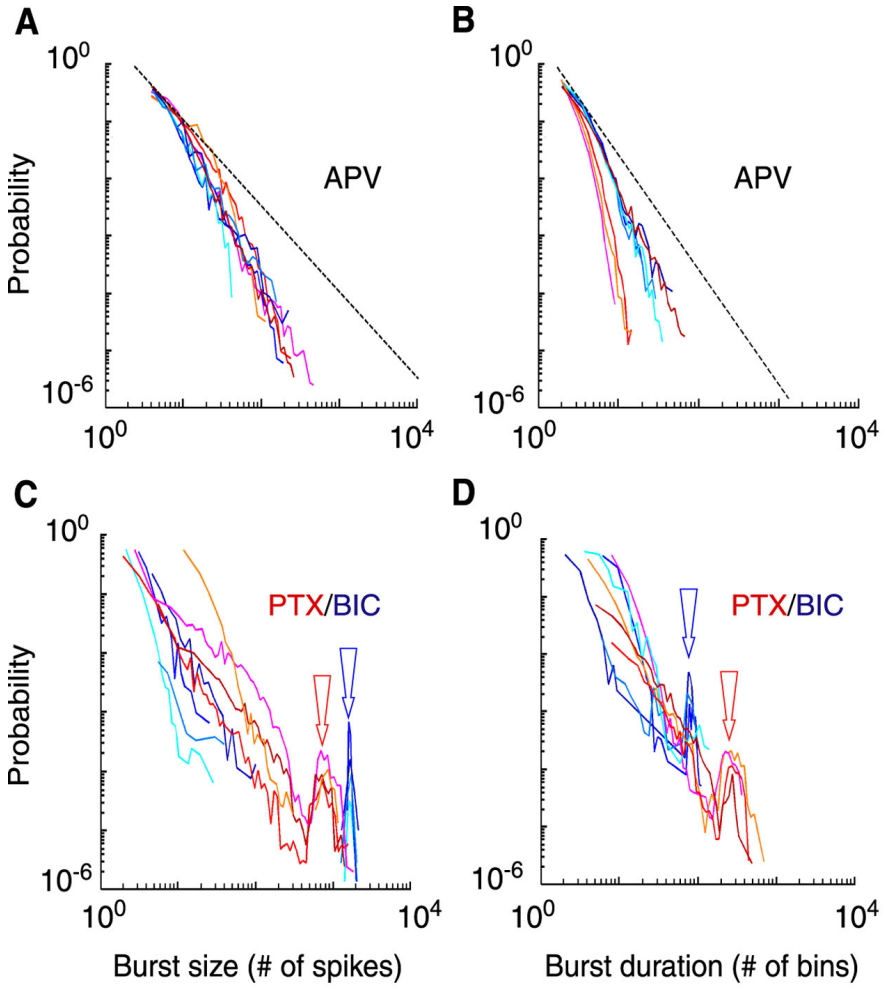

Figure 10 Pharmacological regimes. *Bursts size and duration distributions for leech (reddish lines) and hippocampal (bluish lines) networks obtained using burst definition A.* ***A-B****, In the presence of APV, in both preparations the number of large bursts decreases, (compare to Fig. 4). The black broken line has a slope of –1.5 in (****A****) and of –2 in (****B****).* ***C-D****, In the presence of GABA receptor blockers (PTX/Bicuculline), in both preparations large bursts with characteristic size/duration indicated by the arrows appear. In hippocampal networks, intermediate size bursts are absent as shown by the discontinuity of the distributions.*

Neurons in dissociated cultures are still able to handle and store information, so we investigated the effect of different bursting dynamics on information processing in hippocampal networks. In previous experiments in which isolated pulses were applied to hippocampal networks, blockage of excitatory synaptic pathways mediated by NMDA receptors substantially increased the mutual information between stimuli and evoked electrical activity. An opposite effect was observed when inhibitory synaptic pathways mediated by GABA receptors were blocked (Bonifazi et al. 2005). In the present manuscript, we studied the reliability of the response evoked by trains of pulses in different regimes. We stimulated the hippocampal culture by applying trains of pulses with the same voltage and inter-pulse interval (IPI) to a subset of electrodes while simultaneously recording the evoked and spontaneous activity (see Methods). As indicated by the raster plots (see Fig. 11A) of observed spike trains, in the presence of APV spikes were clustered invariably after the stimulus (yellow vertical bars) and only occasionally were observed before the stimulus or with a significant delay from it. By contrast, in the presence of Bicuculline, spikes could be observed before the stimulus and were not locked to the stimulus as in the presence of APV. An intermediate situation was observed in control conditions. The way in which the network responds to the train of identical stimuli in the different regimes is also illustrated by the network firing rate (see Fig. 11B), which, in the non bursting regime, has well defined peaks after every stimuli. These peaks are progressively less well defined in the control and highly bursting regime. In the non bursting regime, spikes are locked to the applied stimuli and the evoked electrical activity is less affected or disturbed by the spontaneous activity. Differences observed in the considered regimes were quantified by analysing the coefficient of variation (CV) and the signal to noise ratio (SNR) of the evoked response (see Methods).

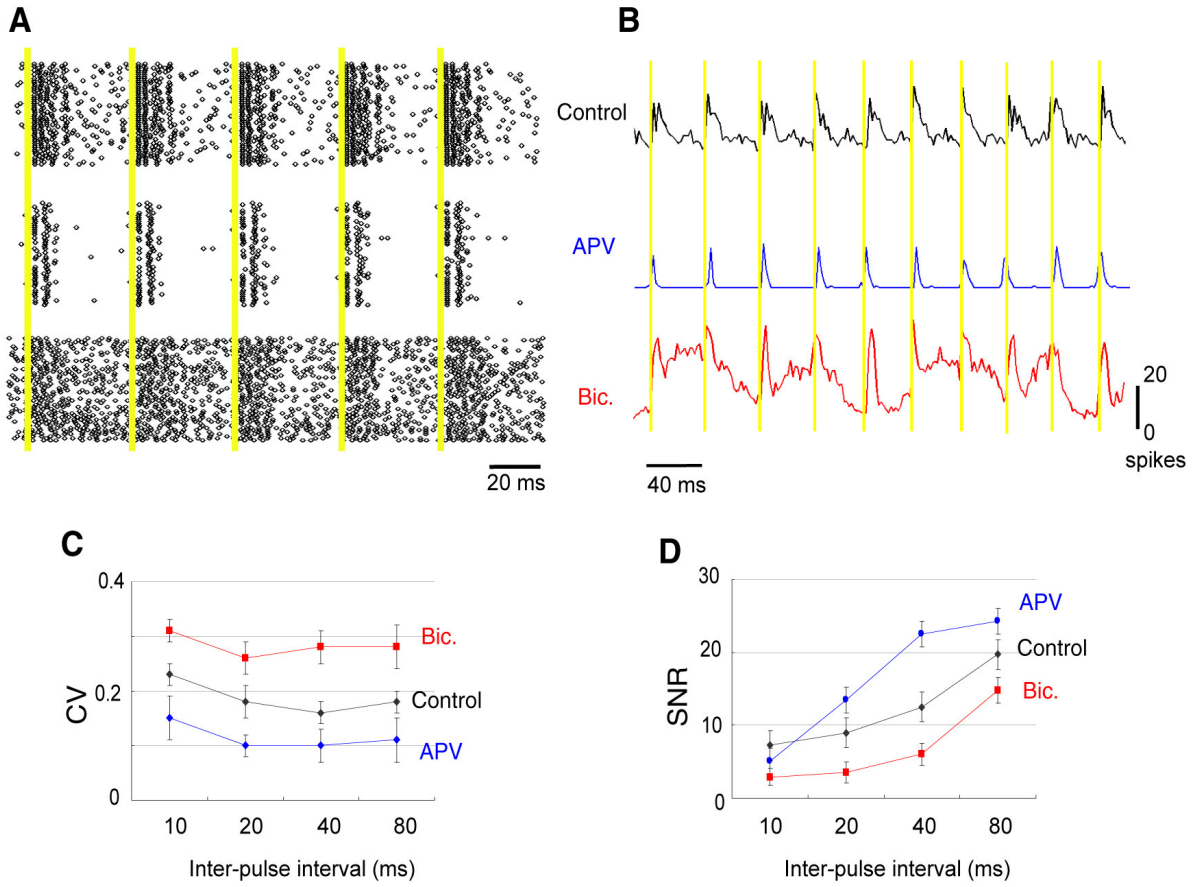

Figure 11. Bursting regimes and evoked activity. ***A****, Evoked activity from a representative electrode recording of an hippocampal network. Raster plots of 50 trials in control (upper panel), in the presence of APV (intermediate panel) and in the presence of Bicuculline (lower panel). Yellow bars indicate occurrence of applied pulses.* ***B,*** *Network firing rate binned at 2 ms from the same hippocampal culture in control (black), APV (blue) and Bicuculline (red). Yellow bars indicate occurrence of applied pulses.* ***C****, Coefficient of variation (CV) and* ***D****, Signal to noise ratio (SNR) of the response of a representative culture in control (black line), APV (blue line) and Bicuculline (red line) for different inter-pulse intervals. Mean and SD calculated over 50 trials.*

For IPIs ranging from 10 to 80 ms, the CV significantly decreased in the presence of APV and increased in the presence of Bicuculline (t test, $p<0.05$, 5/5 see Fig. 11C). In all conditions the CV was stable for IPI>10 ms (t test, $p>0.1$, see Fig. 11C). The SNR of the evoked response was, on the contrary, positively correlated to the IPI (see Fig. 11D). For IPIs greater than 10 ms, the value of SNR was significantly decreased by Bicuculline and increased by APV (t test, $p<0.05$, 5/5, see Fig. 11D). These results show that responses to stimuli are very variable in the presence of a strongly correlated spontaneous activity, typical of the highly bursting regime, and become more reliable in the non bursting regime. These effects were at large extent a consequence of the correlated electrical activity in the network, which is affected by the balance between inhibition and excitation. At the same time the strength of the response is drastically weaker when the excitation is decreased by the presence of APV and the number of neurons involved is smaller (data not shown), and this might make stimuli discrimination more difficult. The spontaneous activity in control represents probably a trade-off between reliability and intensity in the response to the stimuli.

Discussion

Single neuron dynamics

The analysis of ISI distributions of single identified motor neurons allowed to identify three stereotyped distributions: a) exponentially distributed, b) bi-exponentially distributed c) exhibiting two peaks: a larger peak at time T followed by a secondary peak at time 2T (Fig. 3). Firing of *in vivo* motor neurons can be described by a Poisson process (Rieke et al. 1997), i.e. neurons fire stochastically with a given average rate. This mode of firing leads to an exponential ISI distribution, as those observed in present manuscript. Some neurons have episodes of rhythmic firing, reminiscent of the activity of pace-maker neurons (Marder et al. 2005), and this leads to the

presence of a peak in the ISI distribution for an ISI value equal to the period T of the regular activity, and usually also to a smaller peak in 2T corresponding to the times when a spike in the rhythmic episodes failed to be observed. When the overall activity of the network increases, most neurons display a bursting dynamics in which intervals of intense firing are alternated to less active periods. This behavior leads to a bi-exponential distribution of ISI, with a short time constant for spikes occurring during a burst and a longer time constant for spikes occurring between bursts. The possibility of a shift between tonic and bursting activity due to the incoming synaptic inputs is well known (Turrigiano et al. 1994), and has been extensively studied in the leech heartbeat interneurons (Cymbaluk et al. 2002).

Synaptic transmission

The spontaneous activity of both analysed neuronal networks is composed by irregular, arrhythmic bursts of very different sizes. This structure originates from the correlated activity of the neurons forming the networks. Neuronal interactions determining the bursts dynamics act on a timescale of some hundreds of ms (Fig. 2) and are suppressed by APV (Fig. 3 and 5). In the presence of APV both networks enter into a non bursting regime, characterized by a lower correlated electrical activity and a significantly reduced occurrence of large bursts. Excitatory post synaptic potentials (EPSP) mediated by NMDA receptors have a slow kinetics decaying with a time of 50-100 ms and are blocked by APV (Hestrin et al 1990, Koch 1999). These experimental observations suggest that excitatory synaptic pathways mediated by NMDA receptors are responsible for the correlated activity in both networks: long lasting EPSP contrast the effects of inhibition and ensure correlation activity among the neurons. This result was unexpected in leeches, in which the role of NMDA receptors is still unclear (Wu 2002, Burrell and Sahley 2004). In models of spontaneous activity of neuronal networks, NMDA slow inactivation mechanism has proven to have a key role in determining the long duration of activity patterns (Cai et al. 2005) or directly the possibility of stable persistent activity (Wang 1999).

By contrast, when the inhibitory GABA synapses were blocked with PTX in the leech and with Bicuculline in the hippocampal culture, the result was a bi-stable dynamics alternating very large bursts to low activity intervals (Fig. 3 and 5). In both preparations the variability of the signal is

then due to a balance between inhibition and excitation (Shadlen and Newsome 1998) respectively mediated by GABA and NMDA receptors.

Our results show that in both networks the activity involved multiple timescales, as is evident from the 1/f slope of the power spectrum. This dynamics could be originated by a super-imposition of independent processes rather than by interaction among the neurons, but this is not what is happening in our case because a) independent firing would have originated a Poisson distribution of spikes/bin while this distribution is lognormal; b) no single neuron is acting on the very low frequencies (<0.1 Hz) that are dominating the spectrum; c) NMDA receptors blockage results in a flat power spectrum (see Fig. 3), demostrating that the 1/f power spectrum is due to excitatory interactions.

Models of network dynamics

Two common features of the spontaneous activity of both networks were the presence of multiple timescales of interactions, shown by the 1/f power spectrum behavior on the low frequencies range (Fig. 5), and the large variability of the activity, causing the absence of a characteristic scale for bursts as shown by the power law distributions of burst size and duration (Fig. 9).

These observations are in agreement with previous analysis of the spontaneous activity of hippocampal and cortical networks. Segev et al. (2001) observed long-lasting correlation of the spontaneous activity in dissociated hippocampal cultures. Their results were explained in a model of self-organization among integrate-and-fire neurons, based on three hypothesis: a) the network is not homogeneous, i.e. some neurons display fatigue during bursts while others display facilitation (Persi et al 2004); b) the balance of inhibition and excitation is self regulated; c) an internal source of noise drives the network activity (Volman et al. 2004).

In an other paper on spontaneous activity, Beggs and Plenz (2003) recorded local field potentials from cultured cortical rat slices and found evidence for “neuronal avalanches” with amplitude distributions described by a power law over two orders of magnitude. The authors define neuronal avalanches such in a way that they correspond to the avalanches defined in lattice models by the theory of Self Organized Criticality (SOC) (Bak et al. 1988, Jensen, 1998). Their results support the idea that SOC is the dynamics underlying spontaneous activity in the cultures.

In other papers (Linkenkaer-Hansen et al. 2001, Freeman 2004), the presence of SOC dynamics underlying spontaneous activity recorded in human EEG was argued by the presence of long-term correlations (but see also Bedard et al. 2006).

SOC theory describes networks of interacting elements with three basic properties: 1) on a fast timescale active elements excite neighbouring elements with a threshold dynamics; 2) on a slow timescale, external stimuli trigger the activity of the elements of the network; 3) the total energy of the system is constant. These networks have been proven to self-regulate to a critical state, in which the activity is correlated on multiple timescales and is characterized by propagating avalanches. The probability distributions of size and duration of these avalanches are power laws respectively with slope –3/2 and –2 (Vespignani and Zapperi, 1998). When considering neuronal networks, composed by interacting threshold neurons, the avalanches correspond to bursts of spikes. SOC can account for the large variability of the spontaneous activity, and makes predictions about the effect that different modulations can have on the network dynamics.

There are, however, two open problems. First, if conditions 1 and 3 for the presence of SOC are fulfilled by neuronal networks, the validity of condition 2 is less evident: the source of the activity in isolated networks, not receiving external stimulations or chemical triggering, is still unclear (Volman et al. 2004). The second problem is that conditions 1-3 imply the presence of long range correlations and power laws but the opposite is not always true since other mechanisms are known to originate both phenomena (for a review, see Sornette 2004). We think nonetheless that SOC could be a good statistical model for our results on the spontaneous activity. The first problem can be solved by defining "external stimulus" as all the causes found for membrane potential to fluctuate and occasionally cause an action potential in the absence of stimuli from other neurons of the network. We know that untriggered action potentials are indeed present in isolated networks and that are happening rarely, and this match with the condition 2. The second problem cannot be completely solved as long as we do not keep track of every single synaptic interaction. What is possible to do is to test a larger number of predictions of SOC theory to invalidate this hypothesis or limit the alternative possible dynamics.

In both networks bursts size and duration have power law distributions. Many functions (such as lognormal) can be similar to a power law for a short period, but not over the three orders of magnitude displayed for instance by the burst size distribution in hippocampal cultures. Other mechanisms beside SOC, such as multiplicative noise, can lead to power law distributions, but their parameters must be fine tuned to provide the slopes of –3/2 and –2, that are instead necessary consequences of SOC (Zapperi et al. 1995). SOC models predict that decreasing the interactions among network elements will lead to a rapid decay of avalanche size distribution, and that increasing the interactions will lead to a bi-modal distribution with a peak for large bursts (Eurich et al. 2002). This prediction is in contrast with the model of Persi et al. (2004) expecting a decrease in

activity and bursting for small values of inhibition. Results of pharmacological modulation in the inspected networks match with SOC predictions (Fig. 6 and 11).
To our knowledge, this is the first time that such a broad spectrum of SOC predictions regarding the dynamics of spontaneous activity is tested, and it is the first time that these analyses are performed directly at a spike level, instead of using averaged measures of activity such as LFP and EEG. It is also the first time that this model is tested in invertebrate preparations as we will discuss more carefully in the next section.

A common paradigm for the spontaneous activity of leech and hippocampal networks?

In this work we analysed an intact and functional invertebrate network, and a dissociated mammalian neuronal network. The similarity found in the statistical properties of the spontaneous activity of these profoundly different neuronal networks is remarkable. Leech ganglia are composed of approximately 400 neurons, whereas between 10 and 100 thousand neurons form the investigated hippocampal networks. More importantly, the leech ganglion is a hierarchical neuronal network and the hippocampal culture is a random neuronal network. In dissociated cultures the original cytoarchitectural organization is lost during the dissociation, and neurons re-wire with random connections. By contrast, leech ganglia retain a specific internal structure suitable for specific behaviors, composed by mechanosensory neurons, interneurons and the motor neurons from which we are recording. Our results show that most of the features of spontaneous activity are nonetheless shared between the two networks. This suggests that interactions among neurons are sufficient to determine a global behavior, poorly dependent on the specific wiring of the network itself. Even if connections are different, the activity somehow regulates in such a way to have similar long range temporal correlations and largely variable activity, shown by the power law distribution of bursts size and duration.
In this view the functional role of the wiring of leech networks becomes evident just when specific behaviors are initiated by sensory stimuli and/or command neurons (Kristan et al. 2005) activating specified signal pathways (Lewis and Kristan 1998) or central pattern generators (Brodfuehrer and Friesen 1986).
In hippocampal networks, the reduced spontaneous activity and the lower degree of correlation of non bursting regimes make responses more reliable, and allow pooling and averaging spikes to be more efficient (Bonifazi et al. 2005), although optimal information processing is achieved in the critical state (Beggs and Plenz 2003, Kinouchi and Copelli 2006). Large bursts, typical of the highly bursting regime, seem instead essential during neuronal development (O'Donovan 1999) and may

play an important role in motor coordination (Welsh et al. 1995), sleep patterns (Contreras et al. 1995), gene expression (Arnold et al. 2005), perception and recognition (Yu et al. 2004). As different dynamical regimes seem more suitable for different functions, it is very useful to drive a neuronal network from one regime to another, in a controlled way. Tateno et al. (2005) have already demonstrated how these shifts can be obtained by modifying the balance between excitation and inhibition by means of neuromodulators. Such shifts can also occur during development, when GABA mediated synaptic potential can revert its polarity and pass from excitatory to inhibitory (Cherubini et al. 1991). Shifts of a neuronal network dynamical regime are likely to be a basic feature of neural computation (Marder and Thirumalai, 2002).

References

Arieli A, Sterkin A, Grinvald A, Aertsen A (1996) Dynamics of ongoing activity: explanation of the large variability in evoked cortical responses. Science 273:1868-1871.

Arisi I, Zoccolan D, Torre V (2001) Distributed motor pattern underlying whole-body shortening in the medicinal leech. J Neurophysiol 86:2475-2488.

Arnold FJ, Hofmann F, Bengston CP, Wittmann M, Vanhoutte P, Bading H (2005) Microelectrode array recordings of cultured hippocampal networks reveal a simple model for transcription and protein synthesis-dependent plasticity. J Physiol 564:3-19.

Bak P, Tang C, Wiesenfeld K (1988) Self-organized criticality. Physical Review A: Atomic, Molecular, and Optical Physics 38:364-374.

Baker RE, Corner MA, van Pelt J (2006) Spontaneous neuronal discharge patterns in developing organotypic mega-co-cultures of neonatal rat cerebral cortex. Brain Res. 1101:29-35

Beggs JM, Plenz D (2003) Neuronal avalanches in neocortical circuits. J Neurosci 23:11167-11177.

Beggs JM, Plenz D (2004) Neuronal avalanches are diverse and precise activity patterns that are stable for many hours in cortical slice cultures. J Neurosci 24:5216-5229.

Bliss TVP, Collingridge GL (1993) A synaptic model of memory: long-term potentiation in the hippocampus. Nature 361:31-39.

Bonifazi P, Ruaro ME, Torre V (2005) Statistical properties of information processing in neuronal networks. Eur J Neurosci 22:2953-2964.

Brodfuehrer PD, Friesen WO (1986) Control of leech swimming activity by the cephalic ganglia. J Neurobiol. 17: 697-705

Burrell BD, Sahley CL (2004) Multiple forms of Long-Term Potentiation and Long-Term-Depression converge on a single interneuron in the leech CNS J Neurosci 24:4011-4019

Cai D, Rangan AV, McLaughin DW (2005) Architectural and synaptic mechanisms underlying coherent spontaneous activity in V1 PNAS 102:5868-5873

Cherubini E, Gaiarsa JL, Ben-Ari Y (1991) GABA: an excitatory transmitter in early postnatal life. Trends Neurosci 14:515-519.

Cline HT (1986) Evidence for GABA as a neurotransmitter in the leech J Neurosci 6:2848-2856

Connors BW, (1984) Initiation of synchronized neuronal bursting in neocortex. Nature 310:685-687.

Contreras D, Destexhe A, Sejnowski TJ, Steriade M (1997) Spatiotemporal patterns of spindle oscillations in cortex thalamus. J Neurosci 17:1179-1196.

Corral A. Perez CJ, Diaz-Guilera A, (1996) Self-organized criticality induced by diversity Phys. Rev. Lett 78: 1492-1495

Crow EL, Shimitzu K (1987) Lognormal Distributions. New York: Marcel Dekker.

Cymbaluk GS, Gaudry Q, Masino MA, Calabrese RL (2002) Bursting in leech heart interneurons: cell-autonomous and network-based mechanisms J Neurosci 22: 10580-10592

Eurich CW, Herrmann JM, Ernst UA (2002) Finite-size effects of avalanche dynamics. Physical Review E: Statistical, Nonlinear, and Soft Matter Physics 66:66137-66152.

Fiser J, Chiu C, Weliky M (2004) Small modulation of ongoing cortical dynamics by sensory input during natural vision. Nature 431:573-578.

Freeman WJ (2004) Origin, structure, and role of background EEG activity. Part 2. Analytic phase. Clin. Neurophysiol 115:2089-2107.

Garcia-Perez E, Mazzoni A, Zoccolan D, Robinson HPC, Torre V (2005) Statistics of decision making in the leech. J Neurosci 25:2597-2608.

Gonzales-Islas C, Wenner P (2006) Spontaneous network activity in the embryonic spinal cord regulates AMPAergic and GABAergic synaptic strength. Neuron 29:563-575

Hardingham GE, Arnold FJL, Bading H (2001) Nuclear calcium signalling controls CREB-mediated gene expression triggered by synaptic activity. Nat Neurosci 4:261-267.

Hestrin S, Nicoll RA, Perkel DJ, Sah P (1990) Analysis of excitatory synaptic action in pyramidal cells using whole-cell recording from rat hippocampal slices J Physiol (Lon) 422:203-225

Jensen HJ (1998) Self-Organized Criticality – Emergent Complex Behavior in Physical and Biological Systems. Cambridge: Cambridge University Press.

Jones TA, Jones SA (2000) Spontaneous activity in the statoacoustic ganglion of the chicken embryo, J Neurophysiol 83:1452-1468.

Kinouchi O, Copelli M (2006) Physics of psychophysics: dynamic range of excitable networks is optimized at criticality Nature Physics 2:348-351

Koch C (1999) Biophysical computation (Oxford University Press, Oxford)

Krahe R, Gabbiani F (2004) Burst firing in sensory systems. Nat Rev Neurosci 5:13-23.

Kristan WB Jr, Calabrese RI, Friesen WO (2005) Neuronal control of leech behavior. Prog Neurobiol 76:279-327.

Lee IH, Assad JA, (2003) Putaminal activity for simple reactions or self-timed movements. J Neurophysiol 89:2528-2537.

Leinekugel X, Khazipov R, Cannon R, Hirase H, Ben-Ari Y, Buszaki G (2002) Correlated bursts of activity in the neonatal hippocampus *in vivo*. Science 296:2049-2053

Lewis JE, Kristan WB (1998) Representation of touch location by a population of leech sensory neurons. J. Neurophysiol. 80: 2584–2592

Limpert EL, Stahel WA, Abbt M (2001) Log-normal distributions across the sciences: keys and clues. BioSci 51:341-351.

Linkenkaer-Hansen K, Nikouline VV, Palva JM, Ilmoniemi RJ (2001) Long range temporal correlations and scaling behavior in human brain oscillations. J Neurosci 21:1370-1377.

Maimon G, Assad JA (2006) Parietal area 5 and the initiation of self time-movements versus simple reactions. J Neurosci 26:2487-2498.

Marder E, Calabrese RL (1996) Principles of rhythmic motor pattern generation. Physiol Rev 76:687-717.

Marder E, Thirumalai V (2002) Cellular, synaptic and network effects of neuromodulation. Neural Netw 15:479-493.

Mazzoni A, Garcia Perez E, Zoccolan D, Graziosi S, Torre V (2005) Quantitative characterization classification of leech behavior. J.Neurophysiol 93:580-593.

Muller KJ, Nicholls JG, Stent GS (1981) The nervous system of the leech: a laboratory manual. In: Neurobiology of the Leech (Muller KJ, Nicholls JG Stent GS), pp249-275. New York: Cold Spring Harbor Laboratory.

O'Donovan MJ (1999) The origin of spontaneous activity in developing networks of the vertebrate nervous system. Curr Opin Neurobiol 9:94-104.

Papoulis A (1984) Probability, Random Variables, and Stochastic Processes 2nd ed. New York:McGraw-Hill.

Payton B (1981) Structure of the nervous system of the leech. In: Neurobiology of the Leech (Muller KJ, Nicholls JG Stent GS), New York:Cold Spring Harbor Laboratory.

Persi E, Horn D, Volman V, Segev R, Ben-Jacob E (2004) Modelling of synchronized bursting events: the importance of inhomogeneity. Neural computation 16:2577-2595

Rieke F, Warland D, de Ruyter van Steveninck R, Bialek W (1997) Spikes. Exploring the Neural Code. Cambridge, MA: MIT Press

Ruaro ME, Bonifazi P, Torre V (2005) Toward the neurocomputer: image processing and pattern recognition with neuronal cultures. IEEE Trans Biomed Eng 52:371-383.

Schneidman E, Berry MJ, Segev R, Bialek W (2006) Weak pairwise correlations imply strongly correlated network states in neural population. Nature 440:1007-1012.

Segev R, Benveniste M, Hulata E, Cohen N, Palevski A, Kapon E, Shapira Y, Ben-Jacob E (2002) Long term behavior of litographically prepared in vitro neuronal networks. Phys. Rev. Lett. 11:81021-81024

Sornette D (2004) Critical Phenomena in Natural Sciences. Berlin:Springer Verlag.

Stewart CV, Plenz D (2006) Inverted-U profile of dopamine-NMDA-mediated spontaneous avalanche recurrence in superficial layers of rat prefrontal cortex. J Neurosci 26:8148-8159

Tateno T, Jimbo Y, Robinson HP (2005) Spatio-temporal cholinergic modulation in cultured networks of rat cortical neurons: spontaneous activity. Neuroscience 134:425-437.

Turrigiano G, Abbott LF, Marder E (1994) Activity-dependent changes in the intrinsic properties of cultured neurons. Science 264:974-977

Van Pelt J, Wolters PS Corner MA, Rutten WLC (2004) Long-term characterization of firing dynamics of spontaneous bursts in cultured neural networks. IEEE Trans. Biom. Eng. 11:2051-2062

Vespignani A, Zapperi Z (1998) How self organized criticality works: a unified mean field picture. Physical Review E: Statistical, Nonlinear, and Soft Matter Physics 57:6345-6363.

Wang XJ (1999) Synaptic basis of cortical persistent activity: the importance of NMDA receptors to working memory. J Neurosci 19:9587-9603

Welsh JP, Lang EJ, Suglhara I, Llinas R (1995) Dynamic organization of motor control within the olivocerebellar system. Nature 374:453-457.

West AE, Chen WG, Dalva MB, Dolmetsch RE, Kornhauser JM, Shaywitz AJ, Takasu MA, Tao X, Greenberg ME (2001) Calcium regulation of neuronal gene expression. Proc Natl Acad Sci USA 98:11024-11031.

Wiesenfeld K, Moss F (1995) Stochastic resonance and the benefits of noise: from ice ages to SQUIDs. Nature 373:33-36.

Wu E (2002) Evidence against the presence of NMDA receptors at a central glutamatergic synpase in leeches Invert. Neurosci. 4: 157-164

Yu CR, Power J, Barnea G, O'Donnell S, Brown HEV, Osborne J Axel, R Gogos JA (2004) Spontaneous neural activity is required for the establishment and maintenance of the olfactory sensory map. Neuron 42:553-566.

Zapperi S, Baekgaard LK, Stanley HE (1995) Self-organized branching processes: mean-field theory for avalanches. Physical Review Letters 75:4071-4074.

Zohary E, Shadlen MN, Newsome WT (1994) Correlated neuronal discharge rate and its implications for psychophysical performance. Nature 370:140-143.

4

The spontaneous activity of the leech nervous system and the onset of movements

Elizabeth Garcia-Perez, Alberto Mazzoni and Vincent Torre

Paper in preparation

In the absence of external stimuli, animals perform irregular movements to explore the environment. Neuronal networks originating simpler behaviors like withdrawal reflexes or rhythmic movements have been carefully studied, but the mechanisms underlying proactive arrhythmic motion are still largely unknown. In this paper we study the spontaneous activity of leech (*Hirudo medicinalis*) neurons in isolated ganglia, in chains of ganglia and in semi-intact preparations with extracellular recordings. The spontaneous activity in the isolated ganglion is characterized by irregular bursts of all size. When the ganglion was connected with the neighboring ganglia, the synchronization among neurons increased and the spontaneous activity was characterized by very large bursts. Monitoring synchronously the movements of the animal and the electrical activity of mid-body ganglia we studied how these large bursts lead to the motion of the animal.

INTRODUCTION

Understanding how movements are originated is a major issue in neuroscience. The basic mechanisms underlying the control of muscle activation and coordination seem largely shared among different species (Grillner 2003). In particular reflexes, such as the withdrawal from noxious stimulation, and periodic behaviors, such as heartbeat or walking, have been extensively studied. Reflexes originate from feedforward networks initiated by sensory inputs and terminating into the production of movements, (Grillner 2004, Sandrini et al 2005). Periodic movements are produced by central pattern generators (CPGs): networks of neurons able to generate rhythmic behaviors once triggered by an appropriate stimulus (Marder 2001). CPGs have been demonstrated in a variety of preparations in both invertebrates (Nusmbaum and Beenhakker 2002, Marder et al. 2005) and vertebrates (Grillner 2005). However the entire repertoire of animal motions is not exhausted by rhythmic movements or reflexes to external stimuli. In the absence of stimuli, the animals often actively explore the environment in an irregular way, searching for relevant signals or clues (Flanagan 2003, Glimcher 2003, Falck-Ytter 2006). The neuronal mechanisms responsible for such proactive behaviors (Lee and Assad 2003, Maimond and Assad 2006) have been investigated only recently and are largely unknown.

Studies on reflexes and CPGs have shown how the nervous system reacts to stimuli, but for the large and structured spontaneous activity known to be present in the nervous system (Arieli et al. 1996, Fiser et al. 2004, Destexhe and Contreras 2006) is still missing a satisfying description.

The present manuscript studies the spontaneous electrical activity in the leech (*Hirudo medicinalis*) and its relationship to movements. The leech is an ideal preparation to study the neuronal mechanisms underlying a variety of behaviors (Kristan et al. 2005). Neuronal networks controlling the periodic movements of swimming (Brodfuehrer and Friesen 1986, Brodfuehrer and Thorogood, 2001) and crawling (Cacciatore et al. 2000, Eishenart et al. 2000) have been carefully investigated, providing an almost complete description of the underlying CPGs and of the neuronal pathways leading from stimuli to behavior, involving the trigger neurons (Briggman et al. 2006). Neuronal mechanisms initiated by mechanical stimulation and leading to local bending (Lewis and Kristan 1998, Garcia-Perez et al 2004) and to whole body shortening (Shaw and Kristan 1999, Arisi et al. 2001) have also been accurately described.

In previous papers we described the spontaneous behavior of the leech in the absence of direct sensory stimulation (Garcia-Perez et al. 2005) and the spontaneous electrical activity in the leech ganglia (Mazzoni et al. in preparation). To understand the relationship between these two phenomena it is necessary to understand how the spontaneous electrical activity is determined.

In this paper we will analyse the spontaneous activity in the leech nervous system, recording extracellularly from the roots projecting out of the ganglion with suction electrodes. We will initially investigate the spontaneous firing of single neurons and their role in burst initation and participation. Correlations among different roots will be investigated. Then we will compare properties of the spontaneous activity in the ganglion when this is isolated, when is connected to neighboring ganglia, and in semi-intact leeches. This multi-level analysis will be an occasion to investigate spontaneous activity in a structured *in vivo* neuronal network, instead in *in vitro* preparations as usually done (Segev et al. 2001, Beggs and Plenz 2003). Finally, we will analyse the relationship between spontaneous electrical activity and behavior, and in particular how large motor neuron burst are originated and their role in the initiation of spontaneous body motions.

MATERIALS AND METHODS

Animals and Preparations

Medicinal leeches (*Hirudo medicinalis*) were obtained from Ricarimpex (Eysines, France) and kept at 5º C in tap water dechlorinated by aeration for 24 hours. Different kind of preparations were used as summarized in Figure 1A. The simplest preparation consisted in an isolated ganglion (see left panel of Fig. 1A), usually comprised from the 8th and the 13th ganglion of the nerve cord. An isolated ganglion is divided in a left (L) and right (R) semi-ganglion, from which two pairs of roots emerge. Each root was dissected and drawn into glass suction pipettes (Arisi et al. 2001) with which it was possible to record extracellular voltage spikes (see upper panel Fig. 1B). Extracellular voltage spikes were identified as elicited by specific neurons by simultaneously impaling under visual control identified motor neurons. The coincidence of intracellular spikes and extracellular spikes provided an unequivocal way to assign extracellular voltage spikes to identified motor neurons (see Fig. 1B). When the spontaneous activity of an isolated ganglion was analysed 4-8 suction pipettes were used. In this way, it was possible to characterize the firing activity of a large fraction of all leech motor neurons. All preparations were kept in a Sylgard-coated dish at room temperature (20-24°C) and bathed in Ringer solution (in mM: 115 NaCl, 1.8 $CaCl_2$, 4 KCl, 12 glucose, 10 Tris maleate buffered to pH 7.4) (Muller et al. 1981).

A second preparation consisted in a chain of two ganglia linked by the connective fibres (middle of Fig. 1A). Similarly to when isolated ganglia were analysed, the spontaneous activity was analysed with 3-4 suction electrodes recording from roots emerging from each ganglion. We always recorded from pairs of identical roots from the left and right semi-ganglion. We also used semi-intact preparations (Mazzoni et al. in preparation) in which one or two ganglia are disconnected from the body wall but are connected to rest of animal (see right panel of Fig. 1A), which is kept intact. In this preparation it is possible to record electrical signals from the roots emerging from the central ganglia and to observe the motion and behavior of the head and tail of the leech.

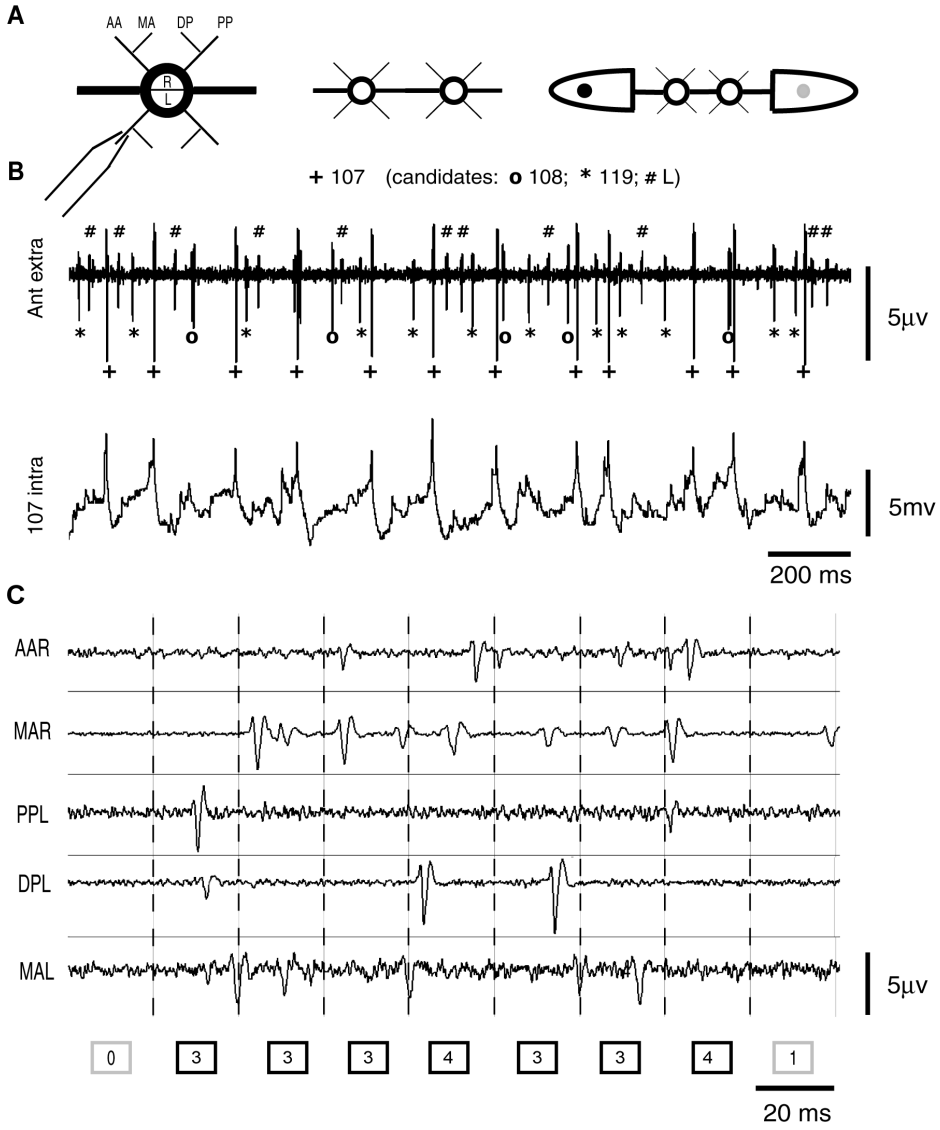

Figure 1: Preparations; neurons and bursts identification ***A,*** *Drawing of used preparations. From left to right: isolated ganglion, pair of connected ganglia and pair of ganglia in semi-intact preparation.* ***B,*** *Extracellular recording from anterior root (top) and intracellular recording from motor neuron 107 projecting to the same root (bottom). Motor neuron 107 was impaled under visual control and its action potentials, recorded with the intracellular electrode, corresponded to the extracellular spikes indicated by the cross +. With this procedure we identified spikes indicated by + as produced by motor neuron 107.* ***C,*** *Extracellular recording from 5 roots of the same ganglion. Recording time is divided into bins (see Methods) and the number of spikes recorded in every bin is indicated in the boxes at the bottom. Dark boxes correspond to active bins, with at least 2 spikes (see Methods). A burst is identified as a strip of consecutive active bins separated by boxes with 0 or 1 spike.*

Spike detection. Spike sorting was carried out for leech networks by using a software developed in our laboratory (Arisi et al. 2001).

Network firing rate (FR). The duration of the recording was divided into bins of constant width. Different widths were used to compare properties at different time scales. In leech networks, for each single neuron the number of spikes occurring in each bin was counted and the resulting discrete time series represented the *neuron firing rate*. The *network firing rate FR* is defined as the sum of all neuron firing rates (i.e. the number of all spikes recorded in the network in each bin)

Lognormal fit. The probability distribution *P(S)* of the number of spikes S per bin of the network firing rate was fitted by a lognormal function:

$$P(S) = \frac{1}{S\sqrt{2\pi}\sigma} \exp\left[-\frac{(\ln S - \mu)^2}{2\sigma^2} \right]$$

where μ and σ are the mean and the variance of the distribution of the logarithm of *S*.

Power spectral analysis The power spectral density (PSD) of the network firing rate obtained with a bin width of 10 ms was computed by using Welch's averaged modified periodogram method (*pwelch* function in Matlab) after a low pass filtering with a cut off frequency of 25 Hz to prevent aliasing.

Correlation. For each pair (i,j) of neurons or electrodes the correlation coefficients (Papoulis, 1984) $\rho_{i,j}$

$$\rho_{ij} = \frac{\sum_n (FR_i(n) - < FR_i >)(FR_j(n) - < FR_j >)}{\sqrt{(< (FR_i(n) - < FR_i >)^2 >)(< (FR_j(n) - < FR_j >)^2 >)}}$$

of the neuron or electrode firing rates $FR(n)$ was computed in a bin width of 500 ms.

Bursts identification. Bursts were identified with a procedure similar to that used previously to identify bursts of local field potentials (Beggs and Plenz 2003). The idea of the procedure is outlined in Fig. 1C, where electrical recordings from several roots are divided into frames of a given duration. The total number of spikes recorded from all suction pipettes were counted, so that at each

frame corresponded a given number of spikes (see the numbers in the box in the lower portion of Fig. 1C). A burst is identified as the electrical activity included between two frames with 0 or 1 spikes with all frames in between with at least more than 1 spikes.

The distribution of inter-spike intervals (ISI) between successive spikes in the network was computed and fitted by a bi-exponential function:

$$P(ISI = t) = C_1 e^{-t/\tau_{long}} + C_2 e^{-t/\tau_{short}}$$

where C_1 and C_2 are two constants and τ_{short} and τ_{long} are a fast and a slow time constant, respectively. The network firing rate with a bin width equal to τ_{long} was calculated and strips of adjacent bins, each counting more than 2 spikes, were considered as bursts. For each experiment, we computed the average inter-spike interval ($\overline{ISI}$) between successive spikes in the network. $\overline{ISI}$ varied from 10 to 50 ms.

Pharmacology: For studying the activity under reduced excitation, the non-competitive NMDA receptor antagonist 2-amino-5-phosphonopentanoic acid (APV) (final concentration, 20μM; TOCRIS) was bath-applied. For studying the activity under reduced inhibition, the ionotropic GABA receptors antagonists picrotoxin (final concentration, 10μM; Sigma) was bath-applied in the leech ganglia.

Behavior analysis: Behavior in leeches was monitored as described in Mazzoni et al. (2005). Briefly two colored beads were glued in the dorsal side of the animal and their motion was tracked in real time with a color CCD camera. In this way it was possible to follow the motion of the head and tail of semi-intact leeches.

One color CCD camera with 640x480 pixels of image size (Watec 231S) and which viewed the leech from above moving in a Petri dish or small tank was mounted on a dissecting microscope and connected via the S-Video-output (PAL) to a frame grabber (PCI-1411, National Instruments) which was installed on a personal computer used to process images in real time. The colored beads placed on the back of the leech were tracked at 10 Hz, by using software developed in our laboratory with LabVIEW 6.1 (National Instruments). The software converted each acquired frame into two binary images, one for each bead. The positions of the beads on the image plane were acquired as Cartesian coordinates, and 4 time series were obtained: [x(n), y(n)] for the head and [x(n), y(n)] for the tail both for $n = 1 \ldots N$ steps, each step corresponding to 50 ms.

The instantaneous values of the speed of the head (S_{head}) and the speed of the tail (S_{tail}) were computed as

$$S_{head}(n) = \sqrt{\left(\frac{dx_{head}(n)}{dt}\right)^2 + \left(\frac{dy_{head}(n)}{dt}\right)^2} \quad \text{and}$$

$$S_{tail}(n) = \sqrt{\left(\frac{dx_{tail}(n)}{dt}\right)^2 + \left(\frac{dy_{tail}(n)}{dt}\right)^2}$$

where the derivatives are obtained convolving the original time series with the derivative of a Gaussian function.

Small values of speed can be associated to noise in the recording or skin deformations, so the leech was considered to be moving just when the speed was >10 pixels/sec.

RESULTS

Leech ganglia are composed of approximately 400 neurons, many of which have been identified and mapped in a stereotyped atlas of the leech ganglion (Muller et al. 1981). Physiological properties of identified leech neurons are remarkably similar in different ganglia and in different animals. Approximately 20 motor neuron pairs have been identified, symmetrically located in the left and right semi-ganglion. The movements of the muscles of every body segment of the leech are caused by the activity of the motor neurons in the corresponding ganglion. Motor neuron firing is at the basis of the leech motor activity and therefore their spontaneous firing determines the leech spontaneous behavior.

The spontaneous activity of single neurons in isolated ganglia

We have studied the spontaneous activity of single neurons by recording extracellular spikes with suction pipettes (see Fig. 1). From the recordings it was possible to sort single neurons activity according to the procedure described in the Methods section. In a previous paper (Mazzoni et al. in preparation) we found that the inter-spike interval (ISI) of the spontaneous firing of leech motor neurons had three stereotyped distributions: exponential, bi-exponential or peaked. The three distribution indicated respectively a Poisson firing, a bursting firing and an almost periodic firing with an average period between successive spikes corresponding to the position of the peak.

As shown in Fig. 2A for some motor neurons the ISI was either bi-exponential or exponential and for other motor neurons the ISI was either bi-exponential or periodic. No identified motor neuron fired spontaneous spikes with a periodic dynamics in some preparations and with an exponential dynamics in other preparations. When the network activity was high the presence of bursts increased the probability of very small inter-spike intervals, making the ISI distribution bi-exponential. We concluded therefore that every identified motor neuron has an intrinsic spontaneous firing dynamics, which is either periodic or exponentially distributed, when the network activity is low, while in the presence of many bursts the ISI distribution becomes bi-exponential. This hypothesis was strengthened by the results of pharmacological manipulations. When 20 μM APV was added to the medium bathing the ganglia, bursts were almost absent, while when 10 μM PTX was added bursts were the dominant feature (Mazzoni et al. in preparation). The mean percentage of bi-exponential neurons in the two conditions was respectively 14% and 56%, both significantly different from the 42% value in control (n=11 control, n=5 APV, n=5 PTX,

ANOVA test p>0.95). Furthermore, the same neuron could display different ISI distributions in the presence of different extracellular medium.

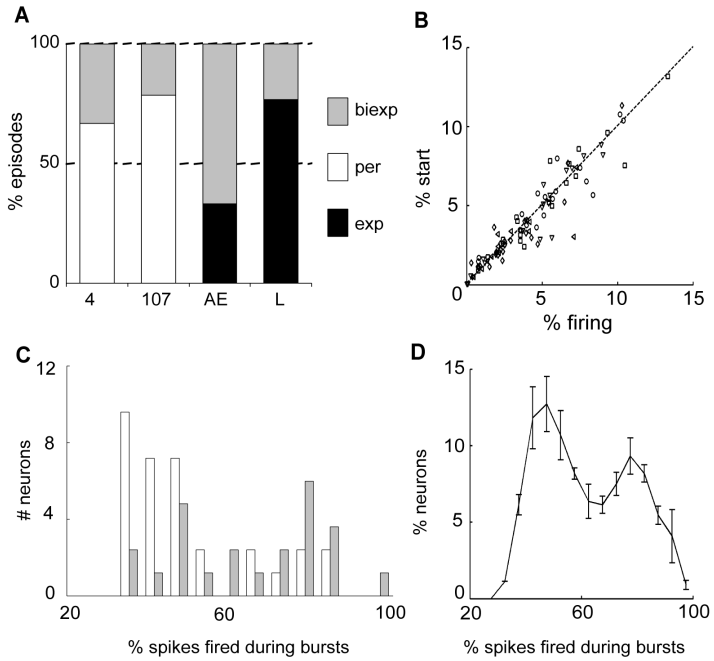

Figure 2 Neurons dynamics and bursts: ***A****, Percentage of experiments in which identified motor neurons (motor neurons # 4, 107, Annulus Erector and Longitudinal motor neurons) had either exponential or bi-exponential or periodic distribution.* ***B,*** *Percentage of bursts started by motor neuron # 101 as a function of the percentage of spikes fired by the same neuron over the total firing of the network. Data collected from 5 experiments, each indicated with a different symbol. Black dashed line has a unitary slope and represents identity. For no experiment the two distributions were significantly different (χ^2 test, p>0.05).* ***C****, Distribution of the percentage of spikes fired during a burst for identified motor neurons in two representative experiments.* ***D,*** *As in C but averaged over 11 experiments.*

Spontaneously occurring bursts were often observed and their detection and characterization is described in detail in the Methods section. As bursts are a major component of the spontaneous electrical activity we asked whether they were initiated by the firing of a specific neuron or set of neurons. We identified which motor neuron fired the first spike of every burst. Then we computed the percentage of spikes fired by every motor neuron *m* ($I_{tot}(m)$) over the total number of recorded spikes during the entire experiment, and the percentage ($I_{start}(m)$) of times in which motor neuron *m*

was the first to fire within a burst. In 11/11 experiment these distributions were not significantly different (paired t-test test, $p>0.05$), indicating that no neuron has a particular role in starting the bursts (see Fig. 2B).

Different neurons, however, participate differently to bursts. For each motor neuron *m* we computed the percentage F(m) of spikes occurring during bursts over the total number of spikes fired by the neuron. The distribution for two representative experiments is shown in Fig. 2C and the one mediated over 11 experiments in Fig. 2D. This distribution do not have a single peak but is bi-modal. The left peak indicates that most motor neurons fire in a similar way during bursts and during the inter-burst intervals. These are the motor neurons with an exponential or periodic ISI. The right peak corresponds to neurons firing preferentially during a burst: these motor neurons have a bi-exponential ISI and fire on average 80% of their spikes during bursts.

Collective properties of the spontaneous activity in isolated ganglia

Pairs of identified motor neurons are symmetrically distributed in the left and right semi-ganglion and their axons emerge from the controlateral roots and innervate the corresponding section of the leech body (Muller et al. 1981). A remarkable exception is represented by the pair of motor neurons 4 and 117 which project into the ipsilateral roots and innervate the ipsilateral body walls (Muller et al. 1981). We recorded extracellular spikes from the roots emerging from the left and right side of the ganglion, and we computed the total firing rate from the left and right roots. We compared the firing rate of every root *n* on the left root (FR_{Ln}) with the firing rate of its homologous root on the right side (FR_{Rn}). FR_{Ln} and FR_{Rn} could be in phase (left panel of Fig. 3A) or in anti-phase (middle panel of Fig. 3A). When the firing rate was low FR_L and FR_R did not have any significant temporal relationship (right panel of Fig. 3A). Collected data, obtained from 11 isolated leech ganglia for a total recording time of about 5 hours, indicate that the percentage of time in which FR_{Ln} and FR_{Rn} were in phase, in anti-phase and uncorrelated was 46±8, 6±2 and 48±10% respectively (see inset of panel A).

Fig. 3B illustrates the cross-correlation between FR_{Ln} and FR_{Rn}, computed on a bin width of 100 ms for 30 seconds frames in which FR_{Ln} and FR_{Rn} had the behavior illustrated in Fig. 4A. The position of the central peak of the cross-correlation (see Fig. 3C) indicates whether homologous roots fired synchronously (the 43%±15% of the time) or the activity of one root preceded the activity of the other (27%±10% leading left, 30%±10% right). No root lead the other root in a consistent manner (ANOVA test, $p>0.5$). The average delay of the activity between the two roots was of 72±29 ms.

The absolute value of the cross-correlation maximum was significantly correlated to the firing rate (n=11, corrcoeff = 0.60 ± 0.14, see Fig. 3D).

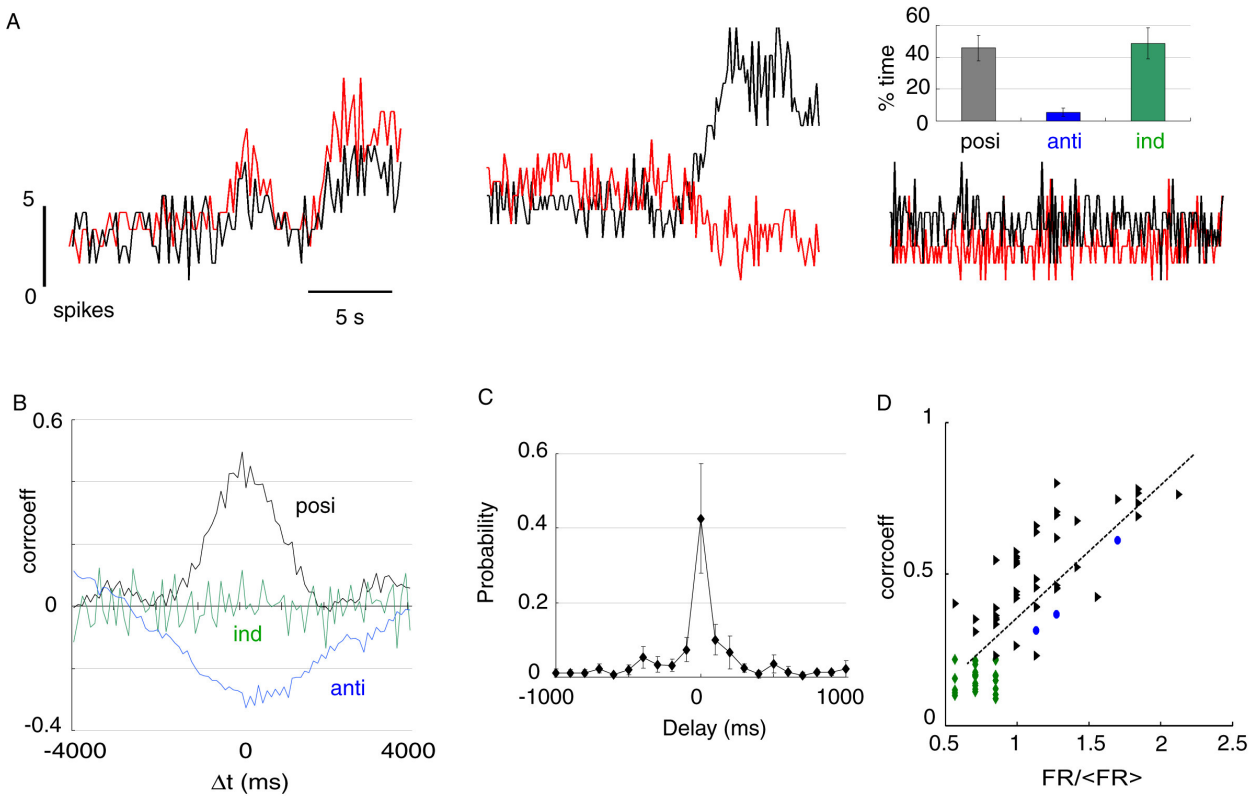

Figure 3 Lateral correlations ***A****, Three possible correlation states between homologous roots. From left to right: positively correlated, anti-correlated, and independent. In the inset: percentage of time spent in each state averaged over 11 exp.* ***B****, Cross-correlation function in the three states.* ***C****, Distribution of the lag corresponding to the correlation peak between homologous roots averaged over 11 experiments.* ***D****, Absolute value of correlation coefficient as a function of the FR for a representative experiment. Black dashed line corresponds to linear regression. The color code is the same of panel A inset and panel B: green corresponds to independence between roots, black to positive correlation, blu to anti-correlation.*

The spontaneous electrical activity in chains of ganglia and in semi-intact preparations

The spontaneous activity observed in a ganglion is affected by electrical signals arriving from the other ganglia and the two primitive brains set in the head and in the tail of the animal (Mazzoni et al. in preparation). These effects are best observed in semi-intact preparations (Fig. 4), in which it is possible to record the activity of ganglia connected to the intact nervous system of the leech. The FR of the ganglion is characterized, in these preparations, by the presence of large bursts of similar size (Fig. 4A). When the ganglion is connected just to one neighbour in the ganglia chain preparation (see Methods), these large bursts become less intense and regular (n=7) as shown in Fig. 4B. When the connective fibres joining the ganglion to the neighbour are cut, and the ganglion is isolated, the FR displays bursts of very variable size (Fig. 4C). Changes of the properties of the FR, visually evident in Fig. 4, were quantified by the comparison of statistical properties of the same ganglion in different configurations (Fig. 5A).

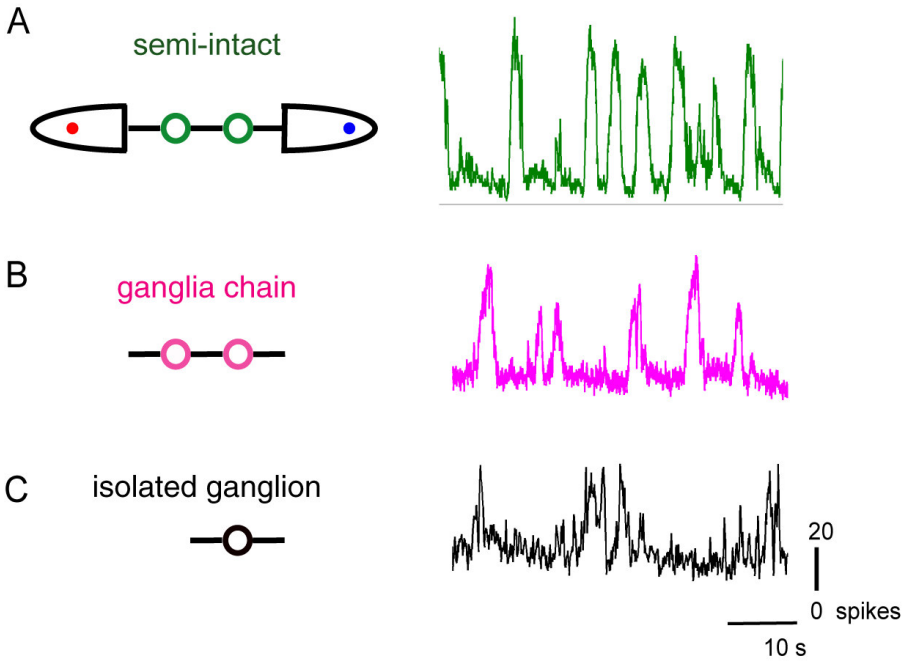

Figure 4. The network firing rate in different preparations *On the left the diagram of the preparation. On the right the recorded FR(t) with four extracellular electrodes.* ***A****, Semi-intact preparation* ***B,*** *Chain of two connected ganglia* ***C,*** *Isolated ganglion. All electrical recordings were obtained from the same ganglion, starting from panel A and subsequently cutting the connective fibers.*

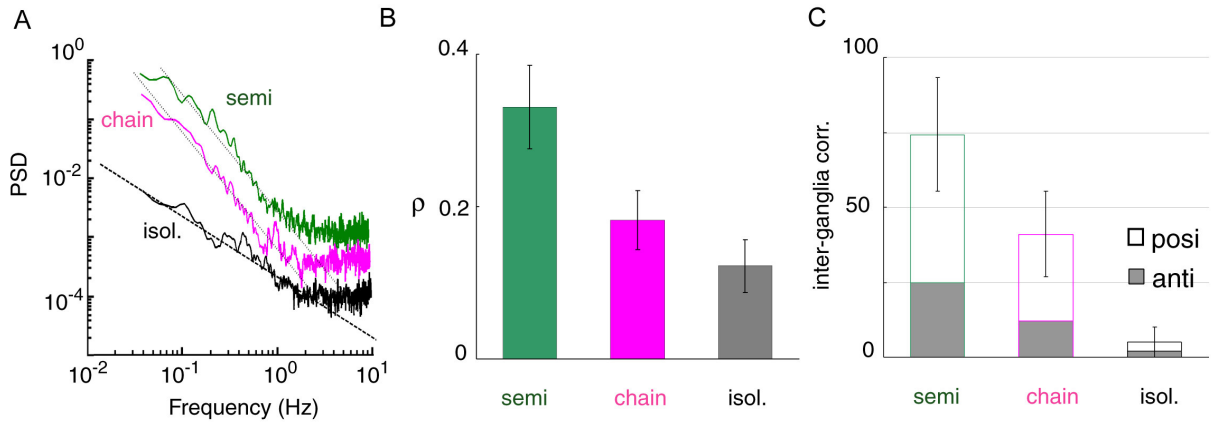

Figure 5 Correlation in semi-intact preparations ***A****, PSD of a single isolated ganglion (black), compared to the PSD from the same ganglion in a chain of two connected ganglia (magenta) and in a semi-intact (green) preparation. Plots of PSD were vertically shifted to allow a better comparison. Black dashed line indicates –1 slope and black dotted lines slope -2.* ***B****, Network correlation coefficient for the three preparations.* ***C****, Percentage of time of correlated activity between the two ganglia in the three different preparations. Correlation can be positive (in phase) or negative (in anti-phase).*

In all experiments (7/7) in semi-intact (green line) and ganglia chain configurations (magenta line) the power spectral density (PSD) of the firing rate, shown in Fig. 5B, had an average slope closer to $1/f^{2}$ (mean = 1.7±0.4). In contrast, in the same ganglion isolated from the rest of the body (black line) the PSD of the firing rate had a 1/f behavior. This change in slope indicates that in semi-intact and ganglia chain preparations low frequency modulations of the firing (i.e. correlations on long timescales) are more relevant than in the isolated ganglion. No peak was present in the PSD of the electrical activity of ganglia in the semi-intact configuration (0/7), indicating the absence of any periodic component in the FR.

We analysed the correlation both between pairs of ganglia and between neurons inside the same ganglion in different configurations. The network correlation coefficient $\bar{\rho}$ among neurons in the same ganglia was 0.30 ± 0.04 in semi-intact leeches, decreased to 0.18 ± 0.2 when the ganglia chain was disconnected from both head and tail and became equal to 0.12 ± 0.2 when ganglia were completely isolated from the rest of the nervous system (Fig. 5B). On average the anterior and the posterior ganglia were correlated (whether positively or anti-correlated) for 74±13% of the time in semi-intact configurations and for the 49±9% of the time in ganglia chain configurations (Fig. 5C).

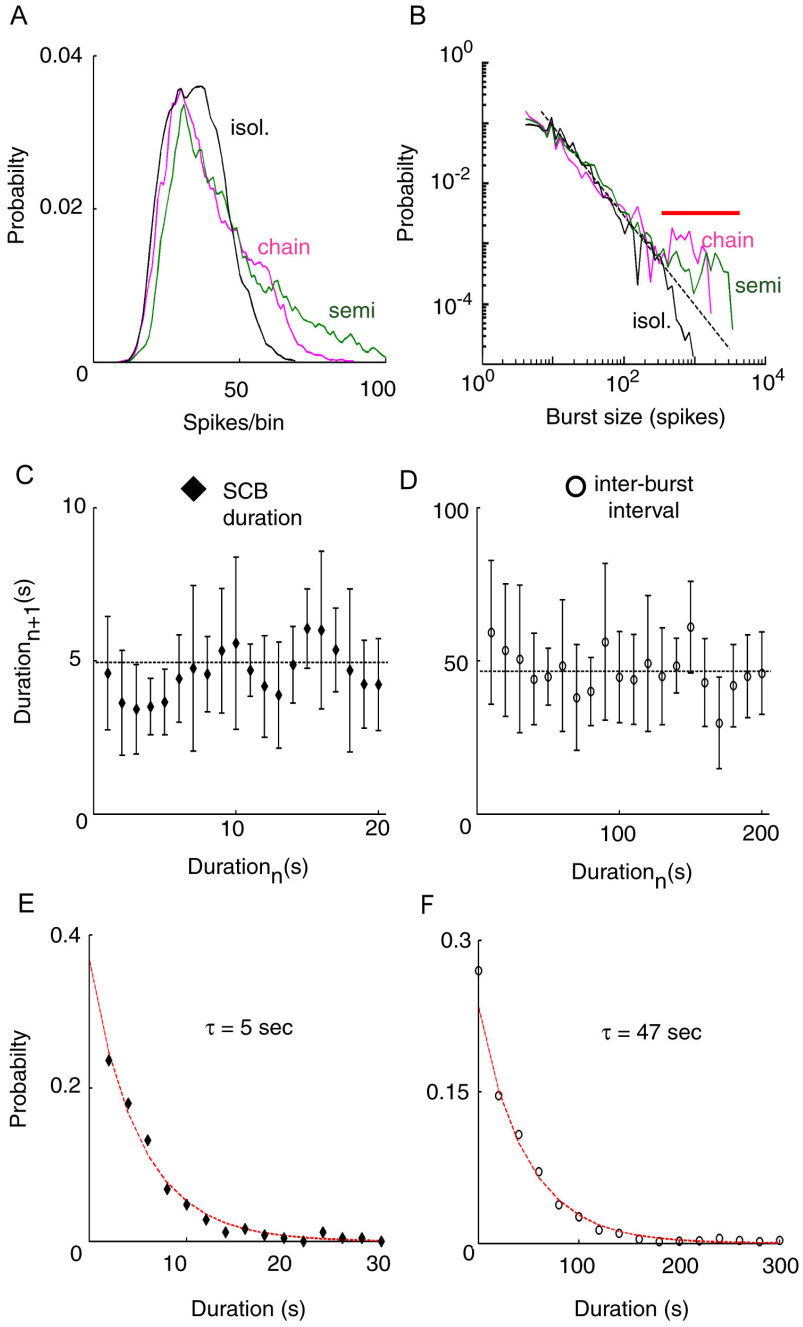

Figure 6 Bursts statistics in semi-intact preparations ***A***, *Spikes/bin distribution for the three preparations. Isolated ganglion distribution is lognormal (χ^2 test, $p>0.05$) while the other distributions are not. (χ^2 test, $p<0.05$).* ***B***, *Burst size distribution for the three preparations. Black dashed lines indicate -3/2 slope. Red line indicates Highly Synchronized Bursts (HSB).* ***C***, *Average duration of an HSB as a function of the duration of the previous HSB. Black horizontal line indicates average duration.* ***D***, *Same as in E but for inter-burst intervals.* ***E,F***, *Distribution of HSB (E) and inter-burst (F) durations. Red line indicates exponential fit (χ^2 test, $p>0.05$).*

The activities of neighbouring ganglia are then significantly (t-test $p<0.05$) more correlated when the ganglia are interacting also with the rest of the body. Therefore in the semi-intact configuration the electrical activity becomes more correlated both between neighbouring ganglia and between neurons in the same ganglion.

The distribution of the number of spikes/bins in semi-intact and ganglia chain configurations is not described by a lognormal distribution (0/7) because of the presence of bins with an unusually high number of spikes (see Fig. 6A). In semi-intact and ganglia chain configurations, the burst size distribution (Fig. 6B) could be described by a power law followed by a peak (indicated by the red bar) corresponding to the occurrence of very large bursts, of a size not observed in isolated ganglia. The same was true for the burst duration distribution (data not shown). Bursts belonging to this second peak will be referred as Highly Synchronized Bursts (HSB).

In order to test whether HSBs were periodic or had some kind of temporal pattern, we analysed the distribution of intervals between successive HSBs and the distribution of their durations. If HSBs were periodic, even for just a subset of the recording time, Inter-Burst Intervals (IBI) and/or HSB durations we expect the n-th value to be similar to the $n+1$th. The two values, instead, are not correlated ($r<0.05$ for both correlations): the IBI and duration of a burst does not depend on the IBI and duration of the previous one, indicating that neither IBI nor HSB duration followed a periodic or regular dynamics (Fig. 6C-D). The distributions of HSB durations and IBI were both exponentially distributed, as shown in Fig. 6E-F. The duration of HSBs was exponentially distributed (χ^2 test, $p>0.05$) with characteristic time $\tau= 5 \pm 1$ s. Inter-burst intervals were distributed according to an exponential distribution (χ^2 test, $p>0.05$) with characteristic time $\tau= 47 \pm 5$ s. HSBs, then, differently from bursts in the isolated ganglion, have a characteristic duration. Furhermore, they do not have a periodic but rather a Poisson-like dynamics, with exponential inter-event intervals distribution.

The relationship between spontaneous electrical activity and behavior

The analysis carried out in previous sections showed that in semi-intact leeches the spontaneous firing activity is characterized by the occurrence of large bursts of spikes, which we refer to as HSBs. These bursts, recorded in motor neurons, are expected to affect the behavior. In order to test this hypothesis we monitored the movements of the leech as described in Mazzoni et al. (2005). Briefly, we attached colored beads on the head and tail of the leech, we recorded the behavior with a CCD camera and we tracked with an algorithm the bead displacements (see Methods). By

simultaneously recording the electrical activity with suction electrodes, as described in previous sections, we were able to compare the global electrical activity and the motion of the head and tail of the leech.

The FR recorded from central ganglia in a semi-intact preparation (shown in black in Fig. 7A) and the speed (see Methods) of the bead glued on the tail (shown in blu Fig. 7A) have similar temporal patterns. We performed an automatic classification of the movement by dividing the recording time into active and resting intervals. The leech was considered to be active when the speed of the tail exceeded a threshold, set according to the level of noise present in the system (see Methods). Active intervals ended when the speed of the tail became lower than the threshold.

Movement onsets (yellow bars in Fig. 7A) usually corresponded to the starting time of a HSB. In order to quantify the degree of correlation between behavior and HSB, we measured the interval between the onset of every movement and the starting time of the closest HSB. The distribution of these intervals collected from 7 different experiments is shown in Fig. 7B. There is a large Gaussian-like peak centred around 200 ms, and two secondary peaks for intervals of 2 sec or more. Movement onset and occurrence of a HSB were considered related if they belonged to the central peak, i.e. they were separated by less than 500 ms (gray area in Fig. 7B), and unrelated if they were separated by a longer time interval (black area in Fig. 7B). With this criterion, the 92% of the movements of the tail were associated to HSBs.

Single leech motor neurons activate leech muscles when their firing exceeds a given threshold (Mason and Kristan 1982). To discover whether such a threshold was present also at a network level we compared network firing rate and speed of the tail. The peak of the distribution in panel 7B indicates that the average delay between onset of bursts and the onset of the related movements is 200 ms. A similar result was obtained computing the cross-correlation between firing rate and speed: the maximum value of correlation was for a lag of 150 ms (n=7, values ranging from 35 to 290 ms) (Fig. 7C).

Accordingly with these results we divided both electrical and behavioral recording in 100 ms frames, and we compared the firing rate at time t with the speed at time $t' = t + \mathrm{Dt}$, with Dt corresponding to the position of the peak of the crosscorrelation. For every value of the FR we have a set of associated speeds of which we computed mean and standard deviation, obtaining in this way the speed as a function of the firing rate. In all the experiments (7/7) the resulting function was the one shown in Fig. 7D: the leech starts moving when the firing rate is over a critical value. Above this value, the motion speed is higher for larger values of the firing rate.

We have then two candidate neuronal mechanisms for the onset of movements. One is that movements are caused by very large bursts. The other one is that movements are caused by high instantaneous value of the firing rate.

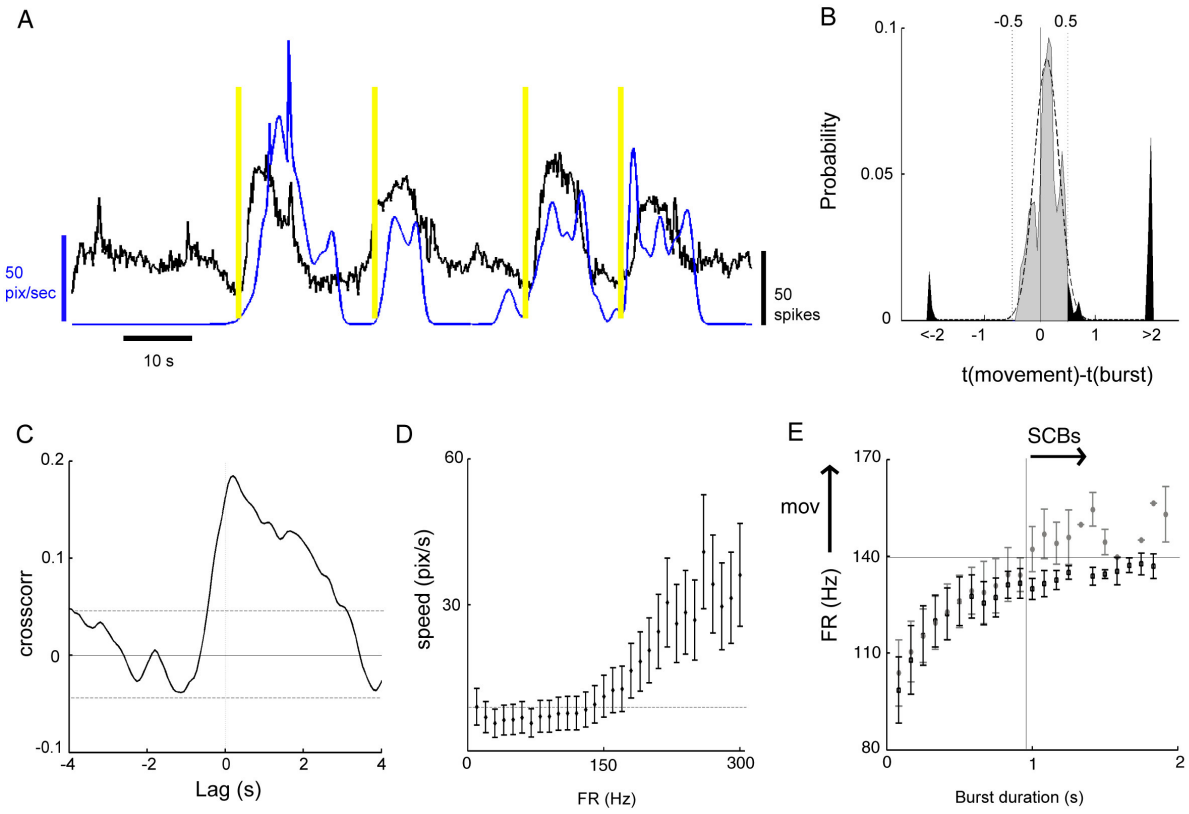

Figure 7 Burst dynamics and onset of bursts ***A***, *Recording from a semi-intact experiment. The network firing rate is displayed in black, tail velocity in blu. Yellow bars indicate movement onset.* ***B***, *Probability distribution of the interval between the movement onset and the closest burst onset. Gray area indicates correlated events (interval < 500 ms) and black area uncorrelated events. Black dashed line represents Gaussian fit.* ***C***, *Cross-correlation between the network firing rate of the posterior ganglion in semi-intact preparation, and speed of the tail. The position of the peak is at about 200 ms.* ***D***, *Tail velocity as a function of body ganglion firing rate for a representative experiment. Horizontal line indicates the maximum velocity that can be accounted for by the noise, above which the leech is moving. A 140 Hz threshold for movement is evident. Above that threshold velocity increases with firing rate.* ***E***, *Burst average firing rate as a function of their duration for the same ganglion shown in panel C in semi-intact preparation (gray) and isolated (black). The vertical line indicates the onset of highly synchronized state in semi-intact preparation. The horizontal line indicates the minimum firing frequency associated to movements.*

As shown in Fig. 7D longer bursts have also a higher instantaneous firing rate. Burst average firing rate increased with burst duration in 11/11 isolated ganglia (see black bars in Fig. 7E). The FR increased with the duration and size of the burst reaching a saturation value, which in isolated ganglia was on average below the rate necessary to trigger movements. In 7/7 semi-intact preparations, the burst average firing rate increased with burst duration (see gray bars in Fig. 7E), but the saturation value for the FR was higher than for isolated ganglia. Indeed, for very large durations corresponding to HSB the FR exceeded the minimum frequency associated with tail movement. Therefore we conclude that the movement is caused by high values of the instantaneous FR but since the instantaneous FR is proportional to the burst duration, the onset of movements is usually associated to long-lasting bursts. Long-range temporal correlations increased the degree of correlated firing among neurons: HSBs already appear when a ganglion is connected to one neighbouring ganglion (see Fig. 4A) and even larger HSBs are observed when the ganglion is receiving synaptic inputs from the whole body (see Fig. 4B).

HSBs propagate from one ganglion to the next, in both directions: from the anterior to the posterior or vice-cersa. A rearward progressing HSB recorded in a mid-body ganglion will reach the tail brain in a time T_1 and from there it will produce a detectable movement of the tail in a time T_2. A HSB originated from the tail will lead to a movement in a time T_2, and will trigger a HSB in the mid-body ganglion in a time T_1 (see the scheme in Fig. 8A). Therefore, two peaks are expected in the movement-burst delay distribution: one peak at $T_2 - T_1$ for forward progressing HSBs, and one peak at $T_2 + T_1$ for rearward progressing HSBs (see Fig. 8B). The presence of negative delays between movements and bursts shown in Fig. 6B is due to the fact that $T_2 < T_1$. The position of the peaks provides an estimate of T_1 and T_2 and the ratio between the areas corresponds to the two peaks the relative probability of the two dynamics.

Fitting the delay distribution with two super-imposed Gaussian functions provided the results shown in Fig. 8C. Two peaks are present at –120±25 ms and 180±25 ms, thus giving as estimate for T_1 of about 150±50 ms in agreement with previous estimates (Shawn and Kristan 1999) and computational models (Zheng et al. 2006) of inter-segmental propagation of electrical activity The value of T_2 was too small (~50 ms) to be properly evaluated with our measures (n=7 experiments for a total of 154 movements associated with HSB). The area corresponding to the rearward progressing HSBs (in red in Fig. 7B-C) is ~4 times larger that the one corresponding to the forward progressing HSBs, suggesting that the first ones are 4 times more probable than the second ones.

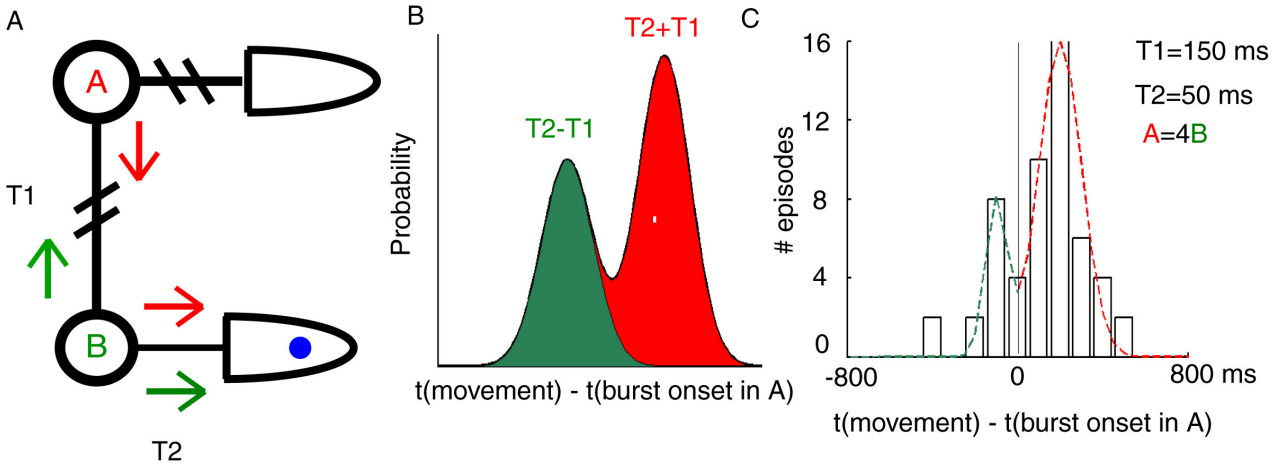

Figure 8 Forward and rearward progressing bursts. ***A****, Scheme of the two possible paths done by a movement-triggering bursts. A is the ganglia from which we are recording, and B the tail brain. The time necessary for the burst to go from A to B in both directions is* T_1*; the time necessary for a burst in B to trigger the movement in the tail is* T_2 ***B****, Model of burst-movement delay distribution. Red area indicates rearward progressing burst, green area forward progressing bursts.* ***C****, Bursts-movement delay distribution for a representative experiment and associated values of the parameters.*

DISCUSSION

The present manuscript provides a detailed analysis of the spontaneous electrical activity of leech neurons. We analysed the spontaneous activity at different levels: from single neurons, to the different functional properties of the roots, up to the activity of the single ganglion when it is connected to the rest of the nervous system. Bursts are a major feature of spontaneous activity: they occur in isolated ganglia but can be modulated by inputs arriving from the rest of the body. Neurons in semi-intact preparations fire spikes with a higher correlation and this leads to highly synchronized bursts (HSBs). These HSBs are able to initiate movements of the entire body of the leech and may play a fundamental role during the spontaneous behavior of the leech (Garcia et al 2005).

Single neurons are displaying both tonic and bursting firing, where the latter rather than to internal switches seems to be associated to the increased activity of the whole network. The diffused origin of network bursts is also suggested by the fact that the different firing rates account for the differences in the probability of starting the bursts: no neuron has a particular role in the onset of bursts. It must be noticed, however, that bursts in motor neurons are probably always triggered by interneurons, from which we are not recording, so from our data we can not directly observe the origin of bursts. Furthermore, some neurons are more likely than others to shift to bursting dynamic. This can bee seen qualitatively in Fig. 2A, and in more detail in the bi-modal distribution shown in Fig. 2C-D: there is one set of neurons firing half of their spikes during bursts and half during inter-bursts intervals, and a second set that is firing mainly during network bursts and is silent in inter-bursts intervals.

The effect of the architecture of the neuronal network in the bursting activity is evident in the ganglia chain. Connecting together two ganglia, individually displaying irregular bursts of a variable size, results in a more synchronized dynamics with a predominance of large bursts, as shown in Fig. 4-5. This increase in the correlation among motor neurons is likely to be due to the activity of the interneurons, that are known to be coupled in neighboring ganglia. The presence of anti-correlated episodes suggest that also inhibitory inter-ganglia pathways are playing a role in spontaneous activity. Synchronization among the activities of different neurons in the ganglion is maximum when the ganglion is connected to the whole nervous system. This is probably due part to the interplay among body ganglia (since the synchronization is evident in the ganglia chain preparation), and part to the inputs received from the head and the tail brain (since the synchronization increases when one or both brains are connected). The correlation lead to highly synchronized bursts.

In agreement with previous experimental results (Linkenkaer-Hansen et al. 2001, Beggs and Plenz 2003) and theoretical suggestions (Jensen 1998, Eurich et al., 2002) we have recently proposed (Mazzoni et al in preparation) that Self Organized Criticality (SOC) theory (Bak et al. 1988, Vespignani and Zapperi 1998), can provide a simple and general explanation for the occurrence of bursts in neuronal networks. A somehow counterintuitive point in SOC models is that, starting from a network displayng critical dynamics such as the isolated leech ganglion (Mazzoni et al. in preparation), an increase in the external stimuli rate is supposed to lead to the same dynamics caused by an increase in correlation among the elements of the network (Vespignani and Zapperi, 1998). This condition is obtained in semi-intact experiments in the leech where the external stimuli consist in both internal fluctuations of the single neurons and the inputs coming from the rest of the body. Our results show that indeed inputs from the other ganglia are causing a dynamics similar to the application of PTX, characterized by an increased bursting activity (Fig. 4) leading to a) increased power associated to low frequencies (Fig. 5A), b) increased correlation (Fig. 5B) c) long-tailed activity distribution (Fig. 6A) and d) a bi-modal distribution of burst size (Fig. 6B).

Previous findings (Mason and Kristan 1982) demonstrated that muscle contractions are activated by motor neuron firing rates exceeding a given threshold. We found the same dynamics at the level of the collective firing of motor neurons: the network FR must exceed a given threshold to cause a detectable motion of leech body wall. The FR reached by HSBs exceeds this threshold, so that HSBs can induce muscle contractions. HSBs trigger movements in the leech body with a delay of some hundreds of ms (Fig. 7), with a positive or negative delay depending on the direction of propagation of the HSB (Fig. 8).

If HSB are the unit responsible for the onset of movements, their statistical properties should affect also the behavior of the intact animal. We have previously analysed the spontaneous behavior of intact leeches in the absence of external stimuli (Garcia Perez et al. 2005) and we found that their behavior can be classified in a limited number of stereotyped states. The duration of stationary states was exponentially distributed with two time constants, one of the order of 5 sec and a longer one varying between 40 and 50 sec, as shown in Fig. 9A. Short stationary states corresponded to pauses in the exploratory motion, while the long stationary states were inactive periods in between two active behaviors. Their distribution is similar to the one of the intervals between successive HSBs, that is exponentially distributed with a time constant of about 47 sec (see Fig. 10B). This suggests that the same process that originates HSBs in our preparation is responsible for the onset of movements in the intact animal. In intact leeches and in the presence of sensory stimuli CPGs are also expected to initiate structured movements (Kristan et al. 2005).

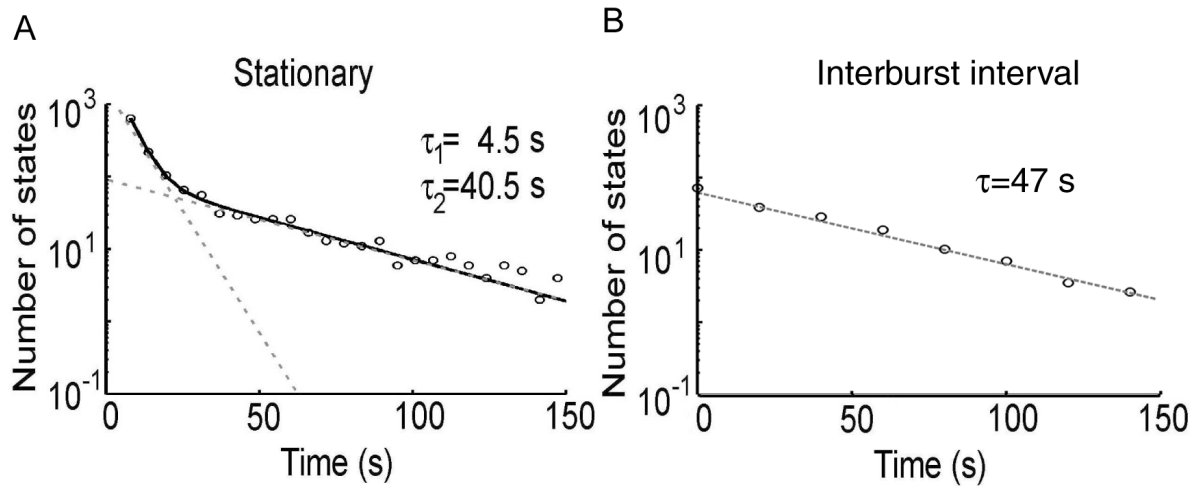

Figure 9 Stationary states and inter-burst intervals ***A*** *Stationary behavioral states distribution redrawn from Garcia Perez et al. (2005)* ***B*** *Inter-burst interval distribution shown in Fig. 5G (lower panel) rescaled to allow comparison. The binning is larger due to the smaller data set available.*

HSB are originated by a modulation of the bursting activity that is present in the ganglion even in the absence of stimuli. The ongoing bursting activity could then be the "internal state" (Brodfuehrer and Thorogood 1993) responsible for the variability of the efficacy of trigger neurons in activating CPGs. Studying the structure of this internal state could help to understand better the process of decision making in the leech.

Limits and perspectives

The main weakness of the present analysis is the limitation of recording only the electrical activity of motor neurons, and the absence of any direct observation of the spontaneous activity of the other neurons constituting the network under investigation. As motor neurons activity is the result of the electrical activity of the neuronal network controlling their firing, we infer properties of the underlying network from the observation of its output. Monitoring the activity of a larger fraction of the ganglion neurons, including interneurons, will result in a stronger test for our models on the dynamics of spontaneous activity. Imaging the leech ganglion with dyes as done in Briggman et al. (2005 and 2006) will provide precious insights on the mechanisms originating spontaneous bursts.
A second limit of our work is that we are recording the electrical activity in midbody ganglia and the movements in the tail. In this way we were able to estimate the propagation speed of HSBs (Fig. 7), but a closer comparison between movements and spontaneous electrical activity in the ganglia

will increase certainly our understanding of the events triggering the movements. These problems could be circumvented by leaving a piece of skin attached to the ganglion, as commonly used in isolated ganglion preparations to study local bending (Zoccolan et al. 2002, Thomson and Kristan 2006) and measure the correlations between skin contractions and spontaneous bursts.

We believe that our approach can be extended to the analysis of the spontaneous activity of a large variety of neuronal networks and can be useful to understand the relationship between spontaneous firing and behavior in several invertebrate species and possibly in some more evolved animals.

References

Arieli A, Sterkin A, Grinvald A, Aertsen A (1996) Dynamics of ongoing activity: explanation of the large variability in evoked cortical responses. Science 273:1868-1871.

Arisi I, Zoccolan D, Torre V (2001) Distributed motor pattern underlying whole-body shortening in the medicinal leech. J Neurophysiol 86:2475-2488.

Bak P, Tang C, Wiesenfeld K (1988) Self-organized criticality. Physical Review A: Atomic, Molecular, and Optical Physics 38:364-374.

Beggs JM, Plenz D (2003) Neuronal avalanches in neocortical circuits. J Neurosci 23:11167-11177.

Briggman KL, Abarbanel HDL, Kristan WB (2005) Optical imaging of neuronal populations during decision making Science 307:896-901

Briggman KL, Abarbanel HDL, Kristan WB (2006) Imaging dedicated and multifunctional neural circuits generating distinct behaviors J. Neurosci. 26:10925-10933

Brodfuehrer PD, Friesen WO (1986) Control of leech swimming activity by the cephalic ganglia. J Neurobiol. 17: 697-705

Brodfuehrer PD, Thorogood MSE (2001) Identified neurons and leech swimming behavior. Prog. in Neurobiol. 63: 371-381

Cacciatore TW, Rozenshteyn R, Kristan WB (2000) Kinematics and modeling of leech crawling: evidence for an oscillatory behavior produced by propagating waves of excitation J Neurosci 20: 1643-1655

Cymbaluk GS, Gaudry Q, Masino MA, Calabrese RL (2002) Bursting in leech heart interneurons: cell-autonomous and network-based mechanisms J Neurosci 22: 10580-10592

Eisenhart FJ, Cacciatore TW, Kristan WB (2000) A central pattern generator underlies crawling in the medicinal leech J Comp Physiol A 186: 631-643

Destexhe A, Contreras D (2006) Neuronal computations with stochastic network states. Science 314: 85-90

Eurich CW, Herrmann JM, Ernst UA (2002) Finite-size effects of avalanche dynamics. Physical Review E: Statistical, Nonlinear, and Soft Matter Physics 66:66137-66152.

Falck-Ytter T, Gredeback G, von Hofsten C (2006) Infancts predict other people's action goals Nat. Neurosci. 9:878-879

Fiser J, Chiu C, Weliky M (2004) Small modulation of ongoing cortical dynamics by sensory input during natural vision. Nature 431:573-578.

Flanagan JR, Johansson RS (2003) Action plans used in action observation Nature 424:769-771

Garcia-Perez E, Zoccolan D, Pinato G, Torre V (2004) Dynamics and reproducibility of a moderately complex sensory-motor response in the medicinal leech J Neurophysiol 92:1783-1795

Garcia-Perez E, Mazzoni A, Zoccolan D, Robinson HPC, Torre V (2005) Statistics of decision making in the leech. J Neurosci 25:2597-2608.

Glimcher P (2003) Decisions, uncertainty, and the brain Cambridge MA MIT Press

Grillner S (2003) The motor infrastructure: from ion channels to neuronal networks Nat Rev. Neurosci. 4: 573-586

Grillner S (2004) Muscle twitches during sleep shape the precise modules of withdrawal reflex Trends in Neurosci. 27: 169-171

Grillner S, Markram H, De Schutter E, Silberberg G, LeBeau FEN (2005) Microcircuits in action- from CPGs to neocortex Trends in Neurosci. 28: 526-534

Jensen HJ (1998) Self-Organized Criticality – Emergent Complex Behavior in Physical and Biological Systems. Cambridge: Cambridge University Press.

Kristan WB Jr, Calabrese RI, Friesen WO (2005) Neuronal control of leech behavior. Prog Neurobiol 76:279-327.

Lee IH, Assad JA, (2003) Putaminal activity for simple reactions or self-timed movements. J Neurophysiol 89:2528-2537.

Lewis JE, Kristan WB (1998) Representation of touch location by a population of leech sensory neurons. J. Neurophysiol. 80: 2584–2592

Linkenkaer-Hansen K, Nikouline VV, Palva JM, Ilmoniemi RJ (2001) Long-range temporal correlations and scaling behavior in human brain oscillations. J Neurosci 21:1370-1377.

Maimon G, Assad JA (2006) Parietal area 5 and the initiation of self time-movements versus simple reactions. J Neurosci 26:2487-2498.

Marder E (2001) Moving rhythms Nature 410:755

Marder E, Bucher D, Schulz DJ, Taylor AL (2005) Invertebrate central pattern generation moves along Curr.Biol. 15:685-699

Mason B, Kristan WB (1982) Neuronal excitation, inhibition and modulation of leech longitudinal muscles J Comp Physiol 146: 527-536

Mazzoni A, Garcia Perez E, Zoccolan D, Graziosi S, Torre V (2005) Quantitative characterization classification of leech behavior. J.Neurophysiol 93:580-593.

Muller KJ, Nicholls JG, Stent GS (1981) The nervous system of the leech: a laboratory manual. In: Neurobiology of the Leech (Muller KJ, Nicholls JG Stent GS), pp249-275. New York: Cold Spring Harbor Laboratory.

Nusbaum MP, Beenhakker MP (2002) A small-systems approach to motor pattern generation Nature 417:343-350

Papoulis A (1984) Probability, Random Variables, and Stochastic Processes 2nd ed. New York:McGraw-Hill.

Rieke F, Warland D, de Ruyter van Steveninck R, Bialek W (1997) Spikes. Exploring the Neural Code. Cambridge, MA: MIT Press

Sandrini G, Serrao M, Rossi P, Romaniello A, Cruccu G, Willer JC (2005) The lower limb reflexion in humans Prog. in Neurobiol. 77:353-395

Segev R, Benveniste M, Hulata E, Cohen N, Palevski A, Kapon E, Shapira Y, Ben-Jacob E (2002) Long term behavior of litographically prepared in vitro neuronal networks. Phys. Rev. Lett. 11:81021-81024

Shaw BK, Kristan WB (1999) Relative roles of the S cell network and parallel interneuronal pathways in the whole-body shortening reflex of the medicinal leech. 82:1114-1123

Thomson EE, Kristan WB (2006) Encoding and decoding touch location in the leech CNS J Neurosci 8009-8016

Vespignani A, Zapperi Z (1998) How self organized criticality works: a unified mean field picture. Physical Review E: Statistical, Nonlinear, and Soft Matter Physics 57:6345-6363.

Turrigiano G, Abbott LF, Marder E (1994) Activity-dependent changes in the intrinsic properties of cultured neurons Science 264: 974-977

Zapperi S, Baekgaard LK, Stanley HE (1995) Self-organized branching processes: mean-field theory for avalanches. Physical Review Letters 75:4071-4074.

Zheng M, Friesen WO, Iwasaki T (2006) Systems-level modeling of neuronal circuits for leech swimming J Comput. Neurosci Epub ahead of print

Zoccolan D, Pinato G, Torre V (2002) Highly variable spike trains underlie reproducible sensorimotor responses in the medicinal leech. J Neurosci 22:10790-10800